University of Glasgow
DEPARTMENT OF
AEROSPACE
ENGINEERING

Implementation Of High Temperature Modelling In Two Dimensional Navier-Stokes Solvers

Laurent Dubuc

GU Aero Report 9330 December 1993

Implementation Of High Temperature Modelling In Two Dimensional Navier-Stokes Solvers

Laurent Dubuc

GU Aero Report 9330 December 1993

Implementation of High Temperature Modelling in Two-Dimensional Navier-Stokes Solvers

L. Dubuc
Aerospace Engineering Department
University of Glasgow,
Glasgow, G12 8QQ, U.K.
EMAIL : laurent@udcf.gla.ac.uk

December 22, 1993

Contents

Abstract

The study reported here is concerned with hypersonic viscous flows and involves the development and implementation of an equilibrium air model within Computational Fluid Dynamics (CFD) codes to account for high temperature effects. This work is included in a research program to develop accurate and efficient computational tools for hypersonic re-entry problems.

The flow regimes encountered by spacecraft vehicles during atmospheric re-entry highlight the need to develop new efficient computational techniques to study chemistry effects. Hypersonic flows are characterized by very strong shock waves, large pressure and heat flux variations and involve chemical processes such as vibrational excitation, dissociation and ionization, which cause air to depart from perfect gas behaviour. As a consequence, the application of CFD techniques to hypersonic flight vehicles requires methods that compute efficiently the composition of air over a wide range of temperatures and densities.

An accurate and efficient equilibrium air model has been developed by J.M. Anderson and is based on the solution of the law of mass action to compute the chemical properties of the gas mixture. The air model currently implemented consists of six chemical species (O_2, N_2, O, NO, N, Ar) and involves three chemical reactions. The model does not take account of ionization. For the temperature range being considered, the assumption of thermal and chemical equilibrium remains valid and air is assumed to be a reacting mixture of thermally perfect gases. The equilibrium chemical composition of the mixture is obtained from the solution of the law of mass action. The thermodynamic properties of the pure species are obtained by using the least-squares method of curve fitting. The thermodynamic properties of the gas mixture are calculated from the thermodynamic species properties and the equilibrium species concentrations. This physically based model was preferred to more general curve fit techniques since it provides a more flexible and more suitable model for CFD applications.

An important aspect for solving the equilibrium equations is the choice of the independent variables. Because the mixture properties are computed on the basis of a uniform equilibrium temperature for all the component species, one needs to retain the equilibrium temperature as an independent variable, the second one usually being density. However, within the time dependent solution of the flow equations, it is the conserved total energy density which is computed as an independent variable and input into the state equations. It is therefore

necessary to develop efficient techniques for inverting the general equations of state to give temperature as a function of energy and density. Due to the complex formulation of the equation of state for air at high temperatures, there is no alternative to resorting to an iterative procedure. Since this iterative process can be quite time consuming, the success of employing such physical model for CFD applications will reside in the efficiency of this procedure. Different techniques have been investigated for inverting the equations of state, and the most efficient is an algorithm based on a Newton-Raphton iteration. The number of iterations is minimized by computing an accurate guess for the equilibrium temperature.

The present model has already been implemented in an implicit central difference scheme for application in one-dimensional nozzle flow problem. Here, the numerical solution of the Navier-Stokes equations is performed by using an upwind scheme together with a finite volume discretization method. The main difficulty which is encountered when extending upwind methods to equilibrium air models is in the formulation of the flux jacobian matrix, which must take into account the temperature variations of the ratio of specific heats. The formulation used here is a generalization of Roe average scheme for equilibrium air and was first proposed by Vinokur & Montagne. A simple explicit time stepping scheme is used and the boundary conditions treatment is based on the method ofn characteristics.

In order to illustrate the application of the equilibrium air model within the CFD environment, a solution of the quasi-one-dimensional Euler equations is given for a hypersonic expansion nozzle flow. Application is then extended to two-dimensional hypersonic inviscid and viscous flows over blunt body shapes. Calculations are performed for both the perfect gas flow and the equilibrium flow for comparison. The effects of the chemistry are discussed.

Chapter 1

The Governing Equations for High Temperature Modelling

1.1 The Navier-Stokes Equations

The full unsteady Navier-Stokes equations represent the most general model to describe aerodynamic flows within the continuum regime. These equations can be obtained directly from conservation principles where no reference to the composition of the gas is required, and therefore apply equally well to perfect gases or chemically reacting gases. In the particular case of a two-dimensional flow, the Navier-Stokes equations can be written in x-y Cartesian coordinate as,

$$
\begin{aligned}
\frac{\partial \rho}{\partial t} + \frac{\partial(\rho u)}{\partial x} + \frac{\partial(\rho v)}{\partial y} &= 0 \\
\frac{\partial(\rho u)}{\partial t} + \frac{\partial(\rho u^2 + p)}{\partial x} + \frac{\partial(\rho uv)}{\partial y} &= \frac{\partial \tau_{xx}}{\partial x} + \frac{\partial \tau_{xy}}{dy} \\
\frac{\partial(\rho v)}{\partial t} + \frac{\partial(\rho vu)}{\partial x} + \frac{\partial(\rho v^2 + p)}{\partial y} &= \frac{\partial \tau_{xy}}{\partial x} + \frac{\partial \tau_{yy}}{\partial y} \\
\frac{\partial(\rho E)}{\partial t} + \frac{\partial(u(\rho E + p))}{\partial x} + \frac{\partial(v(\rho E + p))}{\partial y} &= \frac{\partial(u\tau_{xy} + v\tau_{xy})}{\partial x} + \frac{\partial(u\tau_{xy} + v\tau_{yy})}{\partial y} + \\
& \quad \frac{\partial}{\partial x}\left(k\frac{\partial T}{\partial x}\right) + \frac{\partial}{\partial y}\left(k\frac{\partial T}{\partial y}\right)
\end{aligned}
$$

where ρ, u, v, p, E and T denote the density, the two-cartesian velocity components, the pressure, the total specific energy, and the temperature, respectively. The pressure p can be related to the density ρ and the specific internal energy e by a general equation of state of the form,

$$p = p(\rho, e)$$

The total specific energy E (or total energy per unit mass) is related to the specific internal energy e by

$$E = e + \frac{u^2 + v^2}{2}$$

The unsteady two-dimensional Navier-Stokes equations can be written in conservation form as

$$\frac{\partial \mathbf{U}}{\partial t} + \frac{\partial \mathbf{f}}{\partial x} + \frac{\partial \mathbf{g}}{\partial y} = 0 \tag{1.1}$$

where $\mathbf{U}$ is the solution vector of conservative variables, and $\mathbf{f}$ and $\mathbf{g}$ are the flux vectors which can be split into inviscid and viscous components such as

$$\mathbf{f} = \mathbf{f}^I + \mathbf{f}^V \tag{1.2}$$

$$\mathbf{g} = \mathbf{g}^I + \mathbf{g}^V \tag{1.3}$$

For the Navier-Stokes equations the unknowns and the fluxes have the following non-dimensional form,

$$\mathbf{U} = \begin{pmatrix} \rho \\ \rho u \\ \rho v \\ \rho E \end{pmatrix} \qquad \mathbf{f}^I = \begin{pmatrix} \rho u \\ \rho u^2 + p \\ \rho uv \\ \rho uH \end{pmatrix} \qquad \mathbf{g}^I = \begin{pmatrix} \rho v \\ \rho uv \\ \rho v^2 + p \\ \rho vH \end{pmatrix} \tag{1.4}$$

$$\mathbf{f}^V = \begin{pmatrix} 0 \\ -\tau_{xx} \\ -\tau_{xy} \\ -u\tau_{xx} - v\tau_{xy} + q_x \end{pmatrix} \qquad \mathbf{g}^V = \begin{pmatrix} 0 \\ -\tau_{xy} \\ -\tau_{yy} \\ -u\tau_{xy} - v\tau_{yy} + q_y \end{pmatrix} \tag{1.5}$$

where H denote the total specific enthalpy which is related to the total specific energy as

$$H = E + \frac{p}{\rho}$$

The stress tensor τ and the heat conduction flux q are given by

$$\begin{aligned}
\tau_{xx} &= \frac{2\mu}{3Re}\left(2\frac{\partial u}{\partial x} - \frac{\partial v}{\partial y}\right) \\
\tau_{xy} &= \frac{\mu}{Re}\left(\frac{\partial u}{\partial y} + \frac{\partial v}{\partial x}\right) \\
\tau_{yy} &= \frac{2\mu}{3Re}\left(2\frac{\partial v}{\partial y} - \frac{\partial u}{\partial x}\right) \\
q_x &= -\frac{k}{(\gamma-1)M_\infty^2 RePr}\frac{\partial T}{\partial x} \\
q_y &= -\frac{k}{(\gamma-1)M_\infty^2 RePr}\frac{\partial T}{\partial y}
\end{aligned}$$

where μ and k denote the coefficient of viscosity and thermal conductivity respectively, and γ, M_∞, Re, and Pr denote the ratio of specific heats, the Mach number, the Reynolds number, and the Prandtl number associated with the free stream conditions, respectively.

1.2 The Euler Equations

The Euler equations can be stated by considering the limiting form of the general viscous flow equations in the limit of infinite Reynolds number. The governing equations for an inviscid flow therefore follows from equations (1.1), (1.2), (1.3) wherein the viscous terms have been deleted, leading to

$$\frac{\partial \mathbf{U}}{\partial t} + \frac{\partial \mathbf{f}^I}{\partial x} + \frac{\partial \mathbf{g}^I}{\partial y} = 0$$

with $\mathbf{U}$, $\mathbf{f}^I$ and $\mathbf{g}^I$ defined by (1.4).

1.3 Quasi-One-Dimensional Nozzle Flow

The quasi-one dimensional nozzle flow generally represents a good model problem for algorithm development in computational fluid dynamics. The continuity, momentum, and energy equations for unsteady quasi-one-dimensional flow are given by

$$\begin{aligned} \frac{\partial(\rho A)}{\partial t} + \frac{\partial(\rho u A)}{\partial x} &= 0 \\ \frac{\partial(\rho u A)}{\partial t} + \frac{\partial(\rho u^2 + p)A}{\partial x} &= p\frac{dA}{dx} \\ \frac{\partial(\rho E A)}{\partial t} + \frac{\partial(\rho u H A)}{\partial x} &= 0 \end{aligned}$$

where A is the local cross-sectional area of the nozzle.

The system can be rewritten into the variables $(\rho, \rho u, \rho E)$ in order to define the source term Ω. This leads to the following system

$$\frac{\partial \mathbf{U}}{\partial t} + \frac{\partial \mathbf{f}^I}{\partial x} = \mathbf{\Omega}$$

where

$$\mathbf{U} = \begin{pmatrix} \rho \\ \rho u \\ \rho E \end{pmatrix} \qquad \mathbf{f}^I = \begin{pmatrix} \rho u \\ \rho u^2 + p \\ \rho u H \end{pmatrix} \qquad \mathbf{\Omega} = -\begin{pmatrix} \rho u \\ \rho u^2 \\ \rho u H \end{pmatrix} \frac{d}{dx} \ln A$$

1.4 Equations Of State

The formulation of the governing equations has to be completed by the definition of the equations of state which describe the thermodynamic behaviour of the gas. The equations of state relate the macroscopic quantities of a thermodynamic system, such as the density ρ, the specific internal energy e, the pressure p, the temperature T, and the composition of the gas, either by the number of moles $\mathcal{N}_i$ or by the specific concentration η_i of the species. Two equations of state are generally required to describe a thermodynamic system, although in the limiting case of an ideal gas these two can be combined into one equation. These two equations of state may be written in the general form as

$$\begin{aligned} e &= e(T, \eta_i) \\ p &= p(\rho, T, \eta_i) \end{aligned}$$

The first equation is a caloric equation of state which relates internal energy to temperature. The second equation is a thermal equation of state relating pressure to temperature and density. Different degrees of approximation can be considered to model a thermodynamic system, which allow further simplications in the formulation of the equations of state.

1.4.1 Calorically perfect gas

At room temperature, air is essentially a calorically perfect gas where all intermolecular forces can be neglected. For a gas with only translational and rotational energy, we have

$$\begin{aligned} c_v &= \frac{5}{2}R \\ c_p &= c_v + R = \frac{7}{2}R \\ \gamma &= \frac{c_p}{c_v} = \frac{7}{5} = 1.4 \end{aligned}$$

This result can be obtained either from statistical thermodynamics or kinetic theory and is a consequence of the assumption that the molecules are independent. A calorically perfect gas is therefore characterized by constant specific heats c_p and c_v, and a constant ratio of specific heats $\gamma = c_p/c_v$. This approximation remains valid for temperatures less than approximately 600 K, in which case enthalpy and internal energy are functions of temperature only and are given by

$$\begin{aligned} h &= c_p T \\ e &= c_v T \end{aligned}$$

Referring to the definition of enthalpy, $h = e + p/\rho$, and using the two equations above leads to the general formulation of the thermal equation of state which reads

$$p = \rho RT$$

This equation is commonly referred to as the perfect gas equation of state and holds for a thermally or calorically perfect gas. $R = c_p - c_v$ is the specific gas constant and varies for different gases since it is related to the molecular weight of the gas $\mathcal{M}$ through $R = \mathcal{R}/\mathcal{M}$. In the particular case of a calorically perfect gas, the two equations of state can be combined to produce a simple relation,

$$p = (\gamma - 1)\rho e$$

1.4.2 Thermally perfect gas

When the air temperature reaches approximately 600 K and higher, the vibrational energy of the molecules becomes excited, and this causes the specific heats c_p and c_v to become functions of temperature. In turn, the ratio of specific heats $\gamma = c_p/c_v$ also becomes a function of temperature. For a thermally perfect, non-reacting gas, we have

$$c_p = f_1(T)$$
$$c_v = f_2(T)$$

so that,

$$h = h(T)$$
$$e = e(T)$$

For a non-reacting gas, R is constant and $R = c_p - c_v$ still applies. The perfect gas equation of state is therefore still valid but cannot be further reduced,

$$p = \rho RT$$

1.4.3 Chemically reacting mixture of perfect gas

As the temperature is further increased (above 2000 K), chemical reactions occur, so that air can no longer be considered as a unique component and has to be considered as a mixture of several component species. However, at low densities and high temperatures, where the mean free path is sufficiently large for the molecular force to be ignored, each individual species can be modelled as a thermally perfect gas, and therefore obeys the perfect gas equation of state such as $p_i = \rho_i R_i T$ where p_i, R_i and ρ_i denote the partial pressure, specific gas

constant, and density of species i respectively. Under these conditions, air becomes a chemically reacting mixture of perfect gas, which can be modelled either in equilibrium or in non-equilibrium. If the vibrational excitation and chemical reactions take place very rapidly in comparison to the time it takes for a fluid element to move through the flowfield, we have vibrational and chemical equilibrium flow. If the opposite is true, we have non-equilibrium flow, which leads to considerably more difficult analysis.

In the general non-equilibrium case, the specific heats c_p and c_v, the enthalpy h, and the internal energy e not only depend on the temperature T but also on the chemical composition of the gas through the specific concentrations of the species η_i which in general depend on ρ, T, and the history of the flow,

$$\begin{aligned} h &= h(T, \eta_i) \\ e &= e(T, \eta_i) \\ c_p &= f_1(T, \eta_i) \\ c_v &= f_2(T, \eta_i) \end{aligned}$$

where

$$\eta_i = \eta_i(\rho, T, t), \qquad i = 1, 2, ..., n$$

The perfect gas equation of state still holds

$$p = \sum_{i=1}^{n} p_i = \sum_{i=1}^{n} \rho_i R_i T = \rho R T$$

However, for a chemically reacting gas, R is no longer a constant since it is directly related to the molecular weight of the mixture which is function of the temperature.

If thermodynamic and chemical equilibrium is assumed, the chemical composition of the mixture is uniquely defined for given values of the density and the temperature, and the thermodynamic state of the system can be expressed in terms of either T and p , or T and ρ, so that

$$\begin{aligned} e &= e(\rho, T) \\ p &= p(\rho, T) \end{aligned}$$

1.4.4 Real gas

In contrast to the three previous cases which were essentially concerned with high temperatures, we now consider very high pressure and/or very low temperature conditions wherein the intermolecular forces can no longer be neglected. Under

these conditions, air behaves as a real gas. The molecules are packed closely together and are moving slowly with consequent low inertia. The intermolecular forces thus come to have a large effect on the particle motion and therefore on the macroscopic properties of the system.

Since the perfect gas equation of state is built up on the assumption of a gas model with no interacting force fields, it does not apply to real gas where both the intermolecular forces and the volumes of the molecules themselves have to be taken into account. Various real gas equations of state have been proposed amongst which the most common are those of van der Waals, Berthelot, Dietirici, Wohl, Keyes, Beattie & Bridgeman, and Benedict, Webb, & Rubin. Most of these equations of state are empirical and involve the use of constants which are specific to each gas or gas mixture. Moreover, these modelizations become unaccurate if the state variables are calculated in regions other than those where experimental data were used to estimate the constants.

Under conditions of very high pressures and low temperatures where a real gas is likely to be encountered, the gas is rarely chemically reacting. We can therefore consider the case of a non-reacting real gas, with intermolecular forces, whereby the equations of state can be expressed in terms of ρ and T, or p and T,

$$\begin{aligned} h &= h(p,T) \\ e &= e(\rho,T) \\ c_p &= f_1(p,T) \\ c_v &= f_2(\rho,T) \end{aligned}$$

1.4.5 Summary

As we can see, due to the complexity of the physical and chemical processes involved in the definition of the thermodynamic state of a system, there exists no single universal equation of state which remains valid over the whole range of temperature and density. However, in the light of developing a gas model suitable for atmospheric re-entry problems, whereby the conditions to be encountered are very low densities and very high temperatures, air will be considered as a mixture of thermally perfect gases. Moreover, over a large part of the flight regime, the assumption of thermodynamic and chemical equilibrium is still valid. Although this is a restriction, it appears to be consistent with the high temperature effects arising from the hypersonic velocities encountered at high altitudes.

Chapter 2

The Equilibrium Air Model

2.1 Introduction

The flow regimes encountered by spacecraft vehicles during atmospheric re-entry highlight the need to develop new efficient computational techniques to study chemistry effects. The combination of high speed and high altitude results in the presence of very strong shock waves, and the departure of air from perfect gas behaviour due to vibrational excitation, dissociation and ionization. As a consequence, the application of Computational Fluid Dynamics techniques to hypersonic re-entry problems requires methods that rapidly compute the composition of air over wide ranges of temperature and density.

Previous methods for obtaining equilibrium properties of gas mixtures were based on analytic representations providing tabulated data and curve fits. One of the most popular curve fitting techniques was first developed by Grabau, and employs several polynomial expressions in two variables together with exponential transition functions. Unfortunately, this representation does not provide sufficient continuity and accuracy, especially for the thermodynamic derivatives required for the formulation of the flux jacobian matrix and for the computation of the speed of sound. Furthermore, the original data used to construct the curve fits are not accurate at high temperatures. For that reason, a more accurate representation of the thermodynamic behaviour of air over wide temperature ranges can only be build up using large amounts of data, and therefore tends to be less flexible and computationally more expensive.

In order to overcome some of the limitations inherent in data based approaches to state equation modelling, physically based techniques have been investigated. Most of the available methods are general in nature and employ the *free-energy minimization*. However, the generality of the method has proven to be undesirable since a large fraction of the computational time is spent in

executing the chemistry subroutine. An alternative method has therefore been prefered in this work, which is based on the *law of mass action* and leads to significantly faster computational speeds for the determination of the equilibrium chemical composition. The present method is derived from the model of Prahbu and Erickson [8], and involves the algebraic combination of the reactions of chemical equilibrium, obtained from the law of mass action, with the element conservation laws. Since the law of mass action can be written in terms of equilibrium constants, these methods are sometimes referred to as *equilibrium constant methods.*

2.2 The Law of Mass Action

We consider a chemically reacting mixture of thermally perfect gases. The mixture comprises n different species X_i which are chemically active so that chemical reactions can occur. The general form of the reaction equation is

$$\sum_{i=1}^{n} \nu_i' X_i \rightleftharpoons \sum_{i=1}^{n} \nu_i'' X_i \tag{2.1}$$

where ν_i' and ν_i'' are the stoichiometric coefficients for the chemical species X_i.

The equilibrium condition can be obtained from chemical thermodynamics by formulating the Gibbs equation for a chemically reacting system [10]. For an open system including irreversible chemical processes, the Gibbs equation reads

$$dS = \frac{1}{T} dE + \frac{p}{T} dV - \frac{1}{T} \sum_{i=1}^{n} \hat{\mu}_i d\mathcal{N}_i \tag{2.2}$$

According to the second law of thermodynamics, the expression for entropy production in chemical non-equilibrium is given by

$$dS = d_e S + d_i S \tag{2.3}$$

where $d_e S$ is the flow of entropy into the system from the surroundings and is given by $d_e S = dQ/T$ with $dQ = dE + pdV$. In turn, $d_i S$ is the production of entropy by irreversible processes within the system, and its expression is obtained by combining equations (2.2) and (2.3),

$$d_i S = -\frac{1}{T} \sum_{i=1}^{n} \hat{\mu}_i d\mathcal{N}_i \tag{2.4}$$

The second law requires that $d_i S$ be either positive, corresponding to an irreversible process, or zero, corresponding to a reversible process. Since the chemical equilibrium can be considered as an infinitely slow succession of states of

equilibrium, the condition for chemical equilibrium is therefore that $d_i S$ be zero at all times, which requires that

$$\sum_{i=1}^{n} \hat{\mu}_i d\mathcal{N}_i = 0$$

This equation is the most general description of thermo-chemical equilibrium. It is not restricted to perfect gases and may be looked on as a universally valid formulation of the law of mass action.

In the above equation, $d\mathcal{N}_i$ is the increase in the number of moles of species i due to chemical reactions. $d\mathcal{N}_i$ can be expressed in terms of the stoichiometric coefficients ν_i and the degree of advancement ξ. The equilibrium condition becomes

$$\sum_{i=1}^{n} (\nu_i'' - \nu_i') \hat{\mu}_i^* = 0 \tag{2.5}$$

where $\hat{\mu}_i^*$ is the value of the chemical potential at the equilibrium state. The chemical potential of one gas in a mixture of thermally perfect gases is

$$\hat{\mu}_i = \hat{\mu}_i^0(T) + \mathcal{R}T \ln \frac{p_i}{p_0} \tag{2.6}$$

where $\hat{\mu}_i^0(T)$ is the chemical potential (or Gibbs free energy per mole) of the species in the pure state and for a given temperature.

The equilibrium condition for a mixture of thermally perfect gases is now simply obtained by substituting expression (2.6) for $\hat{\mu}_i$ into the equation (2.5) for reaction equilibrium. This gives for the equilibrium partial pressure p_i^*

$$\sum_{i=1}^{n} (\nu_i'' - \nu_i') \hat{\mu}_i^0 + \mathcal{R}T \sum_{i=1}^{n} (\nu_i'' - \nu_i') \ln \frac{p_i^*}{p_0} = 0 \tag{2.7}$$

Therefore, the system will be in equilibrium if the partial pressures of the reacting species in the mixture satisfy the relation

$$\prod_{i=1}^{n} \left(\frac{p_i^*}{p_0} \right)^{(\nu_i'' - \nu_i')} = K_p(T) \tag{2.8}$$

where

$$K_p(T) = exp \left(- \frac{\sum_{i=1}^{n} (\nu_i'' - \nu_i') \hat{\mu}_i^0}{\mathcal{R}T} \right) \tag{2.9}$$

$K_p(T)$ is the equilibrium constant in terms of partial pressures evaluated at standard state pressure ($p_0 = 101325 N/m^2$). The equilibrium condition can also

be written in terms of the specific concentrations η_i by means of the relation $p_i = \eta_i \rho \mathcal{R} T$,

$$\prod_{i=1}^{n} (\eta_i)^{(\nu_i'' - \nu_i')} = K \tag{2.10}$$

where

$$K = K_p(T) \left(\frac{p_0}{\rho \mathcal{R} T} \right)^{(\nu_i'' - \nu_i')} \tag{2.11}$$

If we consider m independent reactions, equation (2.10) gives m independent relations involving m independent constants $K_r, (r = 1, 2, ..., m)$. This formulation of the law of mass action can be used to calculate the equilibrium composition of a chemically reacting gas at a given temperature and density. However, the equilibrium constants K_r are still not completely known, since they depend on the equilibrium properties of the pure species such as $\hat{c}_{p_i}$, $\hat{h}_i^0$ and $\hat{s}_i^0$, which are derived from statistical mechanics. These are to be discussed in the next section.

2.3 Equilibrium Air Model

Six chemically reacting species are assumed to be present in equilibrium air : diatomic oxygen O_2, diatomic nitrogen N_2, monoatomic oxygen O, nitric oxide NO, monoatomic nitrogen N and Argon Ar. In the temperature range being considered here, we assume that the ionized species (i.e., e^-, NO^+, N^+, O^+, and Ar^+) are in very small quantities and hence are neglected. Futhermore, Argon is treated as an inert gas, and does not take place in any reactions. It does, however, contribute to the internal energy of the gas mixture and therefore must be accounted for.

Under standard conditions of pressure and temperature, air is assumed to consist of O_2, N_2 and Ar in molar proportions of 20.95%, 78.09% and 0.96% respectively. We make the assumption of weakly interacting particles, so that air is assumed to be a reacting mixture of thermally perfect gases. We also make the assumption of thermodynamic and chemical equilibrium. Consequently, all the chemistry will be treated at the state of equilibrium, and the mixture will be characterized by a uniform equilibrium temperature over all the species components.

Three independent chemical reactions involving the chemical species are considered,

(1) $$O_2 + X \rightleftharpoons 2O + X$$

Species Number	Species	Molar mass $\hat{\mathcal{M}}_i$ (kg/mol)	Mole fractions x_i	Mass fractions α_i
1	O_2	0.031999	0.2095	0.2314
2	N_2	0.028013	0.7809	0.7553
3	O	0.015999	0.0000	0.0000
4	NO	0.030006	0.0000	0.0000
5	N	0.014007	0.0000	0.0000
6	Ar	0.039948	0.0096	0.0133
Molar mass of air at T=273.15 K : $\hat{\mathcal{M}} = \sum_{i=1}^{6} x_i \hat{\mathcal{M}}_i = 0.028963$ kg/mol				

Table 2.1: *Low Temperature Composition Air*

(2) $$N_2 + O_2 \rightleftharpoons 2NO$$

(3) $$N_2 + X \rightleftharpoons 2N + X$$

In a dissociation process, a third body can be required to collide with the molecule and part of its internal energy is used to break the bond between the two atoms of the molecules. The third body is only required for the reaction to occur and is not modified by the reaction process. This species can be any atom or molecule present in the mixture, and has been denoted by X in the two dissociation reactions above.

For equilibrium air calculations, the species X is of little significance since it does not modify the equilibrium properties of the mixture. For non-equilibrium calculations, it can however control the effectiveness of the reaction process and acts as a catalyst.

2.4 Thermodynamic Properties of Pure Species

The first step in obtaining the equilibrium properties of a gas mixture is to calculate the thermodynamic properties for each individual species. The exact formulation of thermodynamic properties is obtained from partition functions of statistical mechanics. However, the correct determination of the partition function requires precise values of the quantum energy levels, which gives rise to considerable computing times. A different technique for calculating the species properties has therefore been prefered here, which is based on fitting polynomial

curves to statistically calculated data.

2.4.1 The Exact Formulation of Thermodynamics Properties

For a gas consisting of a single chemical species, the macroscopic equilibrium properties can be obtained from a description of an assembly of microscopic particles using statistical mechanics. When dealing with gases consisting of weakly interacting particles, each energy level can be split into two independent modes, one describing the translational motion of the center of the particle and the other its internal structure. The energy partition function of the system can be written as

$$Q = Q_{trans} Q_{int}$$

For atoms, whose internal structure is due only to orbiting electrons, no further approximations are required to define the model. The only contribution to Q_{int} comes from the quantized electronic levels. Under the assumption of weakly interacting particles, the total energy is simply obtained by summing all the states which have been observed.

For molecules, each energy level associated with the internal structure can be split into two terms, one due to the motion of the electrons about the fixed nuclei, and the other due to the motion of the nuclei in the potential field determined by the electronic energy distribution. However, the exact determination of energy levels for molecules is very difficult when there are more than two atoms. The most accurate method to obtain the energy levels is to solve the vibrational Schrödinger equation [21] which describes the vibrational motion of nuclei in an effective potential field due to the electronic configuration and molecular rotation. The procedures to solve this equation numerically are well known, but can be quite time consuming. For example, in order to calculate the internal energy at 50,000 K, one has to sum between 20,000 and 50,000 bound states for each diatomic species. This obviously gives rise to large computing times and is not viable for CFD calculations.

Various approximate models for diatomic molecules have been proposed by different authors. The most popular is the Classical Rigid Rotator and Harmonic Oscillator model [6] which assumes that the electronic mode, the rotational mode, and the vibrational mode are totally decoupled. The potential for the vibrational mode is that of a simple harmonic oscillator, while the potential for the rotational mode corresponds to a rigid rotator characterized by a constant moment

of inertia. The energy level associated with the internal structure is therefore given as the sum of the energy levels of the different modes, and the partition function can be expanded as

$$Q = Q_{trans} Q_{elec} Q_{rot} Q_{vib}$$

However, the splitting of internal energy into separate macroscopic modes cannot be justified at high temperature, and therefore does not apply for dissociation.

More realistic models based on a higher order expansion of the potential functions have been proposed by different authors (e.g., Dunham, Stupochenko, Jaffe, or Liu & Vinokur) and provide more accurate representations at high temperature at the expense of larger computing times.

2.4.2 Polynomial Curve Fits for the Species Properties

The calculation of the thermodynamic properties for all the species are obtained by using the least-squares method of curve fitting proposed by Prahbu and Erickson [8]. For a thermally perfect gas, the molar heat at constant pressure $\hat{c}_p$ is function of temperature only. The molar heats $\hat{c}_{p_i}$ for all the species can thus be approximated by fifth order polynomials of the form

$$\frac{\hat{c}_{p_i}}{\mathcal{R}} = \sum_{j=1}^{5} a_{i,j} T^{j-1}$$

The corresponding molar enthalpy $\hat{h}_i^0$, molar entropy $\hat{s}_i^0$, and molar Gibbs free energy $\hat{g}_i^0$ are obtained from the classical thermodynamics relations,

$$\hat{h}_i^0 = \int_T^{T_0} \hat{c}_{p_i}(T) dT + \hat{h}_i^{T_0} \tag{2.12}$$

$$\hat{s}_i^0 = \int_T^{T_0} \frac{\hat{c}_{p_i}(T)}{T} dT + \hat{s}_i^{T_0} \tag{2.13}$$

$$\hat{g}_i^0 = \hat{h}_i^0 - T\hat{s}_i^0 \tag{2.14}$$

Hence,

$$\frac{\hat{h}_i^0}{\mathcal{R}T} = \sum_{j=1}^{5} \frac{a_{i,j} T^{j-1}}{j} + \frac{a_{i,6}}{T} \tag{2.15}$$

$$\frac{\hat{s}_i^0}{\mathcal{R}} = \sum_{j=2}^{5} \frac{a_{i,j} T^{j-1}}{j-1} + a_{i,1} \ln T + a_{i,7} \tag{2.16}$$

$$\frac{\hat{g}_i^0}{\mathcal{R}T} = \frac{\hat{h}_i^0}{\mathcal{R}T} - \frac{\hat{s}_i^0}{\mathcal{R}} \tag{2.17}$$

The coefficients $a_{i,6}$ and $a_{i,7}$ are the integration constants. The values of $a_{i,6}$ are determined from the enthalpy of formation for all the species at the reference temperature of 0 K. The values of $a_{i,7}$ are determined from the values of entropy at $T = 298.15K$.

2.5 Equilibrium Species Concentrations

The computational method for calculating the equilibrium chemical composition of air is derived from that developed by Prahbu and Erickson. The method involves the algebraic combination of the reactions of chemical equilibrium with element conservation. The three non-linear equilibrium equations for the three independent reactions (1) to (3) are written here in terms of the specific concentrations η_i,

$$K_1 = \frac{\eta_3^2}{\eta_1} \tag{2.18}$$

$$K_2 = \frac{\eta_4^2}{\eta_1 \eta_2} \tag{2.19}$$

$$K_3 = \frac{\eta_5^2}{\eta_2} \tag{2.20}$$

The equilibrium constants K_r in terms of mole numbers are related to the equilibrium constants K_{p_r} in terms of partial pressures by the following relations,

$$K_r = K_{p_r} \left(\frac{p_0}{\rho \mathcal{R} T} \right)^{\Delta \mathcal{N}_r}$$

where $\Delta \mathcal{N}_r = \sum_{i=1}^{6} (\nu_i^{(r)''} - \nu_i^{(r)'})$ is the increase of the number of moles due to reaction r. The equilibrium constants K_{p_r} are functions of temperature only and are related to the species properties through the Gibbs free energy in the standard state ($i.e., p_0 = 101325 N/m^2$), such as

$$K_{p_r} = \exp\left(-\frac{\Delta \hat{g}_r^0}{\mathcal{R} T} \right) \tag{2.21}$$

where

$$\Delta \hat{g}_r^0 = \sum_{i=1}^{6} (\nu_i^{(r)''} - \nu_i^{(r)'}) \hat{g}_i^0$$

For reactions (1) to (3), we thus have,

$$K_1 = \frac{p_0}{\rho \mathcal{R} T} \exp\left(\frac{\hat{g}_1^0}{\mathcal{R} T} - \frac{2 \hat{g}_3^0}{\mathcal{R} T} \right) \tag{2.22}$$

$$K_2 = \exp\left(\frac{\hat{g}_1^0}{\mathcal{R}T} + \frac{\hat{g}_2^0}{\mathcal{R}T} - \frac{2\hat{g}_4^0}{\mathcal{R}T}\right) \tag{2.23}$$

$$K_3 = \frac{p_0}{\rho\mathcal{R}T}\exp\left(\frac{\hat{g}_2^0}{\mathcal{R}T} - \frac{2\hat{g}_5^0}{\mathcal{R}T}\right) \tag{2.24}$$

Equations (2.18), (2.19), and (2.20) provide a set of three independent relations for the six unknown specific concentrations η_i. The three remaining equations follow from the element conservation laws which require the total number of moles of each element to remain constant. Since Argon is considered as an inert species, its specific concentration η_6 remains constant at the value η_{Ar} corresponding to low temperature. The element conservation laws for oxygen and nitrogen provide two further equations relating the unknown values of η_i to the low temperature concentrations η_N and η_O,

$$2\eta_1 + \eta_3 + \eta_4 = \eta_O \tag{2.25}$$

$$2\eta_2 + \eta_4 + \eta_5 = \eta_N \tag{2.26}$$

$$\eta_6 = \eta_{Ar} \tag{2.27}$$

In principle, it is possible to combine equations (2.18), (2.19), (2.20) and (2.25), (2.26), (2.27) into a single equation in one unknown, so that the full set of equations can be solved, leading to the complete determination of the equilibrium species concentrations at any given temperature and density. However, due to the non-linearity of certain equations, we will sometimes resort to some numerical procedures for solving these equations.

2.6 Low Temperature Considerations

When solving the equilibrium equations, numerical problems such as division-by-zero errors can occur under certain conditions of temperature and density.This problem may be encountered especially at low temperatures where the dissociation of oxygen or nitrogen has not begun yet, so that certain species are present in very small quantities. In order to avoid such problems, we can define an onset temperature for each dissociation reaction, so that we can assume that below certain temperatures the dissociation reactions can be ignored. Consequently, the specific concentrations of the corresponding products of the reaction are set to zero, leading to a simpler resolution of the equilibrium equations.

For the range of temperature being considered here, three cases are to be considered, which are defined in the following sections. Table 2.2 gives a summary of these three models, with the corresponding temperature ranges, the chemical

	Model I	Model II	Model III
Temperature range	$T < 530K$ $\ln K_{p_1} < -100$	$530K < T < 1000K$ $\ln K_{p_3} < -100$	$T > 1000K$
chemical reactions	$N_2 + O_2 \rightleftharpoons 2NO$	$O_2 + X \rightleftharpoons 2O + X$ $N_2 + O_2 \rightleftharpoons 2NO$	$O_2 + X \rightleftharpoons 2O + X$ $N_2 + O_2 \rightleftharpoons 2NO$ $N_2 + X \rightleftharpoons 2N + X$
Major species	O_2, N_2, NO, Ar	O_2, N_2, O, NO, Ar	O_2, N_2, O, NO, N, Ar

Table 2.2: *Equilibrium Air Model*

reactions being considered, and the major species present in the mixture.

2.6.1 Model I : Low Temperatures ($T < 530K$)

We consider here the temperatures which are not high enough for significant dissociation, and therefore reactions (1) and (3) are ignored. At very low temperatures, air is therefore assumed to be a mixture of O_2, N_2, NO and Ar, so that only the reaction (2) for the formation of nitric oxide can occur. The specific concentrations for O and N are set to zero, and the remaining specific concentrations are calculated from the equilibrium equation of reaction (2).

Assumption :

$$\eta_3 = 0$$
$$\eta_5 = 0$$

Equilibrium :

$$K_2 = \frac{\eta_4^2}{\eta_1 \eta_2} \tag{2.28}$$

Nuclear conservation :

$$2\eta_1 + \eta_4 = \eta_O \tag{2.29}$$

$$2\eta_2 + \eta_4 = \eta_N \tag{2.30}$$
$$\eta_6 = \eta_{Ar} \tag{2.31}$$

Equation (2.28) to (2.31) can be combined to form a second order polynomial in η_4 which can be solved analytically. We thus obtain,

$$\eta_4 = \frac{-(\eta_O + \eta_N) + \sqrt{(\eta_O + \eta_N)^2 + (\frac{16}{K_2} - 2)\eta_O\eta_N}}{(\frac{8}{K_2} - 2)}$$
$$\eta_1 = \frac{1}{2}(\eta_O - \eta_4)$$
$$\eta_2 = \frac{1}{2}(\eta_N - \eta_4)$$
$$\eta_6 = \eta_{Ar}$$

2.6.2 Model II : Medium Temperatures ($530K < T < 1000K$)

We consider here temperatures which are high enough for oxygen dissociation but not high enough for significant nitrogen dissociation. Air is assumed to be a mixture of O_2, N_2, O, NO and Ar, and N is still considered as a trace species. The specific concentration for N is set to zero and the remaining specific concentrations are calculated by considering reactions (1) and (2).

Assumption :

$$\eta_5 = 0$$

Equilibrium :

$$K_1 = \frac{\eta_3^2}{\eta_1} \tag{2.32}$$
$$K_2 = \frac{\eta_4^2}{\eta_1\eta_2} \tag{2.33}$$

Nuclear conservation :

$$2\eta_1 + \eta_3 + \eta_4 = \eta_O \tag{2.34}$$
$$2\eta_2 + \eta_4 = \eta_N \tag{2.35}$$
$$\eta_6 = \eta_{Ar} \tag{2.36}$$
$$\tag{2.37}$$

2.6.3 Model III : High Temperatures ($T > 1000K$)

Here, the temperature is high enough for both oxygen and nitrogen dissociation. All the six species are present in air and all three chemical reactions are to be considered.

Equilibrium :

$$K_1 = \frac{\eta_3^2}{\eta_1} \tag{2.38}$$

$$K_2 = \frac{\eta_4^2}{\eta_1 \eta_2} \tag{2.39}$$

$$K_3 = \frac{\eta_5^2}{\eta_2} \tag{2.40}$$

Nuclear conservation :

$$2\eta_1 + \eta_3 + \eta_4 = \eta_O \tag{2.41}$$

$$2\eta_2 + \eta_4 + \eta_5 = \eta_N \tag{2.42}$$

$$\eta_6 = \eta_{Ar} \tag{2.43}$$

$$\tag{2.44}$$

2.6.4 Solution of the Equilibrium Equations

Unlike the low temperature model where the equilibrium equations can be solved analytically, we have to resort to an iterative process for solving the equations for the medium and high temperature models. The method employed in solving the problem is described as follows for the general case of high temperatures, the solution for the medium temperature model simply follows by stating η_5 to zero.

Equations (2.38), (2.39), and (2.40) yield

$$\eta_1 = \frac{\eta_3^2}{K_1}$$

$$\eta_2 = \frac{\eta_5^2}{K_3}$$

$$\eta_4 = \eta_3 \eta_5 K_e$$

where

$$K_e = \sqrt{\frac{K_2}{K_1 K_3}}$$

Substituting the above into equation (2.41) and solving for η_5 in terms of η_3 gives

$$\eta_5 = \left(\eta_O - \frac{2\eta_3^2}{K_1} - \eta_3\right)\frac{1}{\eta_3 K_e}$$

Finally, substituting η_2, η_4 and η_5 in equation (2.42) and simplifying, we obtain the following fourth order equation with η_3 as the unknown,

$$\sum_{i=0}^{4} b^i \eta_3^i = 0 \tag{2.45}$$

where

$$\begin{aligned}
b_0 &= 2K_1\eta_O^2 \\
b_1 &= (-4 + K_3K_e)K_1\eta_O \\
b_2 &= -8\eta_O + 2K_1 + (\eta_O - \eta_N)K_2 - K_1K_3K_e \\
b_3 &= 8 - K_2 - 2K_3K_e \\
b_4 &= (8 - 2K_2)/K_1
\end{aligned}$$

The equation for η_3 is solved by the Newton iteration scheme. The initial value for the unknown η_3 is determined by assuming that η_5 is equal to 0 and that η_2 can be approximated by $\eta_2 = \eta_N/2$. The approximate value for η_4 is obtained by combining equation (2.38) and (2.39),

$$\eta_4 = \eta_3\sqrt{\frac{\eta_N K_2}{2K_1}}$$

Substituting the expression (2.38) for η_1 and the above expression for η_4 into equation (2.41) leads to the following equation in η_3,

$$\frac{2\eta_3^2}{K_1} + \eta_3 + \eta_3\sqrt{\frac{\eta_N K_2}{2K_1}} = \eta_O$$

The solution of this equation therefore gives the initial value for η_3, that is

$$\eta_3^{(0)} = \sqrt{\left(\frac{K_1}{4} + \sqrt{\frac{\eta_N K_1 K_2}{32}}\right)^2 + \frac{\eta_O K_1}{2}} - \left(\frac{K_1}{4} + \sqrt{\frac{\eta_N K_1 K_2}{32}}\right)$$

Equation (2.45) is solved by using the following iterative algorithm,

$$
\begin{aligned}
F^{(i)} &= \sum_{n=0}^{4} b_n \eta_3^{(i)^n} \\
F'^{(i)} &= \sum_{n=1}^{4} n b_n \eta_3^{(i)^{n-1}} \\
\eta_3^{(i+1)} &= \eta_3^{(i)} - \frac{F^{(i)}}{F'^{(i)}}
\end{aligned}
$$

Once a converged solution is obtained for η_3, the remaining specific concentrations are calculated by the following relations.

Model II - Medium Temperatures

$$
\begin{aligned}
\eta_5 &= 0 \\
\eta_4 &= \eta_O - \eta_3 - \frac{2\eta_3^2}{K_1} \\
\eta_2 &= \frac{1}{2}(\eta_N - \eta_4) \\
\eta_1 &= \frac{1}{2}(\eta_O - \eta_3 - \eta_4) \\
\eta_6 &= \eta_{Ar}
\end{aligned}
$$

Model III - High Temperatures

$$
\begin{aligned}
\eta_5 &= \frac{\eta_O - \eta_3 - \frac{2\eta_3^2}{K_1}}{K_e \eta_3} \\
\eta_4 &= K_e \eta_3 \eta_5 \\
\eta_2 &= \frac{1}{2}(\eta_N - \eta_4 - \eta_5) \\
\eta_1 &= \frac{1}{2}(\eta_O - \eta_3 - \eta_4) \\
\eta_6 &= \eta_{Ar}
\end{aligned}
$$

2.7 Thermodynamic Properties of the Mixture

The thermodynamic properties of the gas mixture are calculated from the thermodynamic properties of the pure species and the equilibrium species concentrations.

The pressure p of the mixture is given by the Dalton's Law as the sum of the partial pressures of the various species. Each species behaves like a perfect gas, so that,

$$p = \sum_{i=1}^{6} p_i = \sum_{i=1}^{6} \eta_i \rho \mathcal{R} T = \eta \rho \mathcal{R} T$$

where η is the specific concentration of the mixture, and is given by

$$\eta = \sum_{i=1}^{6} \eta_i$$

The partial pressure of each species can be expressed in terms of the mixture pressure as

$$p_i = \frac{\eta_i}{\eta} p$$

The specific enthalpy of the mixture in terms of the molar enthalpies of the constituent species $\hat{h}_i^0$ and their specific concentrations η_i is given by

$$h = \sum_{i=1}^{6} \eta_i \hat{h}_i^0$$

Similarly, the specific internal energy of the gas mixture is the sum of the energies of all species,

$$e = \sum_{i=1}^{6} \eta_i \hat{e}_i^0 = \sum_{i=1}^{6} \eta_i (\hat{h}_i^0 - \mathcal{R} T) = h - \eta \mathcal{R} T \tag{2.46}$$

The evaluation of the entropy of the mixture requires more care, since the specific entropy of a perfect gas depends on pressure as well as temperature, and the partial pressure is different for each individual species in the gas mixture. However, the specific entropy of the mixture can be expressed as the sum of the partial entropies, each calculated in terms of the appropriate partial pressure, that is,

$$s = \sum_{i=1}^{6} \eta_i \hat{s}_i^0 (T, p_i) \tag{2.47}$$

According to the second law of thermodynamics, the differential form of the entropy of a thermally perfect gas is given by

$$T ds_i = dh_i - \frac{dp_i}{\rho} \tag{2.48}$$

This expression can be rewritten in terms of the specific quantities measured per mole of species (i.e., molar quantities). It becomes

$$d\hat{s}_i = \hat{c}_{p_i}\frac{dT}{T} - \mathcal{R}\frac{dp_i}{p_i} \tag{2.49}$$

Integrating this expression gives

$$\hat{s}_i = \int_{T_0}^{T} \hat{c}_{p_i}\frac{dT}{T} - \mathcal{R}\ln\left(\frac{p_i}{p_0}\right) + \hat{s}_i^{T_0}$$

where $\hat{s}_i^{T_0}$ is the value of $\hat{s}_i$ at the reference temperature T_0 and reference pressure p_0. According to equation (2.13), the above expression becomes

$$\hat{s}_i = \hat{s}_i^0 - \mathcal{R}\ln\left(\frac{p_i}{p_0}\right) \tag{2.50}$$

Substituting expression (2.50) into equation (2.47) gives

$$s = \sum_{i=1}^{6}\eta_i\left(\hat{s}_i^0 - \mathcal{R}\ln\left(\frac{p_i}{p_0}\right)\right)$$

or, in terms of the pressure p of the mixture,

$$s = \sum_{i=1}^{6}\eta_i\left(\hat{s}_i^0 - \mathcal{R}\ln\left(\frac{p_i}{p}\right) - \mathcal{R}\ln\left(\frac{p}{p_0}\right)\right)$$

Hence,

$$s = -\eta\mathcal{R}\ln\left(\frac{p}{p_0}\right) + \sum_{i=1}^{6}\eta_i\left(\hat{s}_i^0 - \mathcal{R}\ln\left(\frac{\eta_i}{\eta}\right)\right)$$

The Gibbs free energy can also be calculated for the mixture as

$$g = h - Ts$$

2.8 Calculation of Thermodynamic Derivatives

2.8.1 The Pressure Derivatives χ and κ

For an equilibrium chemically reacting gas, the two equations of state can be formulated as

$$\begin{aligned} p &= p(\rho, T) \\ h &= h(\rho, T) \end{aligned}$$

so that the total differentials are

$$dp = \left(\frac{\partial p}{\partial \rho}\right)_T d\rho + \left(\frac{\partial p}{\partial T}\right)_\rho dT \tag{2.51}$$

$$dh = \left(\frac{\partial h}{\partial \rho}\right)_T d\rho + \left(\frac{\partial h}{\partial T}\right)_\rho dT \tag{2.52}$$

Expressing dT in terms of dh and $d\rho$ in equation (2.52), and substituting into equation (2.51) gives

$$dp = \left(\frac{\partial p}{\partial \rho}\right)_T d\rho + \frac{\left(\frac{\partial p}{\partial T}\right)_\rho}{\left(\frac{\partial h}{\partial T}\right)_\rho}\left[dh - \left(\frac{\partial h}{\partial \rho}\right)_T d\rho\right] \tag{2.53}$$

Specific enthalpy and internal energy per unit volume are related by

$$h = \frac{1}{\rho}(p + \epsilon)$$

so that,

$$dh = \frac{1}{\rho}(dp + d\epsilon - h d\rho)$$

Substituting dh into equation (2.53) leads to

$$dp = \frac{\left(\frac{\partial p}{\partial \rho}\right)_T \left(\frac{\partial h}{\partial T}\right)_\rho - \left(\frac{\partial p}{\partial T}\right)_\rho \left[\frac{h}{\rho} + \left(\frac{\partial h}{\partial \rho}\right)_T\right]}{\left(\frac{\partial h}{\partial T}\right)_\rho - \frac{1}{\rho}\left(\frac{\partial p}{\partial T}\right)_\rho} d\rho + \frac{\frac{1}{\rho}\left(\frac{\partial p}{\partial T}\right)_\rho}{\left(\frac{\partial h}{\partial T}\right)_\rho - \frac{1}{\rho}\left(\frac{\partial p}{\partial T}\right)_\rho} d\epsilon \tag{2.54}$$

The differential of p can be written as

$$dp = \chi d\rho + \kappa d\epsilon$$

where χ and κ are defined as the partial derivatives of the pressure with respect to density and internal energy per unit volume, respectively. By identification, we thus obtain,

$$\chi = \frac{\left(\frac{\partial p}{\partial \rho}\right)_T \left(\frac{\partial h}{\partial T}\right)_\rho - \left(\frac{\partial p}{\partial T}\right)_\rho \left[\frac{h}{\rho} + \left(\frac{\partial h}{\partial \rho}\right)_T\right]}{\left(\frac{\partial h}{\partial T}\right)_\rho - \frac{1}{\rho}\left(\frac{\partial p}{\partial T}\right)_\rho} \tag{2.55}$$

$$\kappa = \frac{\frac{1}{\rho}\left(\frac{\partial p}{\partial T}\right)_\rho}{\left(\frac{\partial h}{\partial T}\right)_\rho - \frac{1}{\rho}\left(\frac{\partial p}{\partial T}\right)_\rho} \tag{2.56}$$

Equations (2.55) and (2.56) represent the general formulation for the two pressure derivatives χ and κ. These can be further developed by considering particular formulations of the equations of state. For a mixture of thermally perfect gas, we have

$$\begin{aligned} p &= \rho \mathcal{R} T \sum_{i=1}^{6} \eta_i \\ h &= h[T, \eta_i(\rho, T)] \end{aligned}$$

which gives,

$$\left(\frac{\partial p}{\partial \rho}\right)_T = \mathcal{R}T \left[\eta + \rho \sum_{i=1}^{6} \left(\frac{\partial \eta_i}{\partial \rho}\right)_T\right] \tag{2.57}$$

$$\left(\frac{\partial p}{\partial T}\right)_\rho = \rho \mathcal{R} \left[\eta + T \sum_{i=1}^{6} \left(\frac{\partial \eta_i}{\partial T}\right)_\rho\right] \tag{2.58}$$

$$\left(\frac{\partial h}{\partial \rho}\right)_T = \sum_{i=1}^{6} \left(\frac{\partial h}{\partial \eta_i}\right)_T \left(\frac{\partial \eta_i}{\partial \rho}\right)_T \tag{2.59}$$

$$\left(\frac{\partial h}{\partial T}\right)_\rho = \left(\frac{\partial h}{\partial T}\right)_{\eta_i} + \sum_{i=1}^{6} \left(\frac{\partial h}{\partial \eta_i}\right)_T \left(\frac{\partial \eta_i}{\partial T}\right)_\rho \tag{2.60}$$

For a perfect gas,

$$\begin{aligned} p &= \eta \rho \mathcal{R} T \\ h &= c_p T \end{aligned}$$

Equations (2.55) and (2.56) reduce to

$$\begin{aligned} \chi &= 0 \\ \kappa &= \gamma - 1 \end{aligned}$$

As can be seen in equations (2.55) to (2.60), the complete determination of χ and κ require the formulation of the thermodynamic derivatives $(\partial h/\partial T)_{\eta_i}$, $(\partial h/\partial \eta_i)_T$, $(\partial \eta_i/\partial T)_\rho$, and $(\partial \eta_i/\partial \rho)_T$. These derivatives are obtained from the equilibrium equations, and therefore need to be calculated within the same procedure used for solving the equilibrium equations.

2.8.2 The Enthalpy Derivatives

The specific enthalpy of the mixture has already been defined as the sum of the molar enthapies $\hat{h}_i^0$ of the component species, which in turn are given by

polynomial curve fits (see section 2.4.2), so that

$$h = \sum_{i=1}^{6} \eta_i \hat{h}_i^0(T) = \mathcal{R} \sum_{i=1}^{6} \eta_i \left(\sum_{j=1}^{5} \frac{a_{i,j} T^j}{j} + a_{i,6} \right)$$

and

$$\begin{aligned} \left(\frac{\partial h}{\partial T} \right)_{\eta_i} &= \mathcal{R} \sum_{i=1}^{6} \eta_i \left(\sum_{j=1}^{5} a_{i,j} T^{j-1} \right) \\ \left(\frac{\partial h}{\partial \eta_i} \right)_T &= \mathcal{R} \left(\sum_{j=1}^{5} \frac{a_{i,j} T^j}{j} + a_{i,6} \right) \end{aligned}$$

2.8.3 The Specific Concentration Derivatives

Calculation of the derivatives $(\partial \eta_i / \partial T)_\rho$ and $(\partial \eta_i / \partial \rho)_T$ are obtained by considering the differential forms of the equilibrium equations describing each of the three models considered in section 2.6.

Low Temperatures

In the low temperature case, where η_i are explicit functions of the equilibrium coefficient K_2, the derivatives are given by the differential forms of equations (2.28) to (2.30), leading to

$$\begin{aligned} \delta\eta_4 &= \frac{2\eta_1\eta_2}{4\eta_4 + K_2(\eta_1 + \eta_2)} \delta K_2 \\ \delta\eta_1 &= -\frac{1}{2}\delta\eta_4 \\ \delta\eta_2 &= -\frac{1}{2}\delta\eta_4 \\ \delta\eta_3 &= 0 \\ \delta\eta_5 &= 0 \end{aligned}$$

where δ represents either $(\partial/\partial T)_\rho$ or $(\partial/\partial\rho)_T$.

Medium Temperatures

The medium temperature model is governed by equations (2.32) to (2.35). Differentiating these equations leads to the following set of linear equations in $\delta\eta_i$,

$$-K_1\delta\eta_1 + 2\eta_3\delta\eta_3 = \eta_1\delta K_1$$

$$
\begin{aligned}
-\eta_2 K_2 \delta\eta_1 - \eta_1 K_2 \delta\eta_2 + 2\eta_4 \delta\eta_4 &= \eta_1 \eta_2 \delta K_2 \\
2\delta\eta_1 + \delta\eta_3 + \delta\eta_4 &= 0 \\
2\delta\eta_2 + \delta\eta_4 &= 0
\end{aligned}
$$

which can be solved analytically, leading to

$$
\begin{aligned}
\delta\eta_4 &= \frac{2\eta_1\eta_2\delta K_2 - \frac{2\eta_1\eta_2 K_2}{4\eta_3 + K_1}\delta K_1}{4\eta_4 + K_2(\eta_1 + \eta_2) - \frac{\eta_2}{4\eta_3 + K_1}} \\
\delta\eta_3 &= \frac{2\eta_1\delta K_1 - K_1\delta\eta_4}{4\eta_3 + K_1} \\
\delta\eta_1 &= -\frac{1}{2}(\delta\eta_3 + \delta\eta_4) \\
\delta\eta_2 &= -\frac{1}{2}\delta\eta_4 \\
\delta\eta_5 &= 0
\end{aligned}
$$

High Temperatures

Equation (2.38) to (2.42) representing the medium temperature model can be written in differential form as

$$
\begin{aligned}
-K_1\delta\eta_1 + 2\eta_3\delta\eta_3 &= \eta_1\delta K_1 \\
-\eta_2 K_2\delta\eta_1 - \eta_1 K_2\delta\eta_2 + 2\eta_4\delta\eta_4 &= \eta_1\eta_2\delta K_2 \\
-K_3\delta\eta_2 + 2\eta_5\delta\eta_5 &= \eta_2\delta K_3 \\
2\delta\eta_1 + \delta\eta_3 + \delta\eta_4 &= 0 \\
2\delta\eta_2 + \delta\eta_4 + \delta\eta_5 &= 0
\end{aligned}
$$

Although being more complicated, the resolution of this set of equations can still be performed analytically, leading to

$$
\begin{aligned}
\delta\eta_3 &= \frac{1}{A}\left(\left(-4\eta_1\eta_4 - \eta_1\eta_2 K_2 - \frac{4\eta_1^2\eta_5 K_2}{4\eta_5 + K_3}\right)\delta K_1 + (\eta_1\eta_2 K_1)\delta K_2 - \left(\frac{\eta_1\eta_2 K_1 K_2}{4\eta_5 + K_3}\right)\delta K_3\right) \\
\delta\eta_1 &= \frac{2\eta_3}{K_1}\delta\eta_3 - \frac{\eta_1}{K_1}\delta K_1 \\
\delta\eta_2 &= \frac{2\eta_5(4\eta_3 + K_1)}{K_1(4\eta_5 + K_3)}\delta\eta_3 - \frac{4\eta_1\eta_5}{K_1(4\eta_5 + K_3)}\delta K_1 - \frac{\eta_2}{4\eta_5 + K_3}\delta K_3 \\
\delta\eta_4 &= -\frac{4\eta_3 + K_1}{K_1}\delta\eta_3 + \frac{2\eta_1}{K_1}\delta K_1 \\
\delta\eta_5 &= \frac{K_3(4\eta_3 + K_1)}{K_1(4\eta_5 + K_3)}\delta\eta_3 - \frac{2\eta_1 K_3}{K_1(4\eta_5 + K_3)}\delta K_1 + \frac{2\eta_2}{4\eta_5 + K_3}\delta K_3
\end{aligned}
$$

where

$$A = -2\eta_4(4\eta_3 + K_1) - 2\eta_2\eta_3 K_2 - \frac{2\eta_1\eta_5 K_2(4\eta_3 + K_1)}{4\eta_5 + K_3}$$

2.8.4 The Equilibrium Constant Derivatives

The chemical derivatives for η_i can now be completely determined by calculating the derivatives of the equilibrium constants K_r. The three equilibrium constants for the three chemical reactions being considred here are given by equations (2.22), (2.23), and (2.24) in terms of the Gibbs free energies $\hat{g}_i^0$ of the component species. Since the Gibbs free energies $\hat{g}_i^0$ are functions of temperature only, their density derivatives are all zero. Using equations (2.12) to (2.14), the Gibbs free energy can be written as

$$\begin{aligned}\frac{\hat{g}_i^0}{\mathcal{R}T} &= \frac{\hat{h}_i^0}{\mathcal{R}T} - \frac{\hat{s}_i^0}{\mathcal{R}} \\ &= \frac{1}{\mathcal{R}T}\int_T^{T_0} \hat{c}_{p_i}(T)dT + \frac{\hat{h}_i^{T_0}}{\mathcal{R}T} + \frac{1}{\mathcal{R}}\int_T^{T_0} \frac{\hat{c}_{p_i}(T)}{T}dT + \frac{\hat{s}_i^{T_0}}{\mathcal{R}}\end{aligned}$$

Differentiating these equations with respect to temperature T leads to

$$\begin{aligned}\frac{\partial}{\partial T}\left(\frac{\hat{g}_i^0}{\mathcal{R}T}\right) &= -\frac{1}{\mathcal{R}T^2}\int_T^{T_0} \hat{c}_{p_i}(T)dT + \frac{\hat{c}_{p_i}}{\mathcal{R}T} - \frac{\hat{h}_i^{T_0}}{\mathcal{R}T^2} - \frac{\hat{c}_{p_i}}{\mathcal{R}T} \\ &= -\frac{1}{\mathcal{R}T^2}\left(\int_T^{T_0} \hat{c}_{p_i}(T)dT + \hat{h}_i^{T_0}\right)\end{aligned}$$

so that,

$$\frac{\partial}{\partial T}\left(\frac{\hat{g}_i^0}{\mathcal{R}T}\right) = -\frac{\hat{h}_i^0}{\mathcal{R}T^2} \tag{2.61}$$

Using equation (2.61) for each of the five active species, and differentiating equations (2.22) to (2.24) with respect to temperature and density gives,

$$\begin{aligned}\left(\frac{\partial K_1}{\partial T}\right)_\rho &= \frac{K_1}{T}\left(\frac{2\hat{h}_3^0}{\mathcal{R}T} - \frac{\hat{h}_1^0}{\mathcal{R}T} - 1\right) \\ \left(\frac{\partial K_2}{\partial T}\right)_\rho &= \frac{K_2}{T}\left(\frac{2\hat{h}_4^0}{\mathcal{R}T} - \frac{\hat{h}_2^0}{\mathcal{R}T} - \frac{\hat{h}_1^0}{\mathcal{R}T}\right) \\ \left(\frac{\partial K_3}{\partial T}\right)_\rho &= \frac{K_3}{T}\left(\frac{2\hat{h}_5^0}{\mathcal{R}T} - \frac{\hat{h}_2^0}{\mathcal{R}T} - 1\right)\end{aligned}$$

$$\left(\frac{\partial K_1}{\partial \rho}\right)_T = -\frac{K_1}{\rho}$$
$$\left(\frac{\partial K_2}{\partial \rho}\right)_T = 0$$
$$\left(\frac{\partial K_3}{\partial \rho}\right)_T = -\frac{K_3}{\rho}$$

All the chemical and thermodynamic derivatives required in equations (2.55) and (2.56) for the computation of χ and κ have been calculated, and it is therefore possible to compute the equilibrium speed of sound as,

$$c_e = \sqrt{\chi + \kappa h}$$

2.8.5 The Energy Derivatives

Although the energy derivatives are not explicitly required for the resolution of the equilibrium equation, these have to be calculated for the inversion of the equation of state, which will be discussed below.

The internal energy of the mixture has already been expressed as a function of temperature and chemical composition of the mixture, as

$$e = e(T, \eta_i), \qquad i = 1, 2, ..., 6$$

The differential of e therefore reads

$$de = \left(\frac{\partial e}{\partial T}\right)_{\eta_i} dT + \sum_{i=1}^{6} \left(\frac{\partial e}{\partial \eta_i}\right)_{T,\eta_j} d\eta_i \tag{2.62}$$

Furthermore, the equilibrium specific concentrations are functions of temperature and density,

$$\eta_i = \eta_i(\rho, T), \qquad i = 1, 2, ..., 6$$

so that,

$$d\eta_i = \left(\frac{\partial \eta_i}{\partial \rho}\right)_T d\rho + \left(\frac{\partial \eta_i}{\partial T}\right)_\rho dT$$

Since the energy derivative is evaluated at constant density, equation (2.62) becomes

$$de = \left(\frac{\partial e}{\partial T}\right)_{\eta_i} dT + \sum_{i=1}^{6} \left(\frac{\partial e}{\partial \eta_i}\right)_{T,\eta_j} \left(\frac{\partial \eta_i}{\partial T}\right)_\rho dT$$

and therefore,

$$\left(\frac{\partial e}{\partial T}\right)_{\rho} = \left(\frac{\partial e}{\partial T}\right)_{\eta_i} + \sum_{i=1}^{6} \left(\frac{\partial e}{\partial \eta_i}\right)_{T,\eta_j} \left(\frac{\partial \eta_i}{\partial T}\right)_{\rho} \tag{2.63}$$

Refering to equation (2.46), the specific internal energy is related to specific enthalpy and temperature through

$$e = h - \eta \mathcal{R} T$$

and the energy derivatives can therefore be expressed in terms of the enthalpy derivatives as,

$$\begin{aligned} \left(\frac{\partial e}{\partial T}\right)_{\eta_i} &= \left(\frac{\partial h}{\partial T}\right)_{\eta_i} - \eta \mathcal{R} \\ \left(\frac{\partial e}{\partial \eta_i}\right)_{T,\eta_j} &= \left(\frac{\partial h}{\partial \eta_i}\right)_{T,\eta_j} - \mathcal{R}T \left(\frac{\partial \eta}{\partial \eta_i}\right)_{T} = \left(\frac{\partial h}{\partial \eta_i}\right)_{T,\eta_j} - \mathcal{R}T \end{aligned}$$

Replacing the two above derivatives into equation (2.63) gives the following expression for the energy derivatives required for the inversion of the equation of state. This reads,

$$\left(\frac{\partial e}{\partial T}\right)_{\rho} = \left(\frac{\partial h}{\partial T}\right)_{\eta_i} - \eta \mathcal{R} + \sum_{i=1}^{6} \left[\left(\frac{\partial h}{\partial \eta_i}\right)_{T,\eta_j} - \mathcal{R}T \right] \left(\frac{\partial \eta_i}{\partial T}\right)_{\rho} \tag{2.64}$$

Chapter 3

The Transport Properties for High Temperature Air

3.1 The Transport Phenomena

The essence of molecular transport phenomena in a gas is the random motion of atoms and molecules. When a particle (atom or molecule) moves from one location to another in space, it carries with it a certain momentum, energy and mass associated with the particle itself. Part of this momentum, energy, and mass is transferred to other particles through intermolecular collisions, giving rise to the transport phenomena of viscosity, heat conduction, and diffusion, respectively.

The diffusion fluxes are related to the gradient of some macroscopic properties through the different transport coefficients, namely viscosity, thermal conductivity and diffusion coefficient. Contrary to the macroscopic properties, such as pressure, density, temperature, or energy, which are static, equilibrium properties, the transport coefficients μ, k, $\mathcal{D}_{AB}$ are all dynamic, non-equilibrium on a macro-scale, and are ordinarily obtained from kinetic theory.

Mass diffusion arises from chemical imbalance. If the gas remains in chemical equilibrium, mass diffusion is continuously balanced by chemical reactions, and the diffusion process does not need to be considered. Therefore, within the frame of a chemical equilibrium air model, only viscosity and thermal conduction are taken into account for modelling the transport properties of the gas.

Simple correlations for the transport properties of high temperature air are hard to find in the literature. Nevertheless, improved curve fits for the transport properties of equilibrium air have been developed by Srinivasan and Tannehill [18] but are based on a nine species air model, including ionization, and are therefore inconsistent with the six species air model employed here. The most efficient

Species	a_{μ_i}	b_{μ_i}	c_{μ_i}
O_2	0.0449290	-0.0826158	-11.504533
N_2	0.0268142	0.3177838	-13.618136
O	0.0208144	0.4294404	-13.905725
NO	0.0436378	-0.0335511	-11.879328
N	0.0115572	0.6031679	-14.735335

Table 3.1: *Curve fit coefficients for species viscosities*

technique consistent with the present model is therefore to use curve fits for the species transport properties and to estimate the mixture transport coefficients by means of mixture rules such as those developed by Wilke and Cheung et. al.

3.2 Viscosity Coefficient of Pure Species

The results of simple kinetic theory show that viscosity and thermal conductivities of pure gases at low pressure depend only on temperature. Calculation of the transport coefficients can be obtained from a sophisticated kinetic theory treatment by taking into account the relative motion of the molecules within an intermolecular force field. However, poor agreements are generally obtained unless a high order of approximation is used. It is then possible to use curve fits in one variable (i.e., as a function of T) to determine these coefficients in the same fashion as for the species thermodynamic properties. Such a technique has been adopted by Blottner and has been applied to CFD codes by different authors with success.

The viscosity of each species is therefore given according to the Blottner's [4, 5] model as

$$\mu_i = \exp[(a_{\mu_i} \ln T + b_{\mu_i}) \ln T + c_{\mu_i}] \tag{3.1}$$

where μ_i is given in kg/m/s. The constants a_{μ_i}, b_{μ_i}, c_{μ_i} are given in table 3.1. This model provides good results up to 10000 K, which is sufficient for the regions where the effects of viscosity are important.

Figure (A.8) gives the variations of the species viscosities μ_i as a function of T for the five active species present in the equilibrium air model.

3.3 Thermal Conductivity of Pure Species

Conduction of heat is due to the transport of energy by molecular motion. Referring to simple kinetic theory, the thermal conductivity of a monoatomic gas can be written in first approximation as

$$k = \frac{15}{4}\mu R \tag{3.2}$$

One can then define the associated Prandtl number by

$$Pr = \frac{\mu c_p}{k} = \frac{4}{15}\frac{c_p}{R} \tag{3.3}$$

where R is the specific gas constant, and c_p is the specific heat at constant pressure, and both are expressed in J/kg/K. For monoatomic molecules, $c_p = 5/2R$, and equation (3.3) gives $Pr = 2/3$, which is a good representation for such monoatomic gases at low pressure and low temperature. For molecules containing more than one atom, and where the energy is stored under several forms other than translational, the value of c_p is larger than for monoatomic gases, and the model described by equations (3.2) and (3.3) stops to be valid. For diatomic molecules, for which $c_p = 7/2R$, the Prandtl number obtained by equation (3.3) is 0.93, which is far from the usual value of 0.725.

Proper allowance for the distribution of energy between the several modes requires knowledge of the transition probabilities for interchange between them, especially for the transition between the translational and the other degrees of freedom. The Eucken allowance for the internal energy forms is based on the splitting of molecular energy into two components, the first one being associated with the energy of the translational motion, similar to that for a monoatomic gas, and the second one being associated with the internal structure. This may be developed simply as follows [16],

$$k_i = \frac{\mu_i}{\mathcal{M}_i}(\hat{c}_{v_i} + \frac{9}{4}\mathcal{R})$$

where μ_i is the species viscosity calculated by equation (3.1), $\mathcal{M}_i$ is the molecular weight (kg/mol), $\hat{c}_{v_i}$ is the heat capacity per mole at constant pressure (J/mol/K), and $\mathcal{R}$=8.3144 J/mol/K is the universal gas constant.

Figure (A.9) gives the variations of the k_i as a function of T for the five active species present in the equilibrium air model.

3.4 Viscosity of a Gas Mixture

For perfect gas calculations, the most commonly used relation is Sutherland's law, which reads

$$\mu = \mu_0 \sqrt{\frac{T}{T_0}} \frac{1 + S/T_0}{1 + S/T}$$

where T_0 and μ_0 are the reference temperature and reference viscosity, respectively (for example, $\mu_0 = 1.711 \times 10^{-5} Pl$ for $T_0 = 273.15K$), and $S = 110.4K$ is Sutherland's constant. Sutherland's law provides a reliable model for temperatures below 4000K, but may lead to errors larger than 10% for higher temperatures. More reliable models need therefore to be employed in order to calculate the viscosity coefficient for high temperature gases.

The extension of the modern molecular theory to describe the viscosity of non polar gas mixture at low pressure has been summarized by Hirshfelder et. al, but leads to quite complicated relations. Less complex, although less accurate, relations are given by Wilke [3, 5], who has proposed a general equation for viscosity as a function of molecular weights and viscosities of the pure components of the mixture. This reads,

$$\mu = \sum_{i=1}^{n} \frac{\mu_i}{1 + \sum_{j=1, j \neq i}^{n} \left(\frac{X_j}{X_i}\right) \Phi_{ij}} \tag{3.4}$$

with

$$\Phi_{ij} = \frac{1}{\sqrt{8}} \left(1 + \frac{\mathcal{M}_i}{\mathcal{M}_j}\right)^{-1/2} \left[1 + \left(\frac{\mu_i}{\mu_j}\right)^{1/2} \left(\frac{\mathcal{M}_j}{\mathcal{M}_i}\right)^{1/4}\right]^2 \tag{3.5}$$

where μ is the viscosity coefficient of the mixture, μ_i is the viscosity coefficient of species i, $\mathcal{M}_i$ is the molecular weight of species i, and X_i is the mole fraction of species i.

Figures (A.10) and (A.11) give variations of μ as a function of e and T, respectively, with ρ as a parameter. The reference values μ_0, ρ_0, and e_0 are $\mu_0 = 1.748583 \times 10^{-5} Pl$, $\rho_0 = 1.243 kg/m^3$, and $e_0 = 78408.4 J/kg$.

3.5 Thermal Conductivity of a Gas Mixture

The thermal conductivity of a gas mixture is not generally a linear function of the composition of the mixture and may be greater or less than that for any of the

pure constituents [16]. Various semi-empirical relations have been developed for calculating the mixture value of k, but the most suitable is the method proposed by Cheung, Bromley and Wilke. For a gas model consisting of monoatomic and diatomic, non polar species, the thermal conductivity of each component can be split as follows,

$$\begin{aligned} k_i^* &= \left\{ \begin{array}{cc} k_i & for\ monoatomic\ gas \\ \frac{k_i}{1+0.35(\hat{c}_{v_i}/\mathcal{R}-1)} & for\ diatomic\ gas \end{array} \right\} \\ k_i^{**} &= k_i - k_i^* \end{aligned}$$

where $\hat{c}_{v_i}$ is the molar heat at constant volume, and $\mathcal{R}$ is the universal gas constant. The mixture thermal conductivity can then be obtained from the values of k_i^* and k_i^{**} of each of the chemical species by means of a mixture rule similar to equation (3.4), that is

$$k = \sum_{i=1}^{n} \frac{k_i^*}{1 + \sum_{j=1, j\neq i}^{n} \left(\frac{\mathcal{M}_{ij}}{\mathcal{M}_i}\right)^{1/8} \left(\frac{X_j}{X_i}\right) \Phi_{ij}} + \sum_{i=1}^{n} \frac{k_i^{**}}{1 + \sum_{j=1, j\neq i}^{n} \left(\frac{X_j}{X_i}\right) \Phi_{ij}}$$

with

$$\mathcal{M}_{ij} = \frac{1}{2}(\mathcal{M}_i + \mathcal{M}_j)$$

Φ_{ij} is given by equation (3.5).

Figures (A.12) and (A.13) give variations of k as a function of e and T, respectively, with ρ as a parameter. The reference values k_0, ρ_0, and e_0 are $k_0 = 1.87915 \times 10^{-2} J/m/s/K$, $\rho_0 = 1.243 kg/m^3$, and $e_0 = 78408.4 J/kg$.

3.6 The Equilibrium Prandtl Number

The Prandtl number is a dimensionless parameter proportional to the ratio of energy dissipated by friction to the energy transported by thermal conduction, and is expressed as

$$Pr = \frac{\mu c_p}{k}$$

For air at standart conditions, $Pr = 0.725$. However, since Pr is a property of the gas, its value is different for different gases, and has to be estimated through the respective values of μ, c_p and k.

In the case of non-equilibrium gas, the Prandtl number has no real significance. However, under the assumption of local chemical equilibrium, it is possible to define an "equilibrium" Prandtl number Pr_{eq} as

$$Pr_{eq} = \frac{\mu c_p}{k}$$

Figures (A.14) and (A.15) give variations of c_p and Pr_{eq} as a function of temperature with ρ as a parameter. The reference value ρ_0 is $\rho_0 = 1.243 kg/m^3$. Note that in the range of dissociation, Pr_{eq} varies between 0.6 and 0.8.

Chapter 4

The Numerical Solution of the Navier-Stokes Equations

4.1 The Conservative Form of the Equations

The unsteady Navier-Stokes equations form a mixed set of parabolic-hyperbolic partial differential equations for which no analytical solution exists. The solution of these equations can therefore be obtained only by seeking an approximate numerical solution. These equations are derived from the integral form of the general conservation laws of mass, momentum and energy, and can be expressed in various equivalent forms. However, the discretization of the non-conservative form, whereby the equations are expressed in terms of the primitive variables (ρ, u, v, p), gives rise to internal sources which can become important across discontinuities and thereby will not lead to the correct shock intensities. The conservative form of the equations is therefore essential in order to compute the correct propagation speed which will lead to the correct resolution of the discontinuities [2, 3].

The conservative form of the Navier-Stokes equations can be expressed as

$$\frac{\partial \mathbf{U}}{\partial t} + \frac{\partial \mathbf{f}}{\partial x} + \frac{\partial \mathbf{g}}{\partial y} = 0$$

where $\mathbf{U}$ is the solution vector of conserved variables and $\mathbf{f}$ and $\mathbf{g}$ are the flux vectors which can be split into inviscid and viscous components such as

$$\mathbf{f} = \mathbf{f}^I + \mathbf{f}^V$$
$$\mathbf{g} = \mathbf{g}^I + \mathbf{g}^V$$

In the general case of a two-dimensional flow, the unknown vector and the fluxes

have the following non-dimensional form,

$$\mathbf{U} = \begin{pmatrix} \rho \\ \rho u \\ \rho v \\ \rho E \end{pmatrix} \qquad \mathbf{f}^I = \begin{pmatrix} \rho u \\ \rho u^2 + p \\ \rho uv \\ \rho uH \end{pmatrix} \qquad \mathbf{g}^I = \begin{pmatrix} \rho v \\ \rho uv \\ \rho v^2 + p \\ \rho uH \end{pmatrix} \tag{4.1}$$

$$\mathbf{f}^V = \begin{pmatrix} 0 \\ -\tau_{xx} \\ -\tau_{xy} \\ -u\tau_{xx} - v\tau_{xy} + q_x \end{pmatrix} \qquad \mathbf{g}^V = \begin{pmatrix} 0 \\ -\tau_{xy} \\ -\tau_{yy} \\ -u\tau_{xy} - v\tau_{yy} + q_y \end{pmatrix} \tag{4.2}$$

where ρ, u, v, p, E and H denote the density, the two-cartesian components of the velocity, the pressure, the total specific energy and the total specific enthalpy, respectively. The stress tensor τ and the heat conduction flux q are given by

$$\begin{aligned}
\tau_{xx} &= \frac{2\mu}{3Re}\left(2\frac{\partial u}{\partial x} - \frac{\partial v}{\partial y}\right) \\
\tau_{xy} &= \frac{\mu}{Re}\left(\frac{\partial u}{\partial y} + \frac{\partial v}{\partial x}\right) \\
\tau_{yy} &= \frac{2\mu}{3Re}\left(2\frac{\partial v}{\partial y} - \frac{\partial u}{\partial x}\right) \\
q_x &= -\frac{k}{(\gamma-1)M_\infty^2 RePr}\frac{\partial T}{\partial x} \\
q_y &= -\frac{k}{(\gamma-1)M_\infty^2 RePr}\frac{\partial T}{\partial y}
\end{aligned}$$

where μ and k denote the coefficient of viscosity and the coefficient of thermal conductivity, respectively, and γ, M_∞, Re, and Pr denote the ratio of specific heats, the Mach number, the Reynolds number, and the Prandtl number associated with the free stream conditions, respectively.

4.2 The Finite Volume Method

The first step in the definition of a numerical method for solving these equations is the choice of the discretization method which allows the transformation of the differential or integral equations into an algebraic system of equations which can be linear or non-linear. This implies choosing between *finite difference*, *finite element* or *finite volume method*. Although any of these methods can be employed, the finite volume method has proven to be best suited for solving the conservation laws and for tackling the complex flows which are likely to be encountered

in modern CFD problems.

The main idea of the finite volume method is to discretize the integral formulation of the conservation laws directly in the physical space, ensuring thereby that all conservative quantities (mass, momentum, energy) will also remain conserved at the discrete level. This is an essential feature when solving flows where discontinuities are expected. Moreover, the method takes full advantage of an arbitrary mesh, where a large number of options is open for the definition of the control volumes over which the conservation laws are to be satisfied. We shall limit here our discussion to the cell centre finite volume method, where the unknowns hold at the central point of the cell, and the control volume corresponds directly to the cell.

We consider the governing equations in their integral conservation form as

$$\iint_\Omega \frac{\partial \mathbf{U}}{\partial t} d\Omega + \iint_\Omega \left(\frac{\partial \mathbf{f}}{\partial x} + \frac{\partial \mathbf{g}}{\partial y} \right) d\Omega = 0$$

Using Gauss's divergence theorem, the integral over Ω can be transformed into a line integral around its boundary $\partial\Omega$,

$$\iint_\Omega \frac{\partial \mathbf{U}}{\partial t} d\Omega + \oint_{\partial\Omega} (\bar{\bar{\mathbf{F}}} \cdot \mathbf{n}) dl = 0 \tag{4.3}$$

where $\mathbf{n}$ is the outward unit vector normal to the boundary and $\bar{\bar{\mathbf{F}}}$ is a second-order tensor defined as

$$\bar{\bar{\mathbf{F}}} = \begin{pmatrix} \mathbf{f} & \mathbf{g} \end{pmatrix}$$

For cell centre methods, the variable $\mathbf{U}$ is not necessarily attached to a fixed point inside the control volume and can be considered as an average value over the control cell. Equation (4.3) can therefore be approximated by

$$\frac{\Delta \mathbf{U}}{\Delta t} = \frac{1}{\Omega} \oint_{\partial\Omega} -\mathbf{F}_n dl \tag{4.4}$$

where $\mathbf{F}_n$ represents the normal flux and can be split into inviscid and viscous components as

$$\mathbf{F}_n = \mathbf{F}_n^I + \mathbf{F}_n^V = \begin{pmatrix} \mathbf{f}^I & \mathbf{g}^I \end{pmatrix} \cdot \mathbf{n} + \begin{pmatrix} \mathbf{f}^V & \mathbf{g}^V \end{pmatrix} \cdot \mathbf{n}$$

If we assume an average flux along each edge of the control volume, the line integral on the right hand side of equation (4.4) can be expanded as follows

$$\Delta \mathbf{U}_{i,j} = -\frac{\Delta t}{\Omega_{i,j}} \quad (\quad \mathbf{F}_{i-1/2,j} \delta l_{i-1/2,j} + \mathbf{F}_{i+1/2,j} \delta l_{i+1/2,j} + \mathbf{F}_{i,j-1/2} \delta l_{i,j-1/2} + \mathbf{F}_{i,j+1/2} \delta l_{i,j+1/2})$$

where $\mathbf{F}_{i-1/2,j}$, $\mathbf{F}_{i+1/2,j}$, $\mathbf{F}_{i,j-1/2}$, $\mathbf{F}_{i,j+1/2}$ represent the average normal flux along the edge $(i-1/2,j)$, $(i+1/2,j)$, $(i,j-1/2)$ and $(i,j+1/2)$ respectively.

The finite volume discretization method leads to a set of algebraic equations whereby the conservative fluxes have to be evaluated at the interfaces of the control volumes. Because the inviscid terms and the viscous terms are not of the same mathematical nature, the numerical treatment of the different fluxes components can be completely independent. While the viscous fluxes are always discretized by central differencing techniques, the discretization of the convective fluxes can be achieved either by central differencing or upwind differencing.

4.3 Upwind Schemes For the Euler Equations

The accuracy of a numerical solution depends to a large extent on the discretization method employed to evaluate the numerical fluxes at the cell interfaces. Although central differencing is the most straight forward technique to apply, this kind of discretization does not suit very well to discontinuous flows. Most of the central difference schemes suffer from a lack of dissipation, and give rise to large oscillations around discontinuities. All centrally based schemes try to represent derivatives near shock waves using information on both sides of the shock, and therefore do not distinguish upstream from downstream influences. This representation is therefore not consistent with the propagation of physical properties along characteristics, which are typical of hyperbolic equations, and consequently give rise to large oscillations in the vicinity of discontinuities. The success of centrally based schemes in capturing shock waves resides in the introduction of artificial dissipation terms which damp oscillations and prevent the appearance of expansion shock [3]. However, these additional viscous terms tend to spread shock waves over a large part of the flow region, turning them into steep gradients rather than discontinuities.

An alternative is therefore to use upwind schemes, which are based on the introduction of the physical properties of the flow equations into the discretized formulation. The basic idea behind "upwinding" is to relate the characteristic propagation properties and the differencing such as to apply directional space discretizations in accordance with the physical behaviour of inviscid flows. This approach has the great advantage of producing high resolution schemes while preventing the creation of unwanted oscillations.

The introduction of physical properties in the discretization process can be done at different levels, leading thereby to a variety of schemes referred to as as

flux vector splitting or *flux difference splitting* schemes. The first level introduces only information on the sign of the eigenvalues, whereby the flux terms are split and discretized directionally according to the sign of the associated propagation speeds. This leads to the flux vector splitting methods, among which are the Steger & Warming (1981) and Van Leer (1982) schemes.

Alternatively, introduction of the physical properties of the flow equations into the discretization formulation can be done by following the method developed by Godunov (1959), which is based on the solution of a Riemann problem at each cell interface. In Godunov's method, the conservative variables are considered as piecewise constant over the cells at each time step, and the time evolution results from the wave interaction originating at the boundaries between two adjacent cells. Hence, properties derived from the exact local solution of the Euler equations are introduced into the discretization according to the propagation direction of the wave. This family of methods is referred to as flux difference splitting. Since the solution of the Riemann problem requires the resolution of a non-linear algebraic equation which can be quite time-consuming, various approximate solvers have been developed among the most popular are Roe (1981) and Osher (1982) schemes.

In the one-dimensional case, the propagation directions can easily be identified as the characteristic lines and the propagation speeds as the eigenvalues of the flux jacobian matrix. The extension of upwind schemes to two or three dimensions can be achieved in a simple way by treating each flux component as monodimensional wave in some specific directions. For most of the finite volume methods in use, these directions are taken to be normal to the cell interfaces. Although this assumption does not necessarily coincide with the physical behaviour of the flow, it provides a relatively straightforward way of extending the monodimensional analysis to multidimensional problems.

4.4 Roe's Approximate Riemann Solver

Among the various approximate Riemann solvers utilizing the properties of flux jacobian matrices for the treatment of the inviscid terms, Roe scheme is probably one of the most commonly used because of its simplicity and its ability to satisfy the jump conditions across discontinuities exactly. Considering a one-dimensional problem, a hyperbolic system of conservation laws can be written in the general form as

$$\frac{\partial \mathbf{U}}{\partial t} + \frac{\partial \mathbf{f}(\mathbf{U})}{\partial x} = 0$$

where $\mathbf{U}$ is the vector of conservative variables and $\mathbf{f}$ is the flux vector. In Roe's method, the solution of the exact Riemann problem is replaced by the exact solution of an approximate Riemann problem of the form

$$\frac{\partial \mathbf{U}}{\partial t} + \bar{\mathbf{A}} \frac{\partial \mathbf{U}}{\partial x} = 0$$

where $\bar{\mathbf{A}}$ is the flux jacobian matrix. $\bar{\mathbf{A}}$ is a locally constant matrix evaluated at the cell interface and therefore allows the transformation of the initial non-linear problem into a piecewise linear problem. If we consider an interface separating two states U_L and U_R, the numerical flux of Roe is expressed as

$$\mathbf{f}(U_L, U_R) = \frac{1}{2}(\mathbf{f}(U_L) + \mathbf{f}(U_R)) - \frac{1}{2}|\bar{\mathbf{A}}(U_L, U_R)|(U_R - U_L) \tag{4.5}$$

where the Jacobian matrix $\bar{\mathbf{A}}$ has to satisfy the following conditions,

(i) $\quad \bar{\mathbf{A}}(U, U) = \mathbf{A}(U)$

(ii) $\quad \mathbf{f}(U_R) + \mathbf{f}(U_L) = \bar{\mathbf{A}}(U_L, U_R)(U_R - U_L)$

(iii) $\quad$ *The eigenvectors of* $\bar{\mathbf{A}}$ *are linearly independent*

Condition (i) is necessary for consistency. Condition (ii) guarantees that the algorithm will be conservative, and (ii) and (iii) together ensure the correct resolution of discontinuities.

According to equation (4.5), the formulation of the numerical flux of Roe depends on an average matrix $\bar{\mathbf{A}}$ which can be obtained by seeking an average state $\bar{U}$, such that

$$\bar{\mathbf{A}}(U_L, U_R) = \mathbf{A}(\bar{U})$$

$\bar{U}$ is commonly referred to as the Roe-averaged state, and its original derivation relied on the algebraic simplicity of the perfect gas law [14]. While the definition of this average state is quite straight forward in the case of a perfect gas, it becomes a more difficult task when dealing with an equilibrium air model. Accurate numerical calculations for equilibrium air show that the equation of state can be non-convex, i.e. the pressure derivatives can vary non-monotonically with density and internal energy. Consequently it is difficult to define optimum generalizations, valid for all gas laws and all numerical applications. The complexity of generalizing the Roe average for a general equilibrium gas resides in the definition of a unique Roe averaged state. It was originally established [12, 20, 21] that a Roe-averaged state exists for an equilibrium gas, but its precise value is not uniquely defined. Various methods for obtaining a unique state were proposed [22, 9, 11, 17, 1], but the most promising approach is that developed by Vinokur

[20] which proposed an exact definition of a Roe-averaged state. For simplicity, the analysis is presented here for one-dimensional flow, but the generalization to two and three dimensions are presented at the end of this chapter.

4.5 Flux Jacobian Matrices in One-Dimension

We consider the conservative form of the Euler equations written in the one-dimensional case

$$\frac{\partial \mathbf{U}}{\partial t} + \frac{\partial \mathbf{f}}{\partial x} = 0$$

where

$$\mathbf{U} = \begin{pmatrix} \rho \\ \rho u \\ \rho E \end{pmatrix} \qquad \mathbf{f} = \begin{pmatrix} \rho u \\ \rho u^2 + p \\ (\rho E + p)u \end{pmatrix}$$

where ρ is the density, u is the velocity and E is the total energy per unit mass, $E = e + u^2/2$, with e being the internal energy per unit mass (i.e., specific energy). We assume a general equation of state where the pressure p is expressed in terms of the density ρ and the internal energy per unit volume $\tilde{e}$, such as

$$p = p(\rho, \tilde{e})$$

with $\tilde{e} = \rho e$. The differential of p reads

$$dp = \chi d\rho + \kappa d\tilde{e} \tag{4.6}$$

where χ and κ denote the two pressure derivatives with respect to density and internal energy per unit volume, respectively,

$$\chi = \left(\frac{\partial p}{\partial \rho}\right)_{\tilde{e}}$$
$$\kappa = \left(\frac{\partial p}{\partial \tilde{e}}\right)_{\rho}$$

The speed of sound can be expressed as

$$c^2 = \chi + \kappa h$$

where $h = e + p/\rho$ is the specific enthalpy. The flux Jacobian matrix $\mathbf{A}$ can therefore be obtained by formulating the differential expression of the flux $d\mathbf{f}$ in terms of the conserved variables, such that $d\mathbf{f} = \mathbf{A} d\mathbf{U}$. This leads to

$$\mathbf{A} = \begin{pmatrix} 0 & 1 & 0 \\ K_1 - u^2 & (2-\kappa)u & \kappa \\ (K_1 - H)u & H - \kappa u^2 & (1+\kappa)u \end{pmatrix}$$

where $K_1 = \frac{1}{2}\kappa u^2 + \chi$ and $H = h + \frac{1}{2}u^2$ is the total enthalpy per unit mass. The three eigenvalues of A are readily found to be

$$\begin{aligned} \lambda_1 &= u \\ \lambda_2 &= u + c \\ \lambda_3 &= u - c \end{aligned}$$

The corresponding right eigenvector matrix R is

$$\mathbf{R} = \begin{pmatrix} 1 & 1 & 1 \\ u & u+c & u-c \\ K_2 & H+cu & H-cu \end{pmatrix}$$

where $K_2 = \frac{1}{2}u^2 - \chi/\kappa = H - c^2/\kappa$, while the left eigenvector matrix R^{-1} takes the form

$$\mathbf{R^{-1}} = \begin{pmatrix} 1 - K_1/c^2 & \kappa u/c^2 & -\kappa/c^2 \\ \frac{1}{2}(K_1/c^2 - u/c) & -\frac{1}{2}(\kappa u/c^2 - 1/c) & \frac{1}{2}\kappa/c^2 \\ \frac{1}{2}(K_1/c^2 + u/c) & -\frac{1}{2}(\kappa u/c^2 + 1/c) & \frac{1}{2}\kappa/c^2 \end{pmatrix}$$

Considering the case of a perfect gas, the equation of state reads

$$p = (\gamma - 1)\rho e = (\gamma - 1)\tilde{\epsilon}$$

and leads to $\chi = 0$, $\kappa = \gamma - 1$, and $c^2 = \gamma p/\rho$.

4.6 Generalized Roe Average for Equilibrium Real Gas

The definition of the Roe averaged state is presented here following the approach developed by Vinokur [20]. In approximate Riemann solver based on local linearization, the formulation of the numerical flux is based on an averaged matrix $\bar{\mathbf{A}}$ defined as

$$\bar{\mathbf{A}}(U_L, U_R) = \mathbf{A}(\bar{U})$$

which has to satisfy the following condition,

$$\mathbf{f}(U_R) + \mathbf{f}(U_L) = \bar{\mathbf{A}}(U_L, U_R)(U_R - U_L) \tag{4.7}$$

Assuming that the average velocity $\bar{u}$ and the average total enthalpy $\bar{H}$ must be some linear combination of u_L and u_R, and of H_L and H_R respectively, equation (4.7) leads to

$$\bar{u} = \alpha u_L + (1-\alpha)u_R \tag{4.8}$$

$$\bar{H} = \alpha H_L + (1-\alpha)H_R \tag{4.9}$$

where

$$\alpha = \frac{\sqrt{\rho_L}}{\sqrt{\rho_L} + \sqrt{\rho_R}} \tag{4.10}$$

These equations are the identical relations derived by Roe for a perfect gas. The only difference in the generalization to an arbitrary equilibrium gas arises from the new condition,

$$\bar{\chi}\Delta\rho + \bar{\kappa}\Delta\tilde{\epsilon} = \Delta p \tag{4.11}$$

This additional condition is automatically satisfied for a perfect gas, and represents the basis for the definition of the unique Roe-averaged state.

The Roe-averaged specific enthalpy is obtained from the definition of H and by combining equations (4.8) and (4.9),

$$\bar{h} = \alpha h_L + (1-\alpha)h_R + \frac{1}{2}\alpha(1-\alpha)(\Delta u)^2 \tag{4.12}$$

The Roe-averaged speed of sound is given by

$$\bar{c}^2 = \bar{\chi} + \bar{\kappa}\bar{h} \tag{4.13}$$

For a perfect gas, where $\chi = 0$ and κ is a given constant, equation (4.11) is automatically satisfied and consequently equations (4.8), (4.9), (4.10), (4.12), and (4.13) are sufficient to define uniquely the average state $\bar{U}$ and the corresponding eigenvalues and eigenvectors of $\bar{\mathbf{A}}$.

For an arbitrary equilibrium gas, equation (4.11) provides only one relation for the average pressure derivatives $\bar{\chi}$ and $\bar{\kappa}$ and therefore does not allow unique definition of the average state $\bar{U}$.

It is clear however that unique values of $\bar{\chi}$ and $\bar{\kappa}$ must be defined in terms of the thermodynamic states L and R. Following the approach proposed by Vinokur & Montagne [12], the average values $\bar{\chi}$ and $\bar{\kappa}$ can be obtained by integrating equation (4.6) along an arbitrary path between any two states L and R. This path can be defined parametrically by the functions $\rho(t)$ and $\bar{\epsilon}(t)$, where the parameter t is normalized so that $t_L = 0$ and $t_R = 1$. The integration of (4.6) along this path leads to

$$\Delta p = \int_0^1 \chi[\rho(t), \bar{\epsilon}(t)]\rho'(t)dt + \int_0^1 \kappa[\rho(t), \bar{\epsilon}(t)]\bar{\epsilon}'(t)dt \tag{4.14}$$

The simplest choice is the straight-line path defined as

$$\rho(t) = \rho_L + t\Delta\rho \tag{4.15}$$

$$\bar{\epsilon}(t) = \bar{\epsilon}_L + t\Delta\bar{\epsilon} \tag{4.16}$$

Substituting equations (4.15) and (4.16) into (4.14), and comparing to equation (4.11) yields the general relations,

$$\bar{\chi} = \int_0^1 \chi[\rho(t), \bar{\epsilon}(t)]dt \tag{4.17}$$

$$\bar{\kappa} = \int_0^1 \kappa[\rho(t), \bar{\epsilon}(t)]dt \tag{4.18}$$

Equations (4.15) to (4.18) give unique definitions of $\bar{\chi}$ and $\bar{\kappa}$ satisfying equation (4.11) for arbitrary values of $\Delta\rho$ and $\Delta\bar{\epsilon}$, including the limiting case $\Delta\rho = \Delta\bar{\epsilon} = 0$. For a given equation of state, the integrals in equations (4.17) and (4.18) can be evaluated in principle for any two thermodynamic states L and R. However, since the exact evaluation is not computationally practical, some approximate procedure may be required.

One method is suggested by Glaister [9] and consists of introducing two intermediate states A and B defined by $\rho_A = \rho_L$ and $\bar{\epsilon}_A = \bar{\epsilon}_R$, and $\rho_B = \rho_R$ and $\bar{\epsilon}_B = \bar{\epsilon}_L$, respectively. The resultant average pressure derivatives can then be expressed in terms of pressures at certain points and does not require further equilibrium computations. However, due to the non-monotonical behaviour of χ and κ, the introduction of these two fictitious states gives poor results, especially when the states L and R are far apart.

The alternative method proposed by Vinokur & Montagne consists, first, of evaluating two approximations $\hat{\chi}$ and $\hat{\kappa}$ for the two thermodynamic derivatives will not necessarily satisfy (4.11) exactly, and secondly, of obtaining the exact values $\bar{\chi}$ and $\bar{\kappa}$ by projecting the point $(\hat{\chi}, \hat{\kappa})$ onto the straight line defined by equation (4.11). In order to obtain the Roe-averaged state which will be independent of the arbitrary constant in the definition of the energy, equation (4.11) can first be rewritten as follows

$$\Delta\tilde{\epsilon} = \frac{\hat{s}^2}{\bar{\kappa}}\Delta\rho + \frac{\bar{\chi}}{\bar{\kappa}}\Delta p$$

where $\hat{s}$ is a scale factor with the dimension of $\bar{\chi}$. The projection on to the straight line is then defined by the relation

$$\frac{\hat{s}^2}{\bar{\kappa}}\Delta\rho + \frac{\bar{\chi}}{\bar{\kappa}}\Delta p = \frac{\hat{s}^2}{\hat{\kappa}}\Delta\rho + \frac{\hat{\chi}}{\hat{\kappa}}\Delta p \tag{4.19}$$

If one introduces the error

$$\delta p = \Delta p - \hat{\chi}\Delta\rho - \hat{\kappa}\Delta\tilde{\epsilon}$$

and the quantity

$$D = (\hat{s}\Delta\rho)^2 + (\Delta p)^2$$

one can solve equations (4.11) and (4.19) to obtain the final relations,

$$\bar{\chi} = \frac{D\hat{\chi} + \hat{s}^2 \Delta p \Delta \rho}{D - \Delta p \Delta \rho}$$
$$\bar{\kappa} = \frac{D\hat{\kappa}}{D - \Delta p \Delta \rho}$$

A natural choice for the scale factor $\hat{s}$ is

$$\hat{s} = \hat{c^2} = \hat{\chi} + \kappa \hat{h}$$

where we assume that the same quadrature approximation is used to calculate $\hat{\chi}$, $\hat{\kappa}$, and $\hat{c^2}$. Let $\rho_M = (\rho_L + \rho_R)/2$ and $\tilde{\epsilon}_M = (\tilde{\epsilon}_L + \tilde{\epsilon}_R)/2$ define the midpoint state M, then possible quadrature rules for $\hat{\chi}$ are the midpoint rule,

$$\hat{\chi} = \chi_M,$$

the trapezoidal rule,

$$\hat{\chi} = (\chi_L + \chi_R)/2,$$

and Simpson's rule,

$$\hat{\chi} = (\chi_L + 4\chi_M + \chi_R)/6,$$

with analoguous formulas for $\hat{\kappa}$ and $\hat{c^2}$. If the states L and R are reasonably close, either the midpoint rule or the trapezoidal rule should be adequate. For large separation of the two states, Simpson's rule may be required. The quantity D/p_L^2 can be use as a dimensional parameter for measuring the separation of the two states.

4.7 The Entropy Condition

Inviscid flows can undergo a discontinuous behaviour, such as shocks or contact discontinuities, which have to satisfy the Rankine-Hugoniot relations. Contrary to contact discontinuities, shocks are characterized by non-zero mass flow through the discontinuity, which implies a discontinuous variation of entropy across the shock. This entropy variation has to be positive, corresponding to a compression shock, in order to be in accordance with the second principle of thermodynamics. However, expansion shocks, corresponding to a negative entropy variation, are valid solutions of the inviscid equations, since, in the absence of heat transfer, they describe reversible flow variations. It is therefore necessary to impose a condition on the entropy in order to ensure that the obtained solutions of the

inviscid equations are indeed limits of the real fluid behaviour in the limiting case of vanishing viscosity, ensuring thereby that non-physical solutions, such as expansion shocks, will not appear.

This entropy condition can be expressed by different formulations depending on the numerical scheme being considered. Contrary to most of the Godunov-type schemes, Roe's scheme allows expansion shock solutions. In the case of an expansion with a sonic transition where certain eigenvalues are zero, the numerical dissipation vanishes, giving rise to an expansion shock. These solutions, associated with a decrease in entropy, are not physically acceptable and have therefore to be rejected. One technique to avoid the expansion shock was proposed by Harten [3] and consists in introducing a local expansion fan in the approximate Riemann solution when an expansion is detected through a sonic point. This can be realized by modifying the modulus of the eigenvalues $|\lambda_i|$ of $\mathbf{A}$ in equation (4.5) such as follows

$$|\lambda_i| = \left\{ \begin{array}{ccc} |\lambda_i| & if & |\lambda_i| > \epsilon \\ \frac{1}{2}\left(\frac{\lambda_i^2}{\epsilon} + \epsilon\right) & if & |\lambda_i| < \epsilon \end{array} \right\}$$

The parameter ϵ ensures a continuously differentiable correction and its value is usually taken to lie between 0 and 1. However, since no criterion can be used to choose the value of ϵ, this has to be chosen in accordance to the particular numerical application. The numerous calculations done throughout the course of this work have shown that small values of ϵ ($\epsilon < 0.3$) may lead to bad resolution along the symmetric line in particular, and in the transition region between subsonic and supersonic regime. A fixed value of $\epsilon = 0.5$ has therefore been used for all the test cases presented in this report.

4.8 Discretization of the Viscous Fluxes

Independently of the choice of the basic Euler scheme, central or upwind, used for the discretization of the inviscid fluxes, the viscous and thermal terms are always centrally discretized. Defintion of the viscous fluxes is given in equation (4.2). The viscous component of the normal flux with respect to a side with normal $\mathbf{n}(n_x, n_y)$ is given by

$$\mathbf{F}_n^V = \left(\mathbf{f}^V \quad \mathbf{g}^V \right).\mathbf{n}$$

so that,

$$\mathbf{F}_n^V = \begin{pmatrix} 0 \\ \tau_{xx}n_x + \tau_{xy}n_y \\ \tau_{x_y}n_x + \tau_{yy}n_y \\ (u\tau_{xx} + v\tau_{xy} - q_x)n_x + (u\tau_{xy} + v\tau_{yy} - q_y)n_y \end{pmatrix}$$

Since the viscous fluxes functions $\mathbf{f}^V$ and $\mathbf{g}^V$ in the Navier-Stokes equations depend predomimantly on the gradient of the solution vector, a prime requirement is to evaluate the average of these gradients along the edge of each cell. The method presented here consists of evaluating the gradient at the mid-point of the cell edges.

The technique most commonly used in finite volume methods to calculate the gradients of the solution vector is to use a combination of the integral mean value theorem and Gauss's theorem. To illustrate the procedure, we examine the evaluation of the gradient of a scalar function u. We first need to define an appropriate region Ω which surrounds the cell edge where the gradient is to be calculated.

Using Gauss's divergence theorem, the integral of the gradient function of u over Ω can be transformed into a line integral around its boundary $\partial\Omega$, such as

$$\int_\Omega \nabla u d\Omega = \oint_{\partial\Omega} u\mathbf{n}dl \tag{4.20}$$

where $\mathbf{n}$ is the outward unit vector normal to the boundary $\partial\Omega$. Assuming a constant distribution of the gradient over this region, equation (4.20) becomes

$$\frac{\partial u}{\partial x}\mathbf{x} + \frac{\partial u}{\partial y}\mathbf{y} = \frac{1}{\Omega}\oint_{\partial\Omega} u\mathbf{n}dl$$

Consequently, the two components of the gradient in the x and y direction are simply given by the projection of the above expression on to the corresponding basis vector $\mathbf{x}$ or $\mathbf{y}$,

$$\frac{\partial u}{\partial x} = \frac{1}{\Omega}\oint_{\partial\Omega} u(\mathbf{n}\cdot\mathbf{x})dl$$
$$\frac{\partial u}{\partial y} = \frac{1}{\Omega}\oint_{\partial\Omega} u(\mathbf{n}\cdot\mathbf{y})dl$$

The gradient over the cell is then approximated by integrating along the boundary $\partial\Omega$ formed by the four points N_1, N_2, N_3 and N_4. The line integrals on the right hand side can be split into four line integrals along which u is assumed to

be constant. Thus,

$$\frac{\partial u}{\partial x} = \frac{1}{\Omega}\sum_{i=1}^{4} u_i(\mathbf{n_i}\cdot\mathbf{x})\delta l_i$$
$$\frac{\partial u}{\partial y} = \frac{1}{\Omega}\sum_{i=1}^{4} u_i(\mathbf{n_i}\cdot\mathbf{y})\delta l_i$$

where δl_i denotes the length of the edge i, and $\mathbf{n_i}$ the outward unit vector normal to the edge i. The above expressions can be further reduced by expressing the scalar products in terms of the x and y components of each vector. We have

$$\mathbf{n}_i\delta l_i = \begin{pmatrix} \delta y_i \\ -\delta x_i \end{pmatrix} \qquad \mathbf{x} = \begin{pmatrix} 1 \\ 0 \end{pmatrix} \qquad \mathbf{y} = \begin{pmatrix} 0 \\ 1 \end{pmatrix}$$

thus,

$$\frac{\partial u}{\partial x} = \frac{1}{\Omega}\sum_{i=1}^{4} u_i\delta y_i$$
$$\frac{\partial u}{\partial y} = \frac{1}{\Omega}\sum_{i=1}^{4} -u_i\delta x_i$$

Denoting by (x_i, y_i) the cartesian coordinates of each point N_i, the gradients in the x and y directions are completely determined by

$$\frac{\partial u}{\partial x} = \frac{1}{\Omega}(u_1\delta y_{14} + u_2\delta y_{21} + u_3\delta y_{32} + u_4\delta y_{34}) \tag{4.21}$$
$$\frac{\partial u}{\partial y} = -\frac{1}{\Omega}(u_1\delta x_{14} + u_2\delta x_{21} + u_3\delta x_{32} + u_4\delta x_{34}) \tag{4.22}$$

The required values for u_1, u_2, u_3, and u_4 are obtained by calculating the average values of u over the four cells surrounding the corresponding edge. For instance, for the evaluation of the gradient along the edge $(i-1/2, j)$ between the cells $(i-1, j)$ and (i, j), we have

$$u_1 = u_{i,j}$$
$$u_2 = \frac{1}{4}(u_{i,j} + u_{i-1,j} + u_{i,j+1} + u_{i-1,j+1})$$
$$u_3 = u_{i-1,j}$$
$$u_4 = \frac{1}{4}(u_{i,j} + u_{i-1,j} + u_{i,j-1} + u_{i-1,j-1})$$

The average values of u for the edges $(i+1/2, j)$, $(i, j-1/2)$, and $(i, j+1/2)$ are obtained in a similar manner. Equations (4.21) and (4.22) can therefore be used to evaluate the gradient of the two velocity components u and v, and the temperature T.

4.9 Flux Jacobian Matrices in Three-Dimensions

In the general three-dimensional case, the vector $\mathbf{U}$ of conservative variables can be represented by the column vector

$$\mathbf{U} = \begin{pmatrix} \rho \\ \rho\mathbf{u} \\ \rho E \end{pmatrix}$$

where ρ is the density, $\mathbf{u}$ is the fluid velocity vector and E is the total energy per unit mass,

$$E = e + \frac{1}{2}\mathbf{u}.\mathbf{u}$$

with e being the internal energy per unit mass.

Let $\mathbf{n}$ be the normal unit vector in a positive direction to a cell surface in a finite volume grid. This can define the normal velocity component $u_n = \mathbf{u} \cdot \mathbf{n}$. The set of inviscid flux components $\mathbf{F}_n$ is given by the column vector

$$\mathbf{F}_n = \begin{pmatrix} \rho u_n \\ \rho\mathbf{u}u_n + p\mathbf{n} \\ (\rho E + p)u_n \end{pmatrix}$$

The flux jacobian matrix $\mathbf{A}$ is obtained by expressing the differential $d\mathbf{F}_n$ in terms of the differentials of the conservative variables, such that $d\mathbf{F}_n = \mathbf{A}d\mathbf{U}$. This gives

$$\mathbf{A} = \begin{pmatrix} 0 & \mathbf{n} & 0 \\ K_1\mathbf{n} - u_n\mathbf{u} & \mathbf{u}.\mathbf{n} - \kappa\mathbf{n}.\mathbf{u} + u_n\mathbf{I} & \kappa\mathbf{n} \\ (K_1 - H)u_n & H\mathbf{n} - \kappa u_n\mathbf{u} & (1+\kappa)u_n \end{pmatrix}$$

where

$$K_1 = \frac{1}{2}\kappa\mathbf{u}.\mathbf{u} + \chi$$

$H = h + \frac{1}{2}\mathbf{u}.\mathbf{u}$ is the total enthalpy per unit mass, and $\mathbf{I}$ is the identical tensor. The eigenvalues of $\mathbf{A}$ are

$$\begin{aligned} \lambda_1 &= u_n \\ \lambda_2 &= u_n + c \\ \lambda_3 &= u_n - c \end{aligned}$$

with λ_1 being a multiple eigenvalue. The set of linearly independent eigenvectors can be defined in terms of an arbitrary set of spatial basis vectors $\mathbf{a}_i$, and a set

of reciprocal basis vectors $\mathbf{a}^j$ satisfying $\mathbf{a}_i \cdot \mathbf{a}^j = \delta_i^j$, where δ_i^j is the Kronecker symbol. One then can define

$$\begin{aligned} a_{ni} &= \mathbf{n} \cdot \mathbf{a}_i \\ \mathbf{b}_i &= \mathbf{n} \times \mathbf{a}_i \\ a_n^j &= \mathbf{n} \cdot \mathbf{a}^j \\ \mathbf{b}^j &= \mathbf{n} \times \mathbf{a}^j \end{aligned}$$

If β is an arbitrary scalar, the right eigenvector matrix $\mathbf{R}$ can be written in the most general form as

$$\mathbf{R} = \begin{pmatrix} a_{ni} & 1 & 1 \\ a_{ni}\mathbf{u} + \beta \mathbf{b}_i & \mathbf{u} + c\mathbf{n} & \mathbf{u} - c\mathbf{n} \\ a_{ni}K_2 + \beta \mathbf{b}_i \cdot \mathbf{u} & H + cu_n & H - cu_n \end{pmatrix} \tag{4.23}$$

where

$$K_2 = \frac{1}{2}\mathbf{u}.\mathbf{u} - \frac{\chi}{\kappa}$$

The left eigenvector matrix $\mathbf{R}^{-1}$ takes the form

$$\mathbf{R}^{-1} = \begin{pmatrix} a_n^j(1 - K_1/c^2) - \mathbf{b}^j \cdot \mathbf{u}/\beta & a_n^j \kappa \mathbf{u}/c^2 + \mathbf{b}^j/\beta & -a_n^j \kappa/c^2 \\ \frac{1}{2}(K_1/c^2 - u_n/c) & -\frac{1}{2}(\kappa \mathbf{u}/c^2 - \mathbf{n}/c) & \frac{1}{2}\kappa/c^2 \\ \frac{1}{2}(K_1/c^2 + u_n/c) & -\frac{1}{2}(\kappa \mathbf{u}/c^2 + \mathbf{n}/c) & \frac{1}{2}\kappa/c^2 \end{pmatrix} \tag{4.24}$$

In the general three dimensional case, where i and j take on values from 1 to 3, $\mathbf{R}$ is a five column matrix and $\mathbf{R}^{-1}$ is a five row matrix. A useful choice for the basis vectors is to let one of the $\mathbf{a}_i$ be parallel to $\mathbf{n}$, so that the corresponding $\mathbf{b}_i = 0$. The remaining $\mathbf{a}_i$ are then chosen to lie in the plane prependicular to $\mathbf{n}$, so that their corresponding $a_{ni} = 0$.

The generalization of the Roe average for a surface separating two states $\mathbf{U}_L$ and $\mathbf{U}_R$ is defined by the condition $\Delta \mathbf{F}_n = \bar{\mathbf{A}} \Delta \mathbf{U}$,

$$\begin{aligned} \bar{\mathbf{u}} &= \alpha \mathbf{u}_L + (1 - \alpha)\mathbf{u}_R \\ \bar{H} &= \alpha H_L + (1 - \alpha) H_R \\ \bar{h} &= \alpha h_L + (1 - \alpha) h_R + \frac{1}{2}\alpha(1 - \alpha)\Delta \mathbf{u} \cdot \Delta \mathbf{u} \end{aligned}$$

where

$$\alpha = \frac{\sqrt{\rho_L}}{\sqrt{\rho_L} + \sqrt{\rho_R}}$$

4.10 Flux Jacobian Matrices in Two-Dimensions

For a two-dimensional flow, the vector $\mathbf{U}$ of conservative variables reduces to

$$\mathbf{U} = \begin{pmatrix} \rho \\ \rho u \\ \rho v \\ \rho E \end{pmatrix}$$

The fluid velocity vector $\mathbf{u}$ and the normal unit vector $\mathbf{n}$ are

$$\mathbf{u} = \begin{pmatrix} u \\ v \end{pmatrix} \qquad\qquad \mathbf{n} = \begin{pmatrix} n_x \\ n_y \end{pmatrix}$$

and $u_n = un_x + vn_y$. The set of inviscid flux components $\mathbf{F}_n$ is given by

$$\mathbf{F}_n = \begin{pmatrix} \rho u_n \\ \rho u u_n + p n_x \\ \rho v u_n + p n_y \\ (\rho E + p) u_n \end{pmatrix}$$

The flux jacobian matrix $\mathbf{A}$ reduces to

$$\mathbf{A} = \begin{pmatrix} 0 & n_x & n_y & 0 \\ K_1 n_x - u u_n & u n_x - \kappa u n_x + u_n & u n_y - \kappa v n_x & \kappa n_x \\ K_1 n_y - v u_n & v n_x - \kappa u n_y & v n_y - \kappa v n_y + u_n & \kappa n_y \\ (k_1 + H) u_n & H u_n - \kappa u u_n & h n_y - \kappa v u_n & (1+\kappa) u_n \end{pmatrix}$$

The four eigenvalues of $\mathbf{A}$ are

$$\begin{aligned} \lambda_1 &= u_n \\ \lambda_2 &= u_n \\ \lambda_3 &= u_n + c \\ \lambda_4 &= u_n - c \end{aligned}$$

The basis vectors $\mathbf{a}_i$ and $\mathbf{b}_i$ are chosen as follows,

$$\mathbf{a}_1 = \begin{pmatrix} n_x \\ n_y \\ 0 \end{pmatrix} \qquad \mathbf{a}_2 = \begin{pmatrix} -n_y \\ n_x \\ 0 \end{pmatrix} \qquad \mathbf{a}_3 = \begin{pmatrix} 0 \\ 0 \\ 1 \end{pmatrix}$$

$$\mathbf{b}_1 = \begin{pmatrix} 0 \\ 0 \\ 0 \end{pmatrix} \qquad \mathbf{b}_2 = \begin{pmatrix} 0 \\ 0 \\ 1 \end{pmatrix} \qquad \mathbf{b}_3 = \begin{pmatrix} n_y \\ -n_x \\ 0 \end{pmatrix}$$

and

$$\begin{aligned} a_{n1} &= 1 \\ a_{n2} &= 0 \\ a_{n3} &= 0 \end{aligned}$$

The right eigenvector matrix $\mathbf{R}$ is obtained from equation (4.23) by removing the second column and the fourth line, and by taking $\beta = -1$,

$$\mathbf{R} = \begin{pmatrix} 1 & 0 & 1 & 1 \\ u & n_y & u + cn_x & u - cn_x \\ v & -n_x & v + cn_y & v - cn_y \\ K_2 & -un_y + vn_x & H + cu_n & H - cu_n \end{pmatrix}$$

The correspomding left eigenvector matrix $\mathbf{R}^{-1}$ is obtained similarly from equation (4.24) by removing the fourth column and the second line,

$$\mathbf{R}^{-1} = \begin{pmatrix} 1 - K_1/c^2 & \kappa u/c^2 & \kappa v/c^2 & -\kappa/c^2 \\ un_y - vn_x & -n_y & n_x & 0 \\ \frac{1}{2}(K_1/c^2 - u_n/c) & -\frac{1}{2}(\kappa u/c^2 - n_x/c) & -\frac{1}{2}(\kappa v/c^2 - n_y/c) & \frac{1}{2}\kappa/c^2 \\ \frac{1}{2}(K_1/c^2 + u_n/c) & -\frac{1}{2}(\kappa u/c^2 + n_x/c) & -\frac{1}{2}(\kappa v/c^2 + n_y/c) & \frac{1}{2}\kappa/c^2 \end{pmatrix}$$

Chapter 5

Implementation of Equilibrium Air Models within CFD code

5.1 The Choice of the Independent Variables

One of the main difficulties associated with the implementation of equilibrium air models within CFD codes resides in the choice of the independent variables required for solving the equilibrium equations [4]. As already stated, under the assumption of thermal and chemical equilibrium, the thermodynamic state of the system depends on two independent variables only. The optimum choice would obviously be to choose both variables among the conservative variables describing the flow equations, but this is generally not possible since the equations of state are expressed in terms of other variables.

A natural choice for one of the two thermodynamic variables is the density ρ, as it appears explicitly in the flow equations. In the case of a perfect gas, any other thermodynamic variable can be chosen to complete the set of independent variables since the equation of state can be formulated in a simple linear relation. Pressure p, temperature T, or specific internal energy e may indifferently be retained as independent variable.

For equilibrium air model, however, where no simple relation exists between the different thermodynamic variables, the choice of this second variable is not so wide-open. An ideal choice would be to choose the specific internal energy e as it is closely related to the total energy E which has been retained as an independent conservative variable,

$$E = e + \frac{u^2 + v^2}{2}$$

However, this does not represent a practical choice for solving the equilibrium

equations since e generally depends on the gas composition itself. The choice of the remaining thermodynamic variable will therefore be dictated by the formulation of the equation of state. Since the equilibrium air properties are computed on the basis of a uniform equilibrium temperature, one needs to retain the equilibrium temperature as the second independant variable, completing thereby the set of variables required for solving the equilibrium equations.

The set of conservative variables is formed by density, momentum, and total energy, and therefore does not express explicitly in terms of temperature. Consequently, and due to the complex formulation of the equations of state for equilibrium air model, problems will arise when the equilibrium temperature has to be calculated from a given specific internal energy. There is unfortunately no alternative to resorting to an iterative procedure for inverting the equation of state, which will significantly increase the computational time.

5.2 Inversion of the Equation of State

Different techniques have been investigated [4] for inverting the general equation of state in order to obtain the equilibrium temperature for given density and specific internal energy. As already stated, this can only be achieved by means of an iterative procedure because of the complexity of the equations of state. The final choice of a Newton-Raphson iteration scheme was made because of a fast convergence rate and a large flexibility in the choice of the initial value. The most accurate estimate of the initial value of temperature is obtained by using the sixteen coefficient curve fit. The iterative procedure can be summarized as follows :

1) Solving the flow equations in order to obtain values for density ρ and internal energy e.

2) Estimating an accurate initial value for temperature for initializing the iterative process. $T^{(0)}$ is obtained from the 16 coefficient curve fit,

$$T^{(0)} = T(\rho, e)$$

3) Resolution of the equilibrium equations for the given density ρ and the temperature $T^{(n)}$. This provides a new calculated value $e^{(n)}$ for the internal energy,

$$e^{(n)} = e(\rho, T^{(n)})$$

4) Estimating the energy derivative $(\partial e/\partial T)_\rho$

5) The temperature is updated by using the following differential relation,

$$T^{(n+1)} = T^{(n)} - \frac{e^{(n)} - e}{(\partial e/\partial T)_\rho}$$

6) Go back to step 3

The iterative process is repeated until the calculated value for $e^{(n)}$ has converged to the given internal energy e. The equilibrium air properties can then be calculated from the density ρ and the converged temperature $T^{(n)}$. It was shown that a maximum of three iterations are required to achieved a converged solution at low temperatures, and up to five iterations at higher temperatures. The energy derivative $(\partial e/\partial T)_\rho$ follows from the chemical state of the gas and is therefore computed within the same routine than that employed for solving the equilibrium equations.

5.3 The Treatment of Boundary Conditions

5.3.1 The Characteristic Boundary Method

When specifying the values of the unknowns at a boundary, two different types of boundary conditions must be distinguished : the physical and the numerical boundary conditions, which will determine whether the value of the variable has to be imposed or extrapolated from the internal flow domain. The method commonly used to choose the appropriate boundary condition is based on the method of characteristics [3, 7].

The type of boundary condition to apply depends on the direction of propagation of the characteristic waves, namely on the characteristic waves entering or leaving the domain. In the general multi-dimensional case, the eigenvalues of the Jacobian matrix $\mathbf{A}$ are given by $\lambda_1 = U_n$, $\lambda_2 = U_n + c$, and $\lambda_3 = U_n - c$, where λ_1 is a multiple eigenvalue. The sign of these eigenvalues is therefore determined by the velocity component normal to the boundary surface, defining thereby the direction of propagation of the characteristic waves. The choice of the type of boundary condition to apply is therefore directly dictated by the sign of the eigenvalues.

When an eigenvalue is negative, the information carried by the associated characteristics propagates from the boundary towards the interior of the flow domain and a physical boundary condition has to be imposed. On the other

hand, when λ is positive, information is propagated from the flow domain towards the boundary, influencing thereby the boundary surface conditions. In that case, certain variables have to be determined by appropriate numerical procedure, which have to be compatible with the physical flow conditions and the numerical scheme. This forms the basis of the characteristic boundary method.

An important effect of the numerical boundary procedure is to ensure that unwanted perturbations generated in the computational domain, for instance the transient effects in a steady-state flow, leave the domain without being reflected at the boundaries. That implies that the propagation of these perturbations is compatible with the characteristic propagation properties of the flow equations. When this is not the case, the accuracy of the computation can be greatly affected by the reflection occuring at the boundaries. It is therefore recommended to apply, in all cases, characteristic boundary procedures.

5.3.2 Boundary Conditions for Nozzle Flow Problem

In the case of a nozzle flow problem, where the flow is assumed to be quasi-monodimensional, the computational domain is delimited by only two boundaries : the inlet (i.e., reservoir) and the outlet (i.e., exhaust). All the boundaries conditions used for the inlet and the outlet are based on the method of characteristics, and therefore refers to the sign of the eigenvalues of the Jacobian matrix. The treatment of the boundary conditions is generally performed by introducing a set of imaginary elements which are obtained by symmetry with respect to the boundary itself. The idea is then to specify the variables for these imaginary cells such as to satisfy particular boundary conditions. The variables at the element adjacent to the boundary inside the flow domain will be denoted by subscript L, and the variables at the imaginary cells by subscript R.

Subsonic Inlet

If the inlet is supersonic ($u < c$), one of the eigenvalue is negative and the associated characteristic wave is travelling out the flow domain. In that case, one variable needs to be extrapolated from the inside flow, corresponding to a numerical boundary condition. The two remaining variables being imposed by physical boundary conditions. The choice of the variable to be extrapolated is not imposed, but it may have an influence on the stability of the algorithm. We therefore choose to extrapolate velocity, and to impose pressure and density by the inlet conditions. The variables at the imaginary cells are therefore defined

by,

$$\begin{aligned} \rho_R &= \rho_{inlet}/\rho_0 \\ p_R &= p_{inlet}/p_0 \\ u_R &= u_L \end{aligned}$$

where p_0 and ρ_0 denote the stagnation pressure and the stagnation density, respectively.

Supersonic Outlet

If the outlet section is supersonic ($u > c$), all three eigenvalues are positive, corresponding to three characteristic waves carrying information outside the flow domain, and the three variables ρ, p, and u are obtained by linear extrapolation from inside the domain. For a first order scheme, the variables at the imaginary cells can be taken equal to the variables at the adjacent cells, that is

$$\begin{aligned} \rho_R &= \rho_L \\ p_R &= p_L \\ u_R &= u_L \end{aligned}$$

Subsonic Outlet

If the flow is subsonic at the exhaust ($u < c$), one characteristic wave is travelling from outside the domain towards the boundary, and one variable can be specified. This is commonly chosen to be the exhaust pressure $p_{exhaust}$. The two remaining variables are obtained by extrapolation. Thus,

$$\begin{aligned} \rho_R &= \rho_L \\ p_R &= p_{exhaust}/p_0 \\ u_R &= u_L \end{aligned}$$

5.3.3 Boundary Conditions for Two-Dimensional Problems

Here again, all boundary conditions are treated by the method of characteristics, by considering the eigenvalues of the Jacobian matrix $\mathbf{A} \cdot \mathbf{n}$, where $\mathbf{n}$ is

the outward unit vector normal to the boundary. This defines locally quasi-one-dimensional propagation properties so that the treatment of boundary conditions for multi-dimensional problems can be performed by analogy with the one-dimensional case. Same notations are used to denote the variables at the adjacent and imaginary cells. The only difference comes from the treatment of the wall boundary condition where certain variables are directly evaluated at the boundary interface. These variables will be denoted by subscript s.

Supersonic Inlet

If the flow is supersonic in the direction normal to the entry surface, the four eigenvalues are negative, and four variables have to be imposed by the free-stream conditions,

$$\begin{aligned} \rho_R &= 1 \\ u_R &= \cos\alpha \\ v_R &= \sin\alpha \\ p_R &= \frac{1}{\gamma M_\infty^2} \end{aligned}$$

where α is the angle of attack, γ is the free-stream ratio of specific heat, and M_∞ is the free-stream Mach number.

Supersonic outflow

At the outflow boundary, assuming that the flow is still supersonic, all the eigenvalues are positive and the four characteristic waves are travelling out of the computational flow domain, propagating the information from the interior domain towards the boundary. No physical conditions can be imposed. All the variables are extrapolated from the interior points and, for a first order scheme, they can be taken equal to the variables at the adjacent cells, that is

$$\begin{aligned} \rho_R &= \rho_L \\ u_R &= u_L \\ v_R &= v_L \\ p_R &= p_L \end{aligned}$$

Symmetric line

For a two-dimensional or axisymmetric flow at zero angle of attack, the solution can be sought for only half of the domain, introducing the symmetric line as a boundary condition. Since the symmetric line can be identified as a stream line, the symmetry condition requires a zero normal velocity along this line, so that

$$\begin{aligned} \rho_R &= \rho_L \\ u_R &= u_L \\ v_R &= -v_L \\ p_R &= p_L \end{aligned}$$

Solid wall boundary for the Euler equations

The boundary condition along the body in the case of an inviscid flow is the usual slip-condition, which states that the velocity must be tangent to the surface ($\mathbf{u} \cdot \mathbf{n} \doteq 0$, where $\mathbf{n}$ is normal to the surface). In that case, the normal velocity is zero, so that one eigenvalue is negative (one characteristics enters the flow domain) and only one physical condition can be imposed, namely $U_n = 0$. The other variables, such as the tangential velocity, the density and the pressure, have to be obtained from the interior domain by applying the characteristic relations. In terms of the Riemann invariants, we have

$$\begin{aligned} U_{n_s} + \frac{2}{\gamma - 1} c_s &= U_{n_L} + \frac{2}{\gamma - 1} c_L \\ V_{t_s} &= V_{t_L} \\ U_{n_s} &= 0 \\ Z_s &= Z_L \end{aligned}$$

where Z is the unscaled entropy defined by

$$Z = ln\left(\frac{p}{\rho^\gamma}\right)$$

Hence

$$\begin{aligned} c_s &= c_L + \frac{\gamma - 1}{2} U_{n_L} \\ \rho_s &= \left(\frac{c_s^2}{\gamma} e^{-Z_L}\right)^{\frac{1}{\gamma - 1}} \\ p_s &= \frac{\rho_s c_s^2}{\gamma} \end{aligned}$$

As a consequence of the slip-condition at the wall, the normal component of the inviscid flux vector reduces to

$$\mathbf{F}_n^I = \begin{pmatrix} 0 \\ p_s n_x \\ p_s n_y \\ 0 \end{pmatrix}$$

Hence, the only contribution to the normal flux at the wall is due to the pressure.

Solid wall boundary for the Navier-Stokes equations

An important difference between inviscid and viscous flows is the wall boundary condition. Due to the existence of friction, the flow can no longer slip along the wall, and the boundary condition to be used here is the no-slip boundary condition, which states that the velocity is zero at the wall,

$$\begin{aligned} u_s &= 0 \\ v_s &= 0 \end{aligned}$$

In addition, due to the energy transport by thermal conduction, an additional boundary condition is required at the wall, which can be expressed in terms of temperature. If the wall is at constant temperature, this boundary condition is simply expressed as

$$T_s = T_w$$

where T_w denotes the specified wall temperature. Unfortunately, in a high speed flow problem, the wall temperature is usually one of the unknowns, and the above condition cannot be used. Instead, the boundary condition can be given in terms of the heat flux by using Fourier's law of heat conduction. A special case of heat transfer wall boundary is the adiabatic wall condition, which corresponds to a zero temperature gradient at the wall,

$$\left(\frac{\partial T}{\partial n}\right)_w = 0$$

Another condition follows from the boundary layer assumption which assumes a constant pressure gradient through the boundary layer in the direction normal to the surface, so that

$$\left(\frac{\partial p}{\partial n}\right)_w = 0$$

The variables at the imaginary cell are therefore given by

$$
\begin{aligned}
u_R &= -u_L \\
v_R &= -v_L \\
p_R &= p_L \\
T_R &= \left\{ \begin{array}{ll} 2T_w - T_L & for\ constant\ wall\ temperature \\ T_L & for\ adiabatic\ wall \end{array} \right\} \\
\rho_R &= \rho_L \frac{T_L}{T_R}
\end{aligned}
$$

5.4 Time Stepping Scheme

The discretization of the Navier-Stokes equations in space transforms the governing equations into a set of coupled ordinary differential equations that must be integrated in time to obtain the steady state solution. As already discussed in a previous chapter, the finite volume discretization leads to the following set of equations at each grid point,

$$\Delta \mathbf{U}_{i,j} = -\frac{\Delta t}{\Omega_{i,j}} \sum_{s=1}^{4} (\mathbf{F}_s^I + \mathbf{F}_s^V) \delta l_s$$

where $\Omega_{i,j}$ is the area of the control volume (i,j), and $\mathbf{F}_s^I$ and $\mathbf{F}_s^V$ are the discrete approximations to the convective fluxes and the viscous fluxes, respectively. The above equations can be integrated in time by using the simplest explicit scheme, for which the fluxes are expressed only in terms of the solution vector at the n^{th} time step, so that the solution is updated as

$$\mathbf{U}_{i,j}^{n+1} = \mathbf{U}_{i,j}^{n} - \frac{\Delta t}{\Omega_{i,j}} \sum_{s=1}^{4} [\mathbf{F}_s^I(\mathbf{U}_{i,j}^n) + \mathbf{F}_s^V(\mathbf{U}_{i,j}^n)] \delta l_s$$

For steady problems, the numerical solution is obtained as a result of balancing all the fluxes entering the domain. Various methods may be employed to accelerate the convergence of the Navier-Stokes equations to the steady state. When time accuracy is not required, such as for steady problems solved with a time dependent method, one can apply a simple convergence acceleration technique by using local time steps. These are calculated from the local flow properties and enable the scheme to operate everywhere at its stability limit. Consequently, the solution progresses in time towards the steady solution with a different pace at each grid point.

The stability of the time stepping scheme is of crucial importance. It can be defined as the ability to damp the perturbations generated by the approximation of the numerical scheme. Thus, stability limitations due to both the convective and diffusive terms in the Navier-Stokes equations must be considered, and a stability analysis has to be performed in both cases in order to determine the appropriate local time step.

Local Time Step for the Euler Equations

Determination of the allowable time step follows from a dimensional analysis of the equations together with the application of a CFL stability condition, which states that the domain of dependence of the discretized equations must at least contain that of the original differential equations [3]. The local time step for the two-dimensional Euler equations can be determined by analogy with the linear advection equation in one-dimensional problem. The time step $\Delta t_{i,j}$ associated with the cell (i,j) is then given by

$$\Delta t = CFL \frac{\Omega_{i,j}}{\mathbf{u}_{i,j} \cdot \eta_{i,j} + c_{i,j} \parallel \eta_{i.j} \parallel + \mathbf{u}_{i,j} \cdot \xi_{i,j} + c_{i,j} \parallel \xi_{i.j} \parallel}$$

where $\mathbf{u}_{i,j}$ is the velocity vector, $c_{i,j}$ is the local speed of sound, and $\eta_{i,j}$ and $\xi_{i,j}$ are two local normal vectors.

Local Time Step for the Navier-Stokes Equations

For the two-dimensional Navier-Stokes equations, the local time step is determined in a similar manner by analogy with the advection-diffusion equation for a one-dimensional problem. This leads to

$$\Delta t = CFL \frac{\Omega_{i,j}}{\mathbf{u}_{i,j} \cdot \eta_{i,j} + c_{i,j} \parallel \eta_{i.j} \parallel + \alpha \parallel \eta_{i.j} \parallel^2 + \mathbf{u}_{i,j} \cdot \xi_{i,j} + c_{i,j} \parallel \xi_{i.j} \parallel + \alpha \parallel \xi_{i.j} \parallel^2}$$

where

$$\alpha = \frac{2\mu\gamma}{\rho_{i,j} RePr}$$

Chapter 6

Results

Several numerical tests have been conducted to evaluate the accuracy, efficiency and robustness of the present model. The algorithm is first validated with a quasi-one-dimensional flow problem, namely a hypersonic expansion nozzle. Two-dimensional test cases over blunt body shapes are then presented for inviscid and viscous flows. The aim is to demonstrate the ability of the present numerical method in handling thermodynamic and chemical equilibrium flows with very strong shock waves.

The following non-dimensional coefficients are defined in accordance with the definitions given in the Workshop of Hypersonic Flows for Reentry Problems [13].

Pressure coefficient

$$C_p = \frac{p - p_\infty}{1/2\rho_\infty u_\infty^2}$$

where ρ_∞ and u_∞^2 are the density and the velocity at infinity.

Skin friction coefficient

$$C_f = \frac{\tau_w}{1/2\rho_\infty u_\infty^2}$$

where $\tau_w = \mu(\partial u/\partial n)_w$ is the wall shear stress.

Heat flux coefficient

$$C_h = \frac{q}{1/2\rho_\infty u_\infty^3}$$

where $q = k(\partial T/\partial n)_w$ is the normal heat flux at the wall.

Stanton number

$$S_t = \frac{q}{\rho_\infty u_\infty c_{p_\infty}(T_{0_\infty} - T_w)}$$

where c_{p_∞} is the free stream specific heat at constant pressure, T_{0_∞} is the isentropic stagnation temperature and T_w is the wall temperature.

6.1 Hypersonic Expansion Nozzle Problem

Several test cases for one-dimensional flow have been considered for the validation of the algorithm, but only the expansion nozzle flow problem with high inlet temperature and pressure is presented here, since it is the best test case for illustrating the efficiency and accuracy of the equilibrium air model [4]. In this case, the computation domain consists of 200 equally-spaced nodes. The area distribution is given by the following equation,

$$A(x) = \exp(\sum_{i=0}^{3} c_i x^i)$$

where the coefficients c_i are determined in accordance with the throat and exhaust locations and sections. Here, the throat and exhaust locations are taken to be x_T=0.1 m and x_E=1.0 m, respectively, and the corresponding section radii r_T=5.0 mm and r_E=182.7 mm, which gives,

$$\begin{aligned} c_0 &= -9.165624 \\ c_1 &= -5.923050 \\ c_2 &= 32.576744 \\ c_3 &= -19.743499 \end{aligned}$$

The geometry of the nozzle is illustrated in figure B.1.

The stagnation conditions for this test case were chosen in order to give an expansion through a region of thermally imperfect gas behaviour. The stagnation conditions at the inlet are

$$\begin{aligned} p_0 &= 25.167 \times 10^6 \ N/m^2 \\ \rho_0 &= 6.425 \ kg/m^3 \\ h_0 &= 25.164 \times 10^6 \ J/kg \\ s &= 11310.0 \ J/kg/K \\ T_0 &= 9434.8 \ K \end{aligned}$$

The inflow section is assumed to be subsonic so that the inflow boundary conditions are completely defined by the inlet static pressure and density,

$$\begin{aligned} p_{inlet} &= 21.167 \times 10^6 \ \ N/m^2 \\ \rho_{inlet} &= 5.640 \ \ kg/m^3 \end{aligned}$$

No exhaust pressure is imposed, so that the flow is expanded throughout the nozzle without a shock wave forming. As can be seen in figure B.9, the flow is hypersonic at the outlet, with an exhaust Mach number above 6.

To illustrate the effects of the equilibrium air properties, results are given together with the equivalent perfect gas solution which was obtained with the same stagnation conditions as above. The molar mass of the gas is held constant and equal to its stagnation value, and the equivalent ratio of specific heats γ was obtained from the stagnation conditions by the following equation,

$$\gamma = \frac{1}{1 + p_0/\rho_0 h_0}$$

Thus,

$$\begin{aligned} \hat{\mathcal{M}} &= 0.020026 \ \ kg/m \\ R &= \hat{\mathcal{R}}/\hat{\mathcal{M}} = 415.18 \ \ J/kg/K \\ \gamma &= 1.184 \end{aligned}$$

Figures B.2 to B.9 show the variations of the different thermodynamic properties of the gas throughout the nozzle for both the equilibrium air model and the equivalent perfect gas model. No significant differences are shown for the variations of pressure, density, enthalpy, and internal energy, between both representations. The most noticeable difference arising from the temperature variations. As the gas expands through the nozzle, the decrease of temperature and pressure causes the dissociated species O, N, and NO, to recombine to form O_2 and N_2. In the process of recombination, chemical energy is converted to thermal energy which consequently slows down the rate of decrease of temperature. Since the ideal gas model does not account for the chemical processes, it predicts larger and faster temperature decreases during the expansion. This is illustrated in figure B.6. The perfect gas solution over-predicts the temperature drop, and this is due to the incorrect modelling of the internal energy modes at high temperature. This therefore highlights the need to resort to a more reliable model.

Due to the high temperatures and pressures involved, very intensive chemical reactions occur in the front section of the nozzle, and species mole fractions change significantly from their initial values. The composition of air at the inflow consists mainly of O, N, and N_2. As the recombination processes proceed, the mole fraction of N rapidly decreases (see figure B.13). The variations of the mole fractions of the other species are not as significant as for monoatomic nitrogen, due principally to the conservation of mass and the counterbalance of the other chemical reactions.

Figures B.11 and B.12 give the variations of the two thermodynamic derivatives χ and κ. These variations exhibit very strong variations together with a turning point around x=0.6 m. The peak value of κ corresponds to the maximum rate of the dissociation reactions.

6.2 Hypersonic Blunt Body Problem (Inviscid Flow)

An inviscid test case was then considered for validation of the two-dimensional Euler code. This case consists of an inviscid hypersonic flow over a blunt body, with a free stream Mach number of 15. Reference conditions were chosen to correspond to atmospheric conditions at an altitude of 45 km,

$$\begin{aligned} p_\infty &= 170 \ N/m^2 \\ \rho_\infty &= 0.002 \ kg/m^3 \\ T_\infty &= 295 \ K \end{aligned}$$

The same problem was calculated by Grossman & Walters [22], and Drikakis & Tsangaris [19], and therefore the results could be validated against previously published results.

The geometry of the blunt body is defined by a cylinder (R=1 m) extended by a wedge of 5 degree of incidence. This problem was resolved in both the ideal gas and the equilibrium gas model for comparison. The ideal gas solution was generated with the same free stream conditions and $\gamma = 1.4$. The computational meshes for both calculations are made of 41×81 grid points. Some attempts at mesh adaptation were made in order to refine the mesh along the shock wave to produce sharper resolution. Figures C.1 and C.2 show the two final meshes used for the perfect gas and the equilibrium calculations.

	Perfect gas ($\gamma = 1.4$)	Equilibrium air
p/p_∞	292.6	302.3
ρ/ρ_∞	6.13	12.0
T (K)	14081	5727
δ/R	0.387	0.219

Table 6.1: *Comparison of stagnation point values for Mach 15 blunt body problem*

Figures C.3 to C.10 show the isoline contours for Mach number, density, pressure, and temperature for both calculations. We note that the mesh refinement enables a very sharp resolution of the shock wave. As expected, the shock wave moves clearly closer to the body when the equilibrium reactions are included. We also note that the temperature gradients are much smaller for the equilibrium calculation. This is due by the dissociation reactions involved which are endothermic chemical processes and therefore slow down the increase in temperature for the equilibrium flow.

Figures C.11 to C.13 compare the distribution of pressure, temperature, and density along the symmetric line. The calculated pressure levels behind the shock are approximately similar in both the perfect gas and the equilibrium air model, which would prove that the pressure is hardly affected by the chemistry. However, equilibrium the temperature and density predictions are significantly different than those obtained by the perfect gas model. Density behind the shock increases and temperature decreases. The lower temperatures are the results of air dissociation and the increased specific heats at high temperature. As the shock stand-off distance is inversely proportional to the density ratio across the shock, the larger density ratio obtained for the equilibrium calculations explains why the shock is closer to the boundary.

Figures C.14 to C.16 shows the pressure, temperature and density distributions along the body surface. Again, the perfect gas and the equilibrium gas pressure distribution coincide, whereas there are significant differences in the temperature and density distributions, especially near the stagnation point. Table 6.1 compares the stagnation point values of pressure, density, and temperature as well as the shock stand-off [1] distance for perfect gas flow and equilibrium gas flow. All the above results are in good agreement with the corresponding results from the literature.

[1] distance from nose to shock

Species	Minimum values	Maximum values	Stagnation point values
O_2	0.02%	20.9%	0.02%
N_2	52.1%	78.9%	52.1%
O	0.0%	33.5%	31.5%
NO	0.0%	3.7%	0.68%
N	0.0%	14.9%	14.9%
Ar	0.74%	0.96%	0.74%

Table 6.2: *Minimum, maximum, and stagnation point values of the different species mole fractions for Mach 15 blunt body problem*

Species mole fraction contours for the equilibrium calculation are shown in figure C.17 to C.21, and table 6.2 gives the minimum, maximum, and the stagnation point values of the different species mole fractions. Oxygen dissociates nearly completely in the stagnation region. Nitrogen dissociates to a lesser extent. At the stagnation point, the gas is made approximatly of 31% monoatomic oxygen, 15% monoatomic nitrogen, and 52% diatomic nitrogen. The amount of NO never exceeds 3.7%.

6.3 Hypersonic Hyperbola Problem (Viscous Flow)

Validation of the Navier-Stokes code was performed for a hypersonic viscous flow over a hyperbola. Calculations were carried out for both the ideal gas flow and the equilibrium flow with a free stream Mach number $M = 10$ and a Reynolds number $Re = 1.2 \times 10^4$. Reference conditions correspond to atmospheric conditions at an altitude of 52 kilometers [19, 15],

$$\begin{aligned} p_\infty &= 48.67 \ N/m^2 \\ \rho_\infty &= 7.7 \times 10^{-4} \ kg/m^3 \\ T_\infty &= 225 \ K \end{aligned}$$

The no-slip condition for the velocity ($U_w = 0$) and the adiabatic wall condition ($(\partial T/\partial n)_w = 0$) for the temperature were used at the wall boundary. The hyperbola is given by the equation

$$\left(\frac{x}{500mm} + 1\right)^2 - \left(\frac{y}{88mm}\right)^2 = 1$$

	Perfect gas ($\gamma = 1.4$)	Equilibrium air
p/p_∞	129.4	133.5
ρ/ρ_∞	6.01	9.35
T (K)	4840	2945
δ (mm)	1.2	0.7

Table 6.3: *Comparison of stagnation point values for Mach 10 hyperbola problem*

Figures D.17 shows the computational grid used for both the ideal gas and the equilibrium calculations. The mesh consists of 61 $\times$ 61 grid points.

Isoline contours are given in figures D.1 to D.8 for Mach number, density, pressure and temperature for both calculations. The pressure, temperature and density distributions along symmetric line are given in D.9 to D.11, and the wall distributions for pressure, temperature, and density are given in figures D.12 to D.14. Table 6.3 compares the stagnation point values of pressure, density, and temperature as well as the shock stand-off distance for both calculations. The same comments as those already made for the previous test case remain valid here. The pressure field is quite similar in both cases although the shock wave stands closer to the body for the equilibrium flow. The main differences between the perfect gas and the equilibrium gas flow are in the temperature and density predictions.

The surface distribution for pressure coefficient C_p and skin friction C_f are given in figures D.15 and D.16. The heat transfer distribution has no real significance for this test case since the wall of the hyperbola was assumed to be adiabatic. The present results exhibit a slight difference for the skin friction distribution compared with the previously published results [19, 15]. The skin friction coefficient is a very sensitive numerical quantity since it is calculated from the velocity gradient normal to the wall, and is therefore heavily influenced by the mesh and the repartition of the grid points in the boundary layer. A finer mesh near the wall would probably produce more accurate results. The differences may also be explained by a different modelization of the transport coefficients μ and k.

Conclusions

The present equilibrium air model has been implemented and tested on high Mach number and high Reynolds number flows over two-dimensional blunt body shapes. Good results have been obtained and comparison have been made between perfect gas and equilibrium flow, which lead to the following conclusions.

The pressure field is hardly affected by the chemistry, the main differences arising from the density and temperature predictions behind the shock. Density behind the shock increases and temperature decreases. Due to a larger density ratio across the shock for the equilibrium calculation, the shock wave stands closer to the body.

The physical model presented here to compute the chemical composition and the thermodynamic properties of the gas mixture provides more suitable and more flexible technique over any curve fitting technique. The chemical composition can easily be modified to represent different standard conditions and the model can easily be extended to account for ionization by including additional species.

The greatest disadvantage of using this technique is in the iterative process used to invert the general equation of state. This has proven to increase significantly the computational time. It was shown however that the chemical routine could be called every five, ten or twenty iterations without affecting the convergence nor the accuracy of the solution. Further improvements may be obtained in that direction in order to reduce the call of the chemistry routine. This can be achieved by defining a local equivalent ratio of specific heats $\bar{\gamma}$ as

$$\bar{\gamma} = 1 + \frac{p}{\rho e}$$

This equivalent $\bar{\gamma}$, which will vary over the whole flow field, can be updated every ten or twenty iterations by the chemistry routine. This would allow the code to run as for a perfect gas computation. This should significantly decrease the computational time and consequently make the equilibrium code more efficient.

Some attempts at mesh refinement have been made with success and should be pursued in order to provide more suitable meshes for choked flows and viscous flows.

Appendix A

Equilibrium Air Model

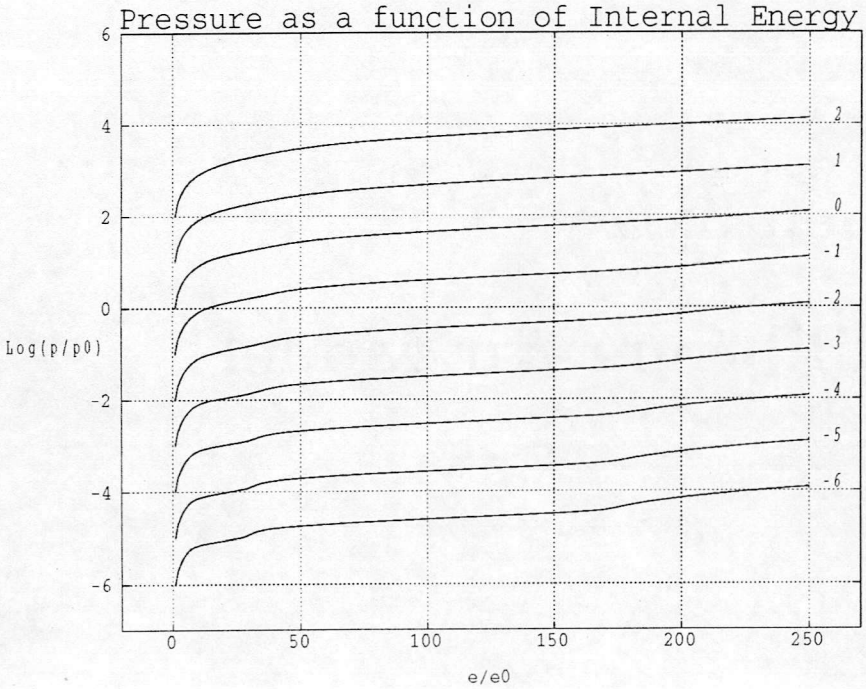

Figure A.1: *Pressure as a function of internal energy for constant values of* $log_{10}(\rho/\rho_0)$

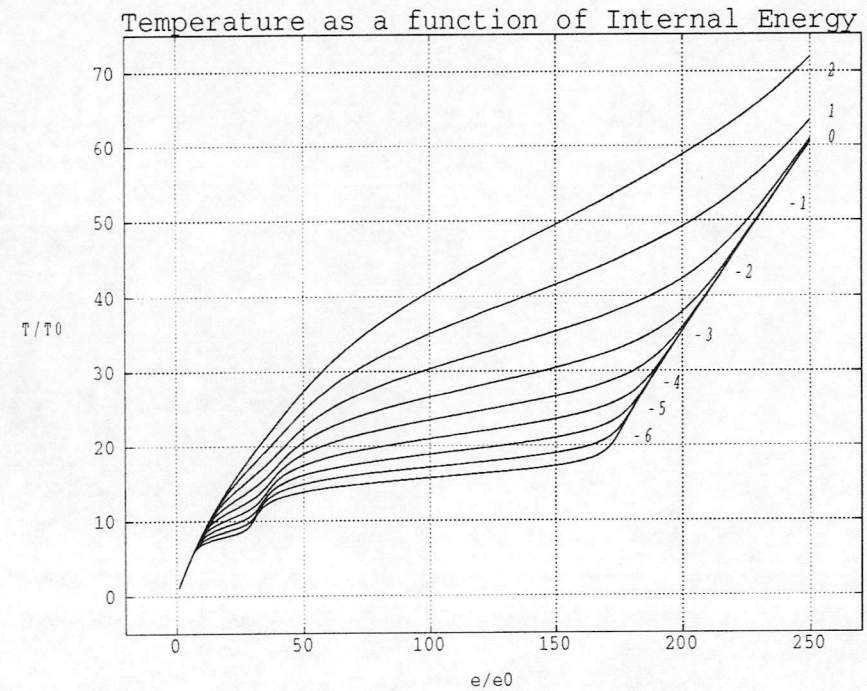

Figure A.2: *Temperature as a function of internal energy for constant values of* $log_{10}(\rho/\rho_0)$

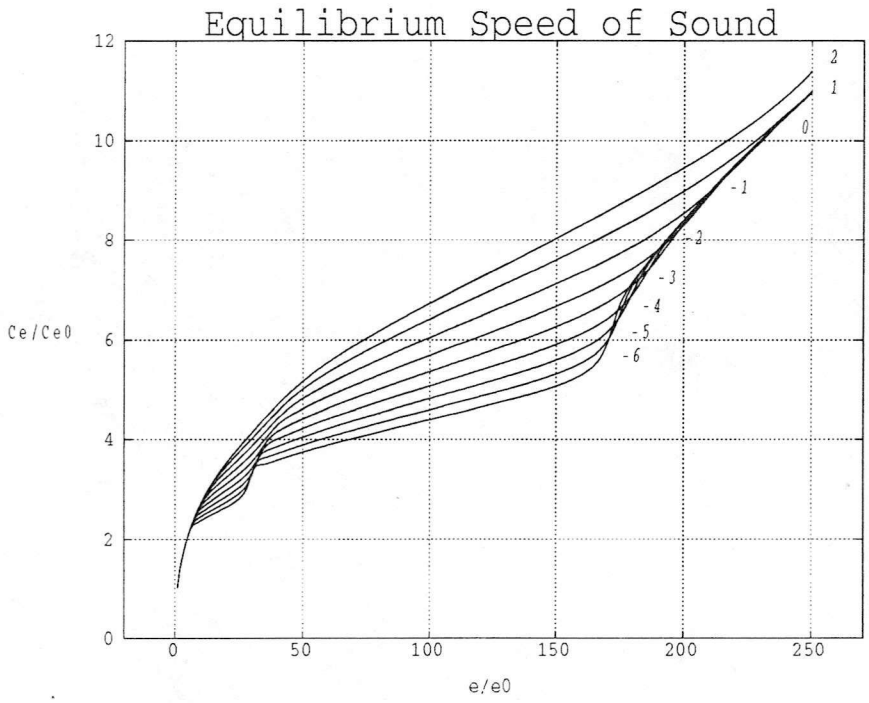

Figure A.3: *Equilibrium speed of sound as a function of internal energy for constant values of* $log_{10}(\rho/\rho_0)$

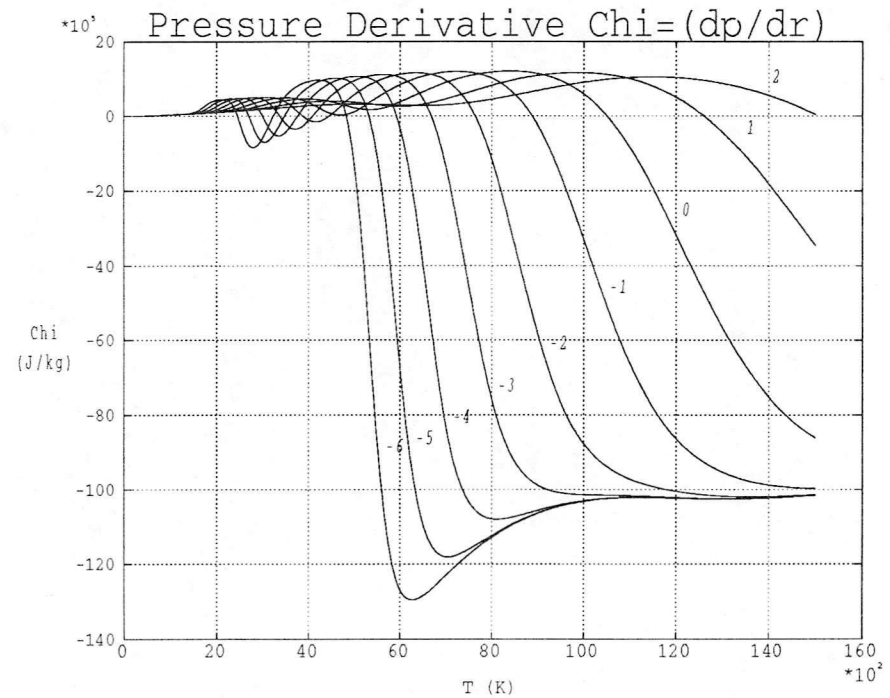

Figure A.4: *Pressure derivative* $\chi = (\partial p/\partial \rho)_\epsilon$ *as a function of temperature for constant values of* $log_{10}(\rho/\rho_0)$

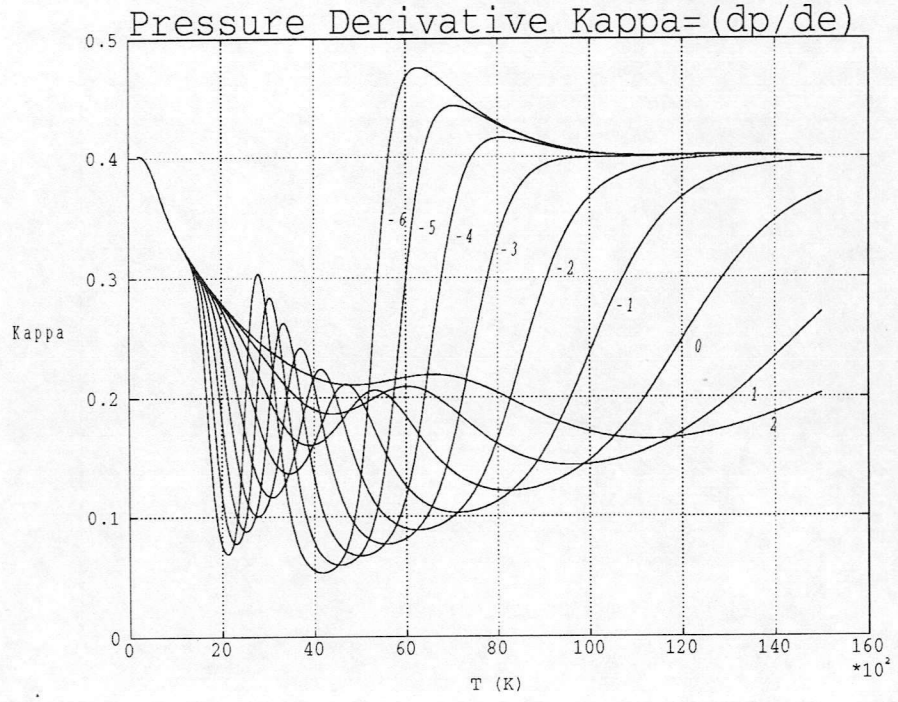

Figure A.5: *Pressure derivative* $\kappa = (\partial p/\partial \epsilon)_\rho$ *as a function of temperature for constant values of* $log_{10}(\rho/\rho_0)$

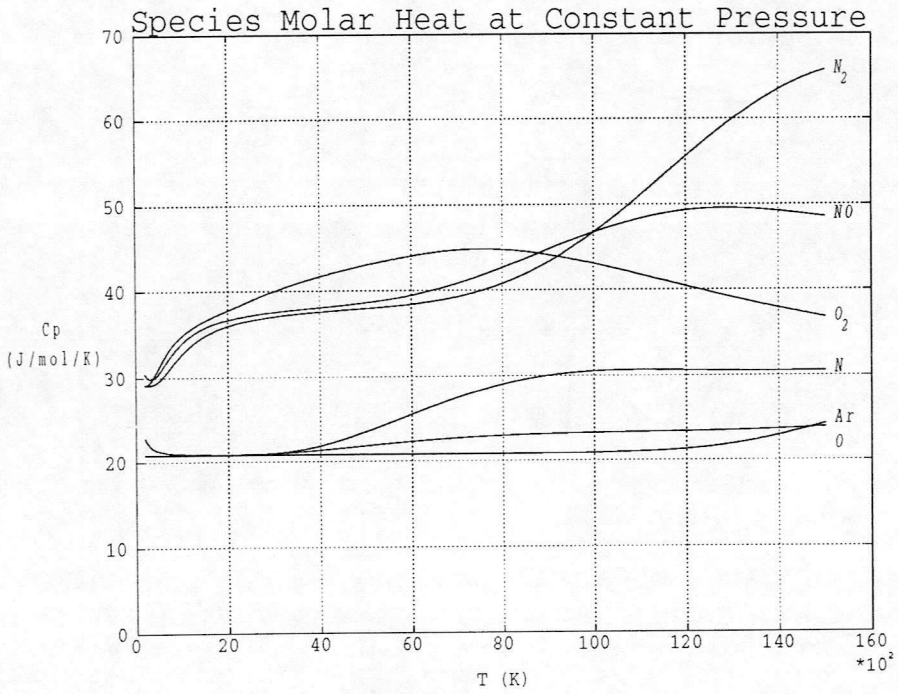

Figure A.6: *Species molar heat at constant pressure* $\hat{c}_p$*as a function of temperature. Curve fit calculation*

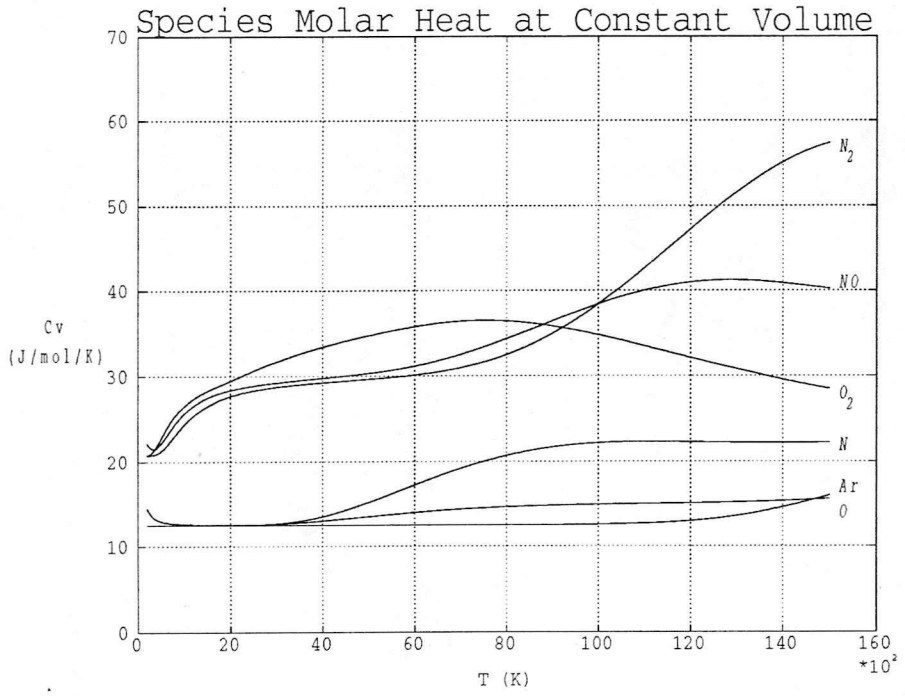

Figure A.7: *Species molar heat at constant volume $\hat{c}_v$ as a function of temperature.* $\hat{c}_v = \hat{c}_p - \hat{R}$

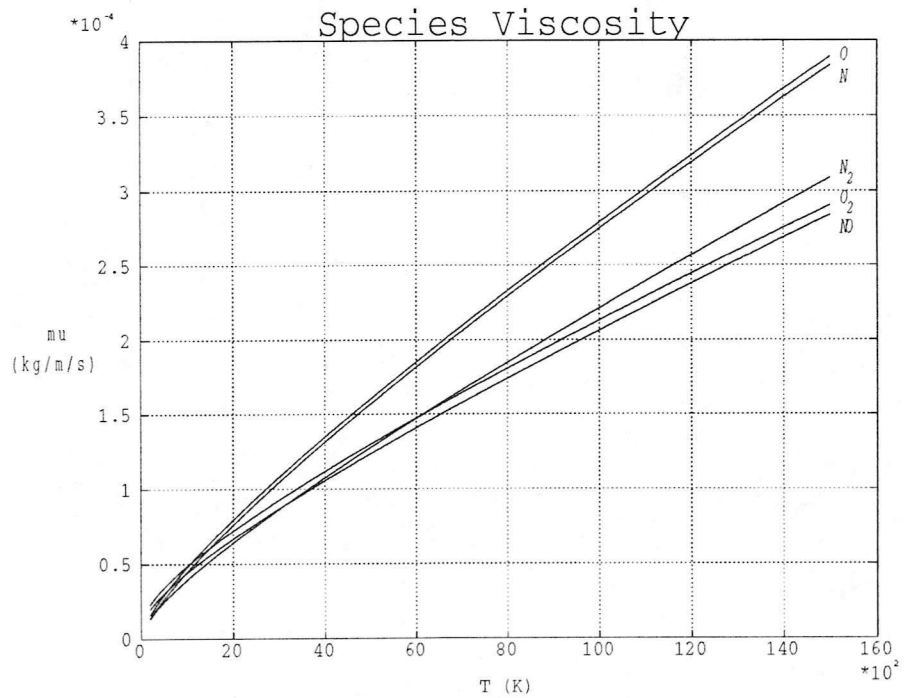

Figure A.8: *Species viscosity μ_i as a function of temperature. Curve fit calculation.*

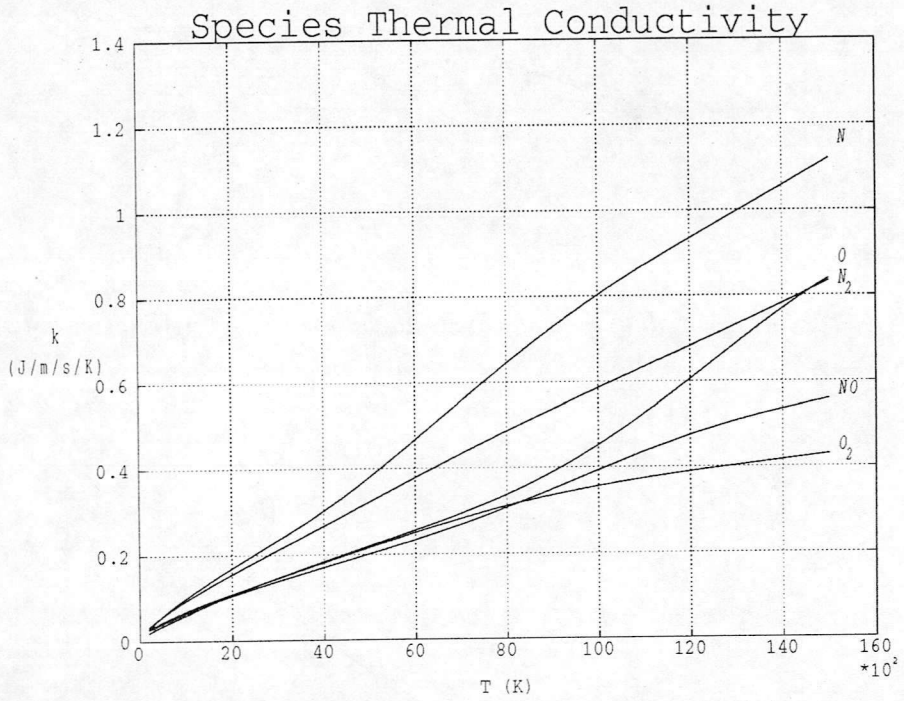

Figure A.9: *Species thermal conductivity k_i as a function of temperature. Curve fit calculation.*

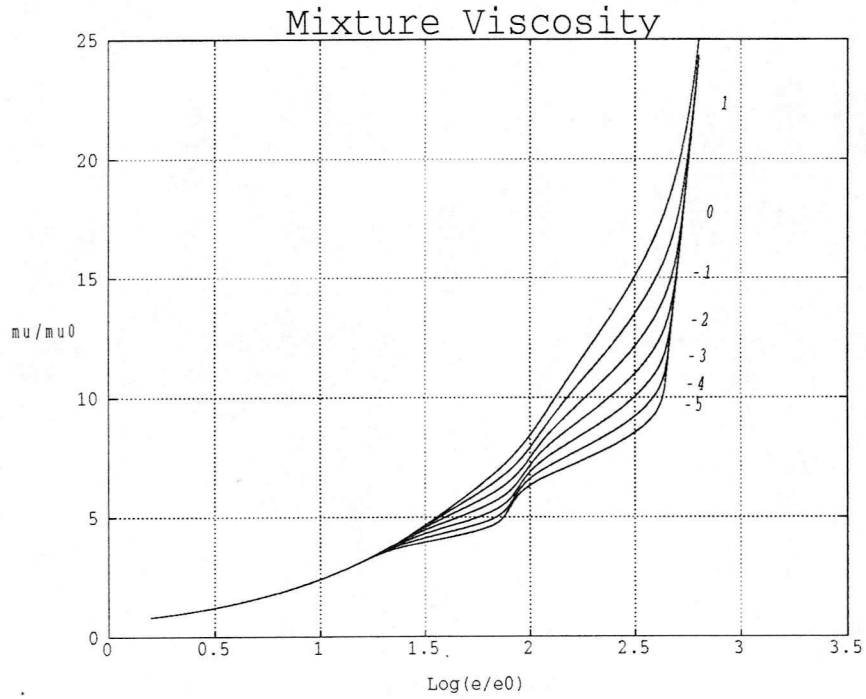

Figure A.10: *Mixture viscosity μ as a function of internal energy for constant values of $log_{10}(\rho/\rho_0)$*

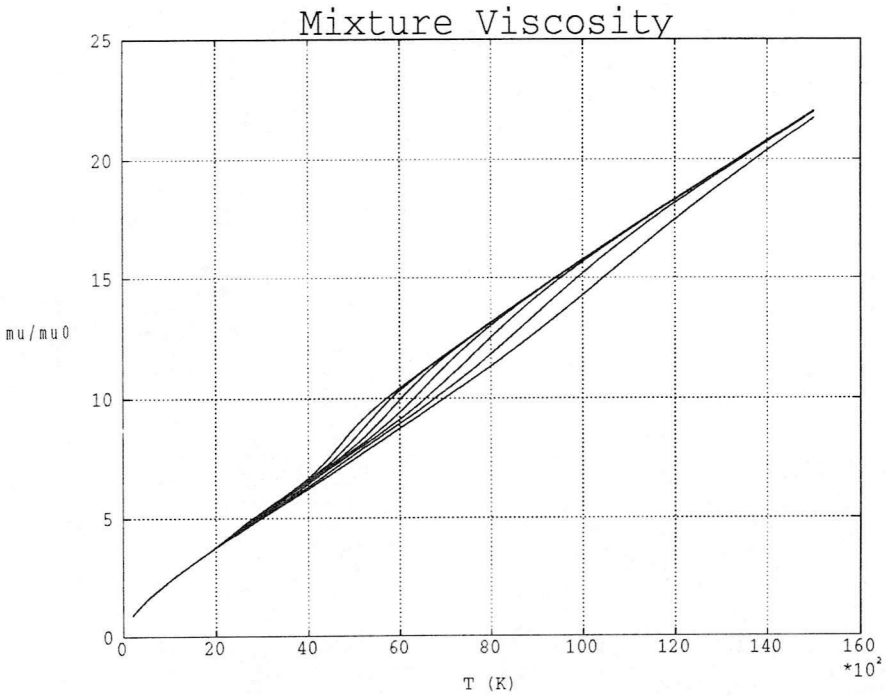

Figure A.11: *Mixture viscosity μ as a function of temperature for constant values of $log_{10}(\rho/\rho_0)$*

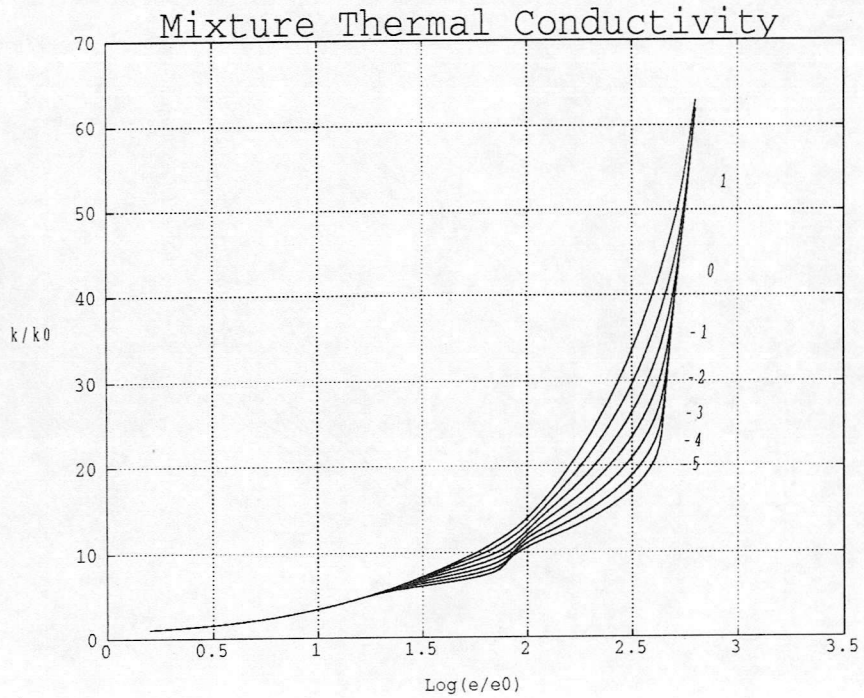

Figure A.12: *Mixture thermal conductivity k as a function of internal energy for constant values of* $log_{10}(\rho/\rho_0)$

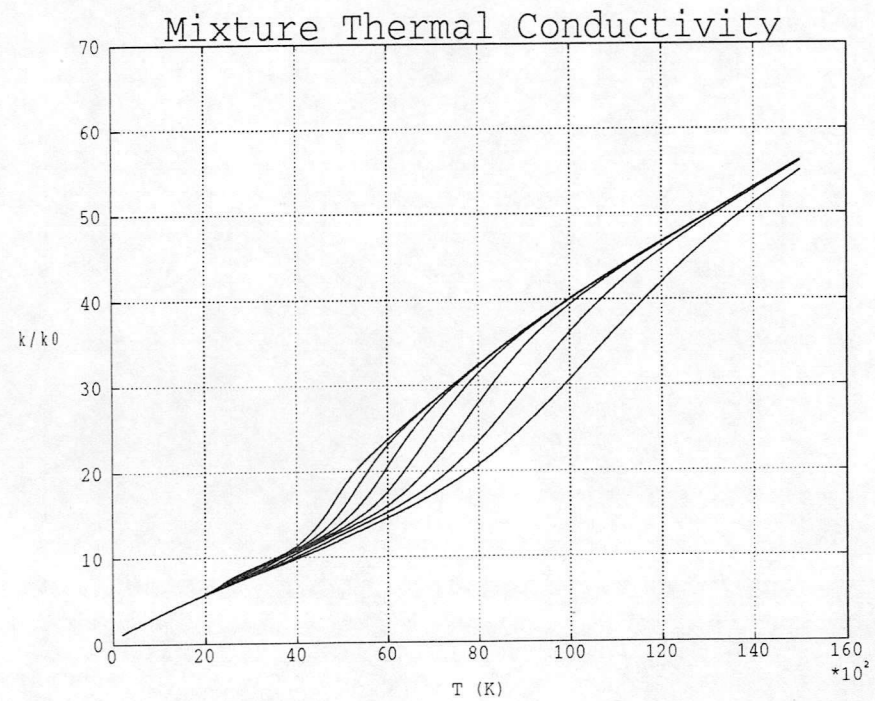

Figure A.13: *Mixture thermal conductivity k as a function of temperature for constant values of* $log_{10}(\rho/\rho_0)$

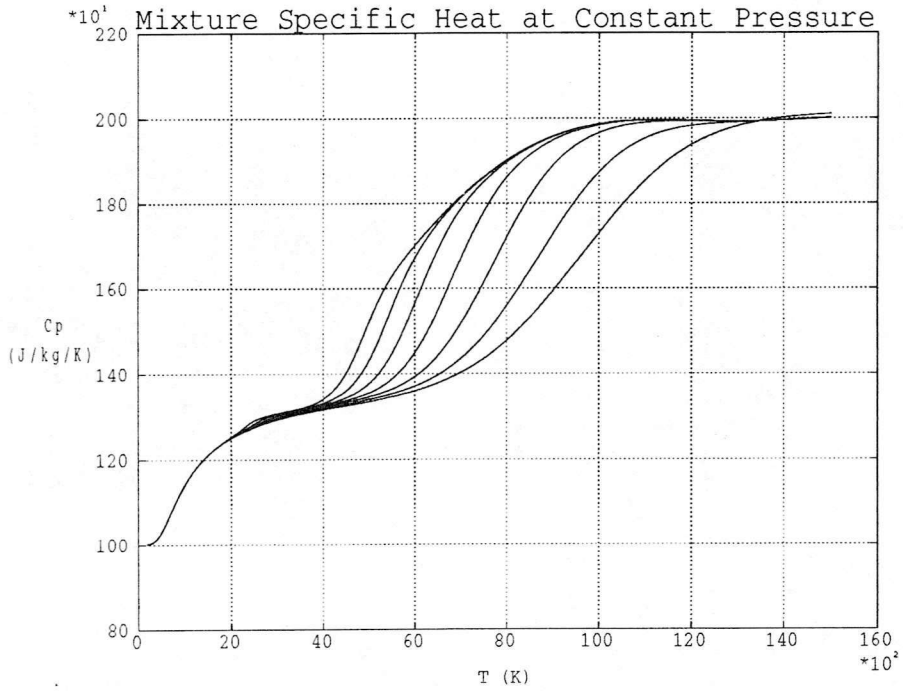

Figure A.14: *Mixture specific heat at constant pressure c_p as a function of temperature for constant values of $log_{10}(\rho/\rho_0)$*

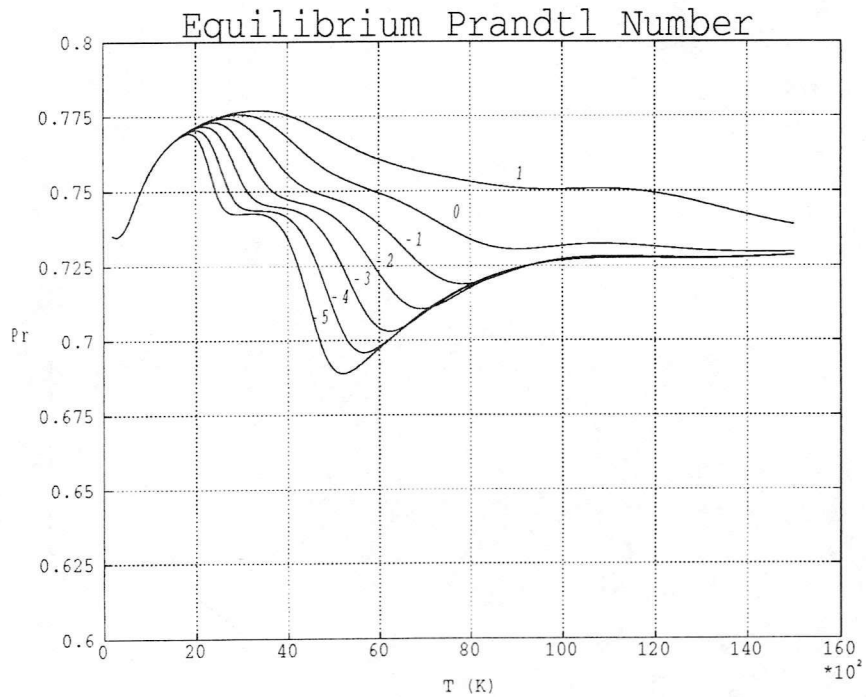

Figure A.15: *Equilibrium Prandtl number Pr_e as a function of temperature for constant values of $log_{10}(\rho/\rho_0)$*

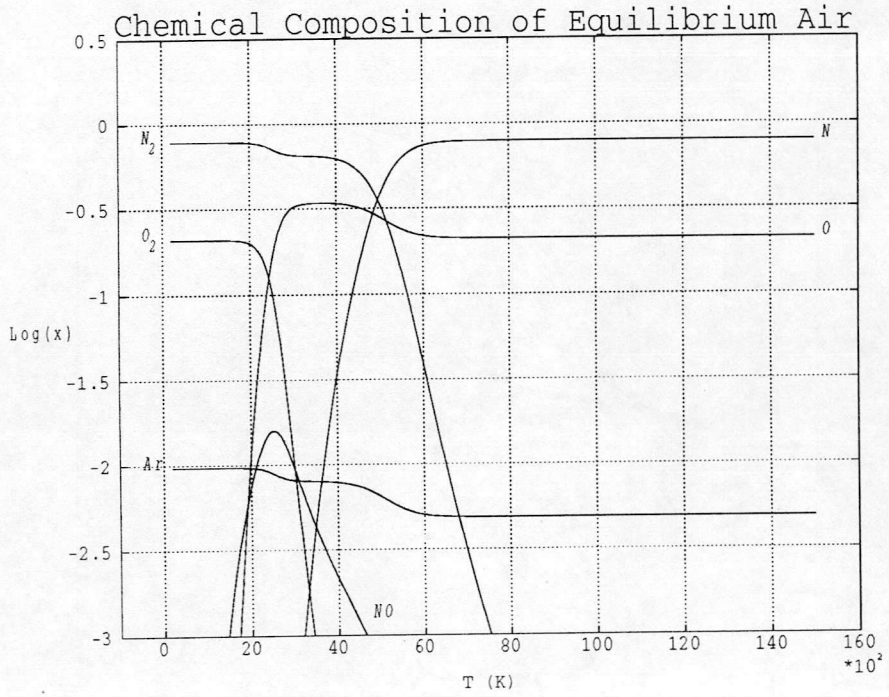

Figure A.16: *Chemical composition of equilibrium air as a function of temperature.* $\rho = 1.225x10^{-4} kg/m^3$

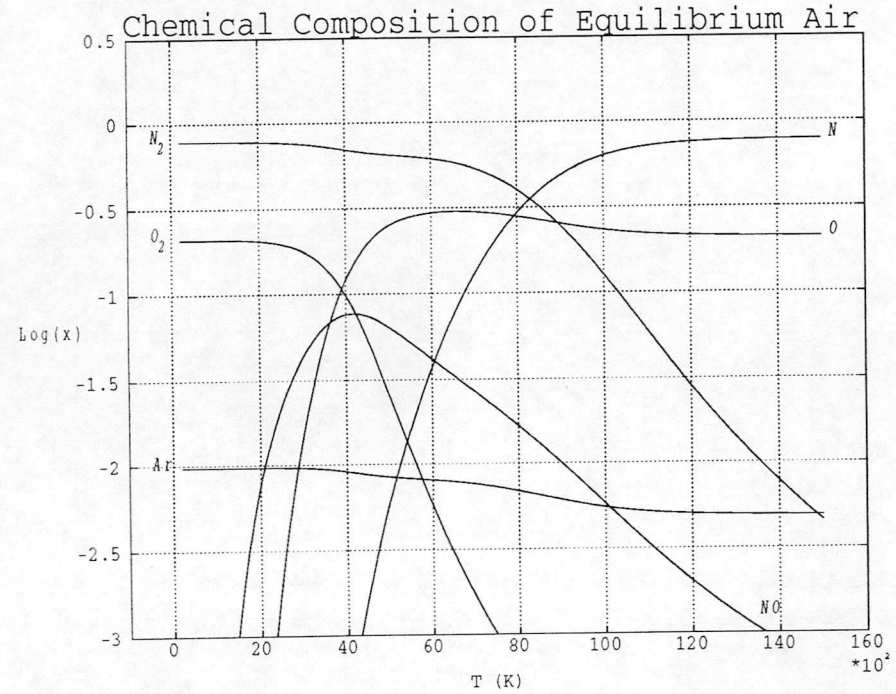

Figure A.17: *Chemical composition of equilibrium air as a function of temperature.* $\rho = 1.225 kg/m^3$

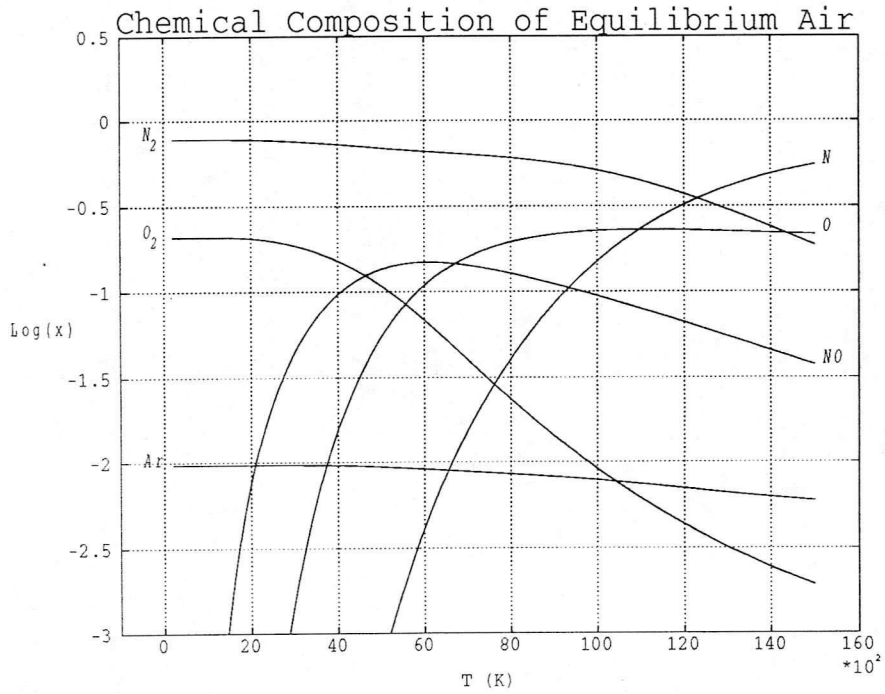

Figure A.18: *Chemical composition of equilibrium air as a function of temperature.* $\rho = 122.5 kg/m^3$

Appendix B

Hypersonic Expansion Nozzle Problem

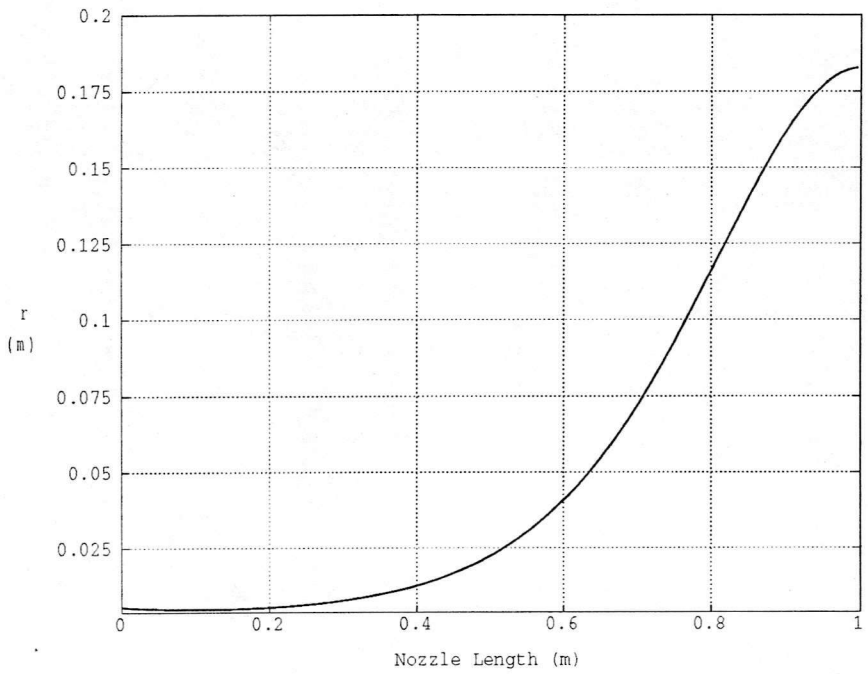

Figure B.1: *Nozzle radius variation.*

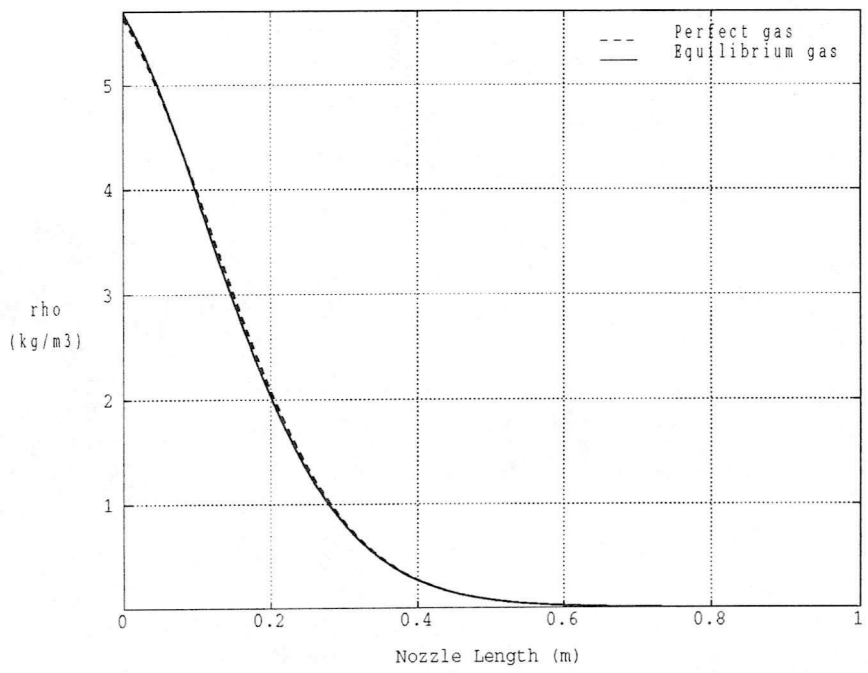

Figure B.2: *Density variation.*

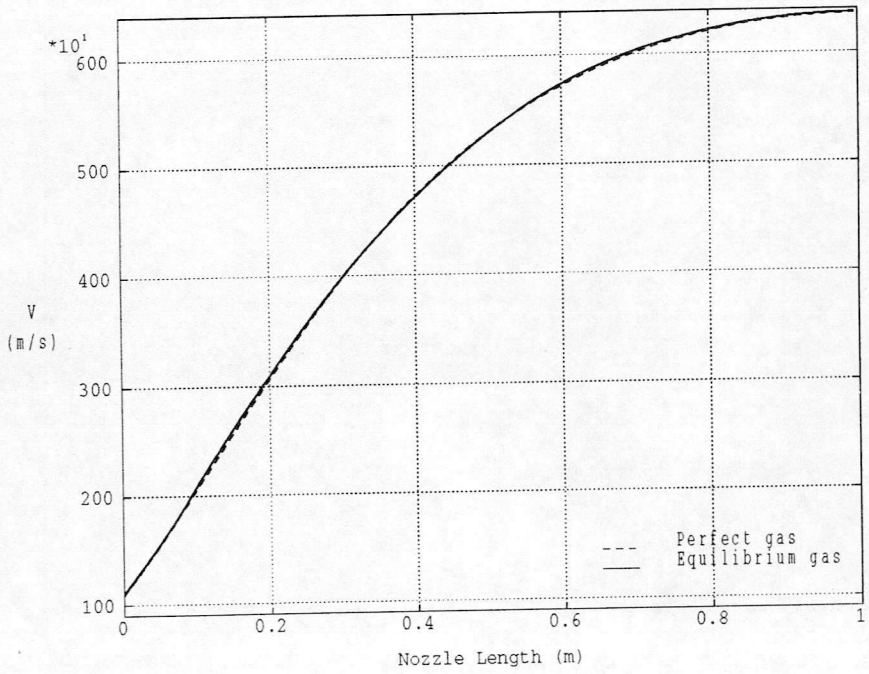

Figure B.3: *Velocity variation.*

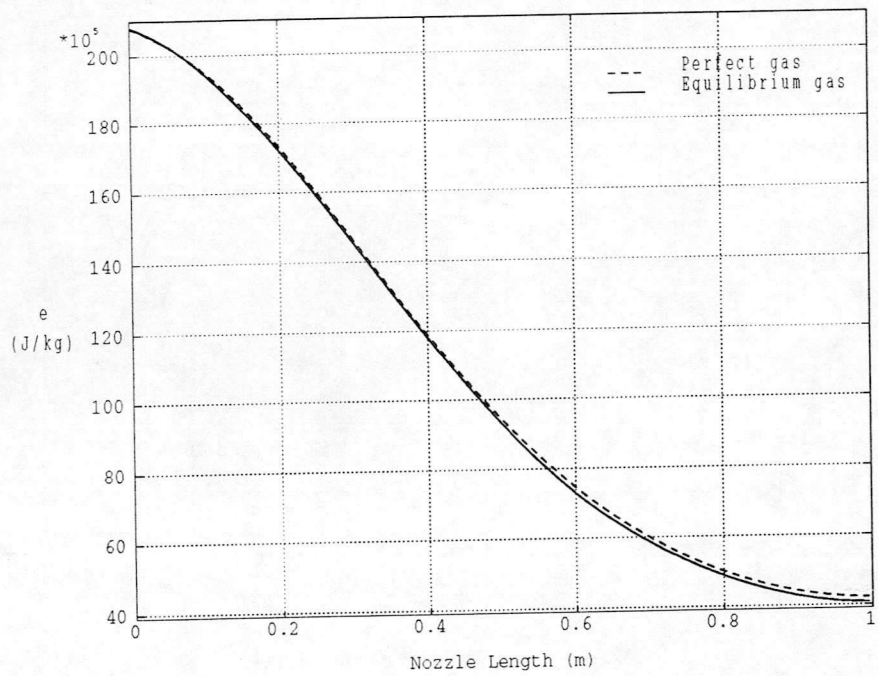

Figure B.4: *Internal energy variation.*

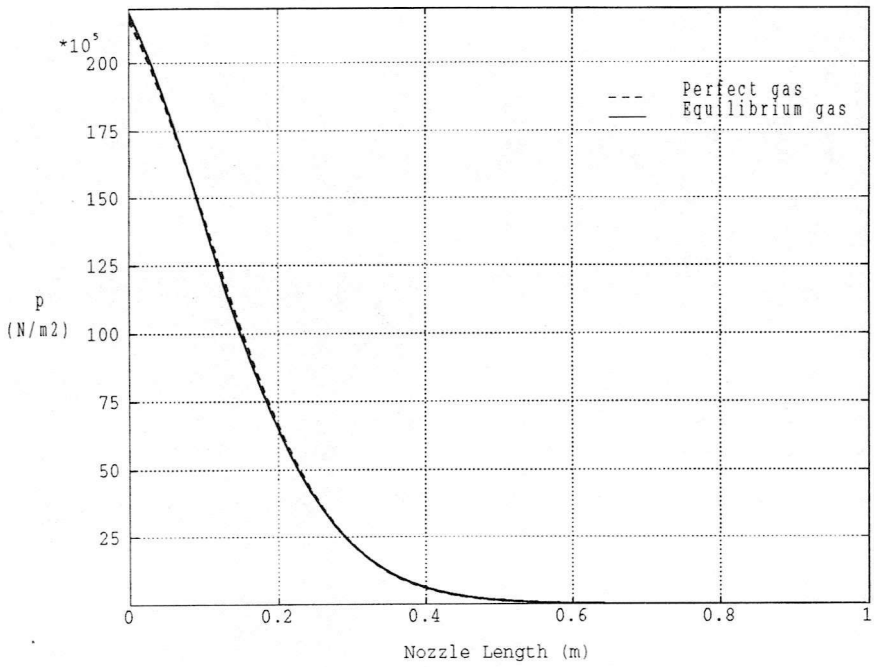

Figure B.5: *Static pressure variation.*

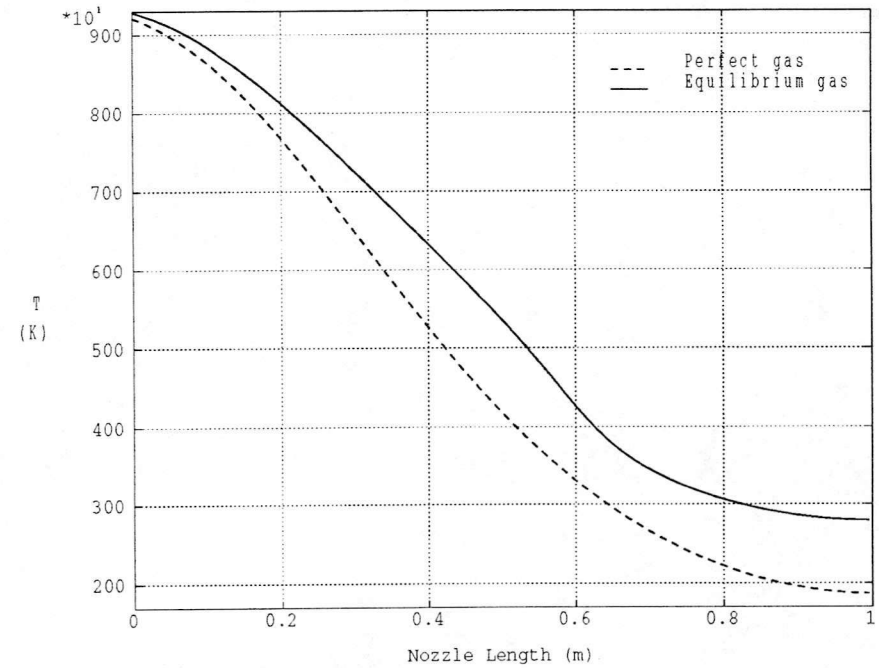

Figure B.6: *Temperature variation.*

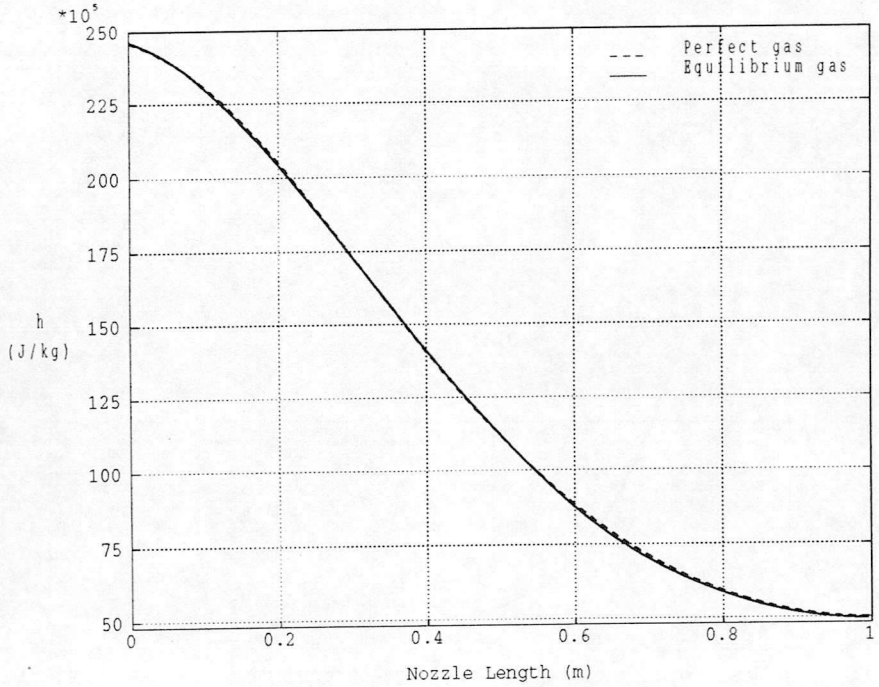

Figure B.7: *Specific enthalpy variation.*

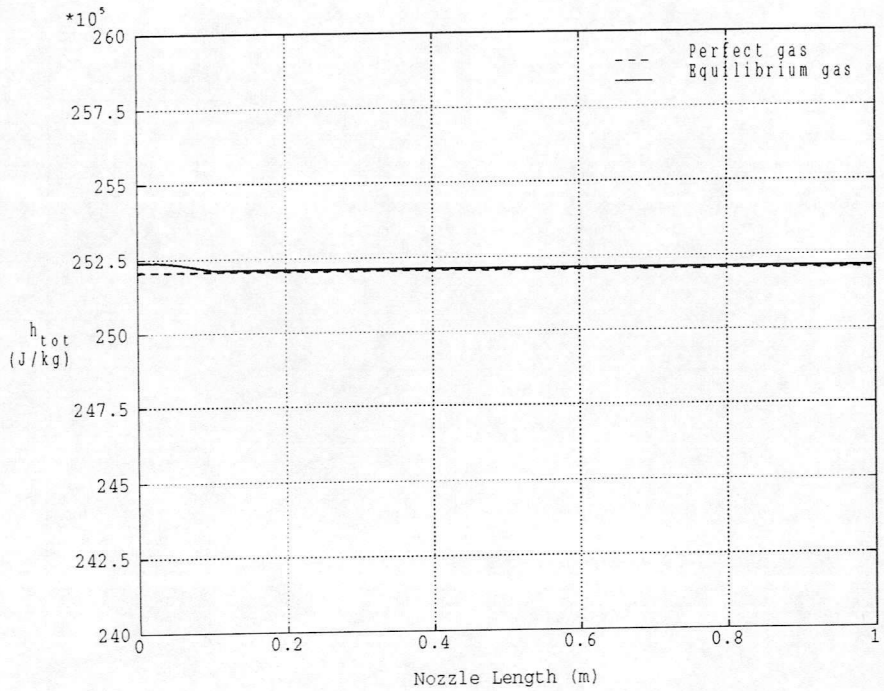

Figure B.8: *Total enthalpy variation.*

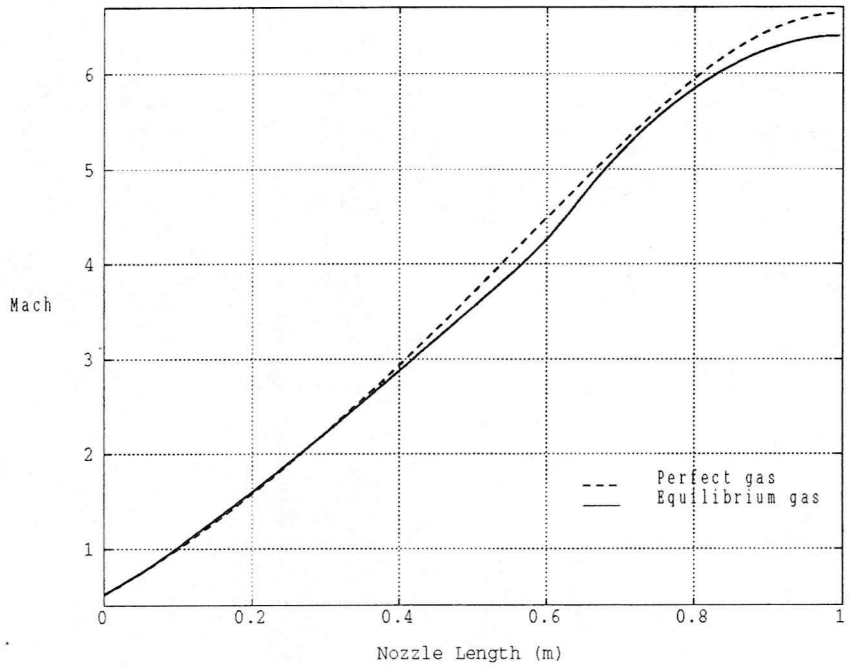

Figure B.9: *Mach number variation.*

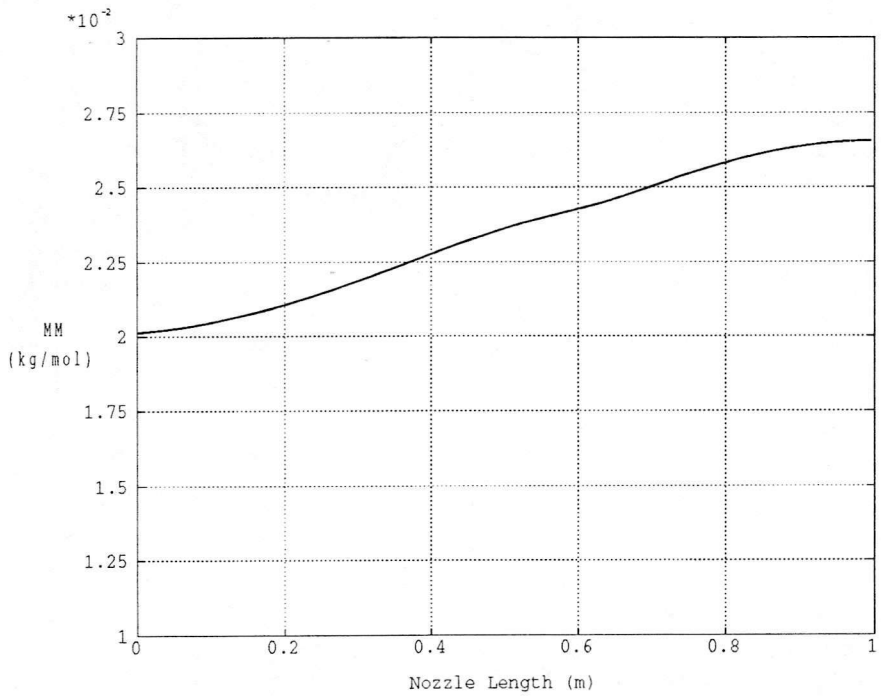

Figure B.10: *Molar mass variation.*

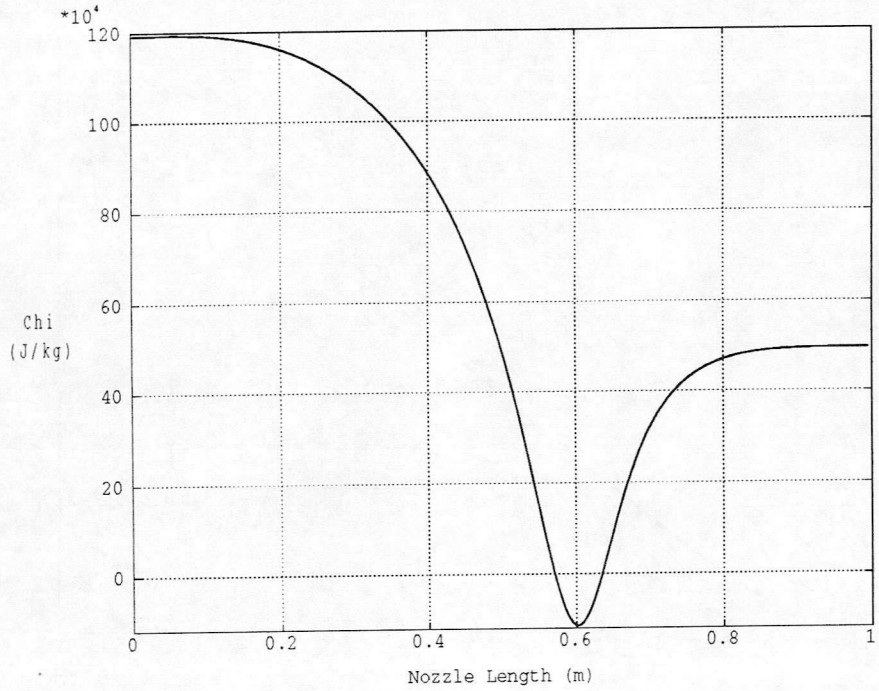

Figure B.11: *Pressure derivative* $\chi = (\partial p/\partial \rho)_\epsilon$ *variation.*

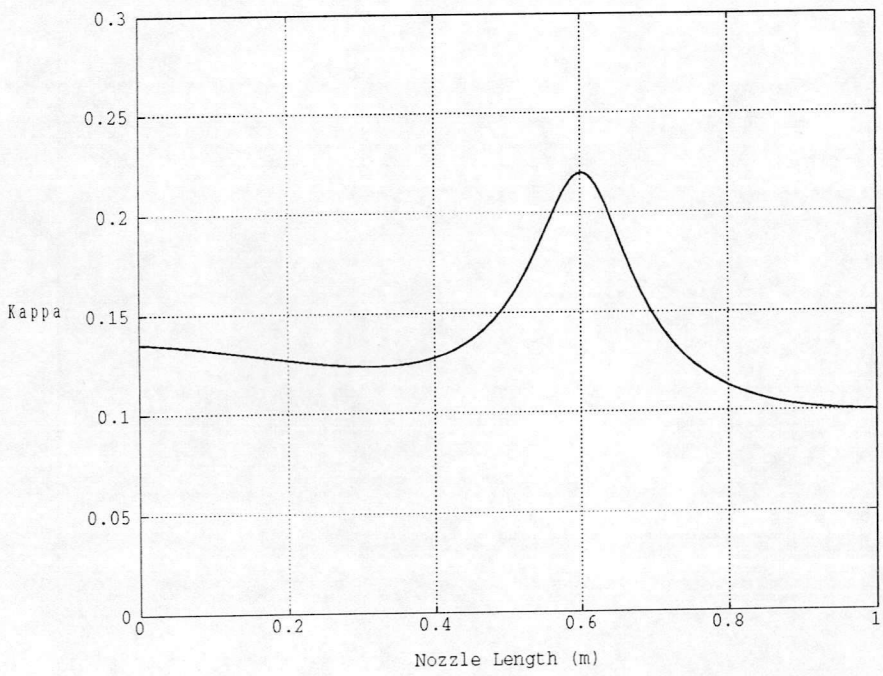

Figure B.12: *Pressure derivative* $\kappa = (\partial p/\partial \epsilon)_\rho$ *variation.*

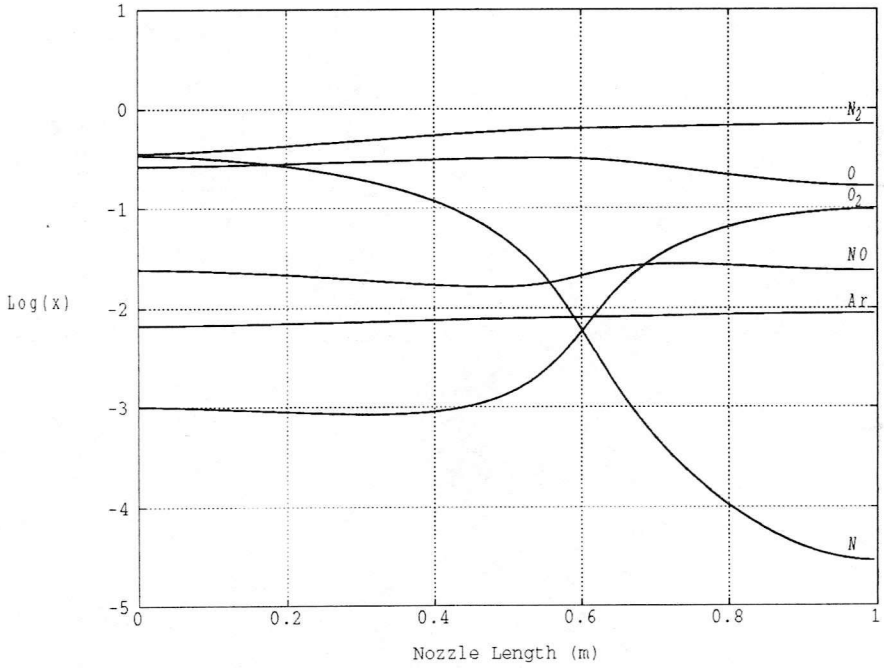

Figure B.13: *Chemical composition of equilibrium air. Species mole fractions* x_i.

Appendix C

Hypersonic Blunt Body Problem

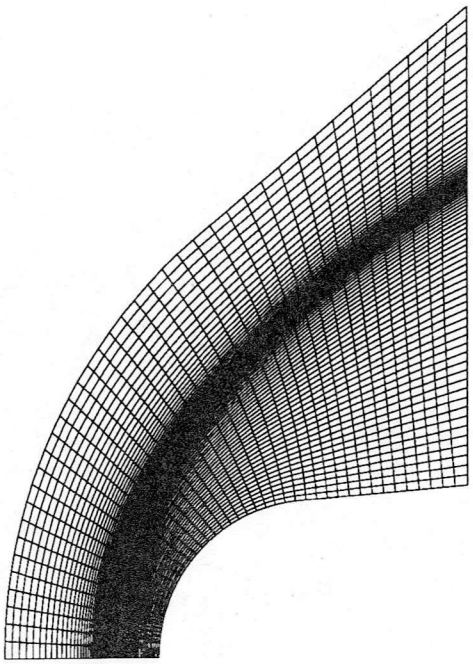

Figure C.1: *Mesh for perfect gas model* (40×80)

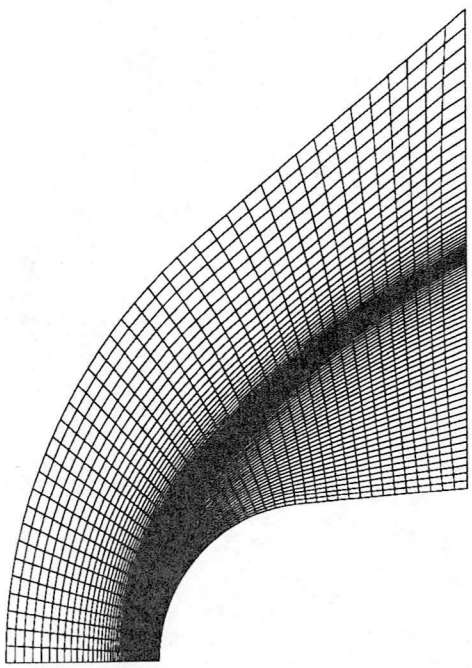

Figure C.2: *Mesh for equilibrium gas model* (40×80)

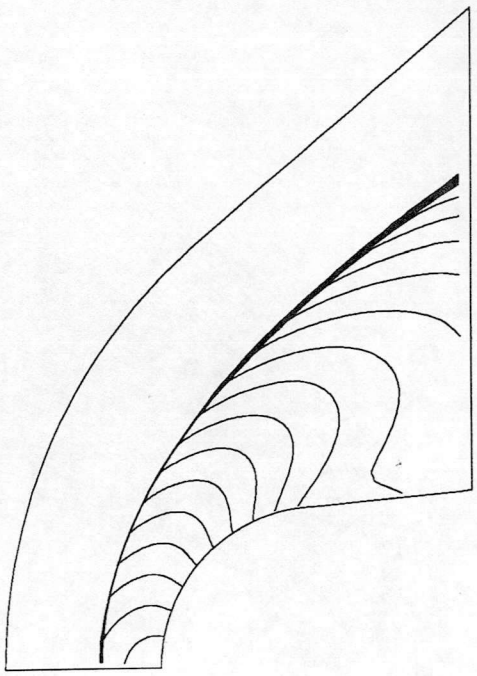

Figure C.3: *Mach number contours (Perfect gas)* - $\Delta M = 0.2$

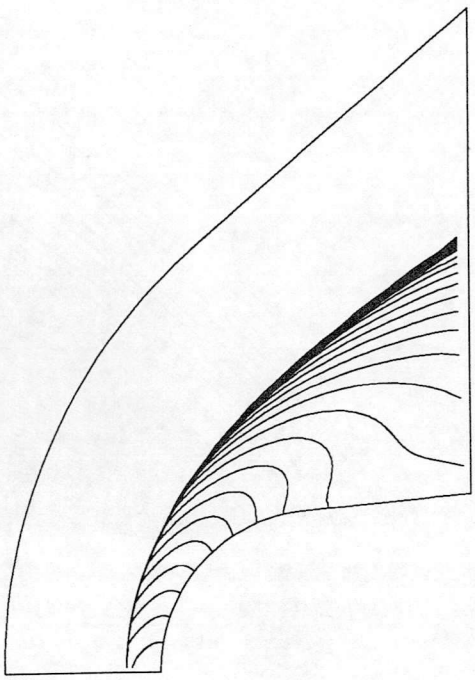

Figure C.4: *Mach number contours (Equilibrium gas)* - $\Delta M = 0.2$

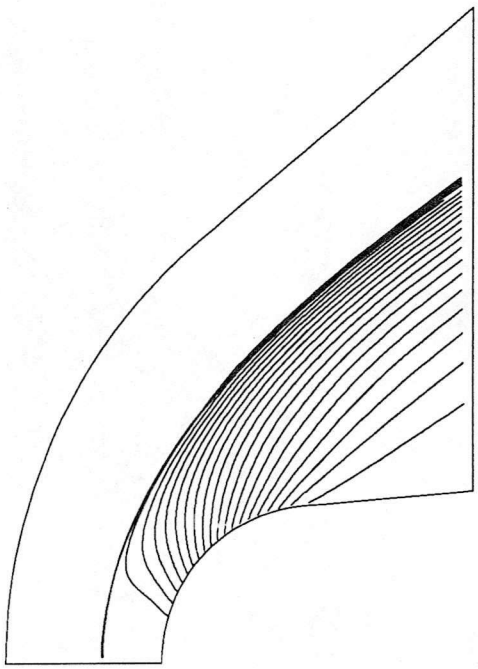

Figure C.5: *Density contours (Perfect gas)* - $\Delta\rho = 0.5 \times 10^{-3}$

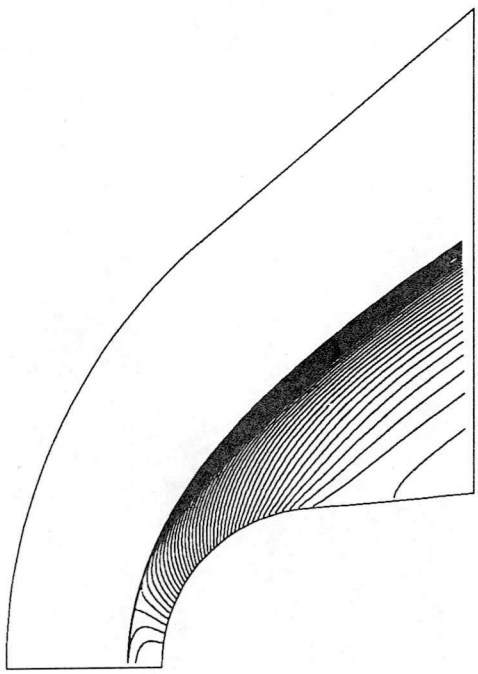

Figure C.6: *Density contours (Equilibrium gas)* - $\Delta\rho = 0.5 \times 10^{-3}$

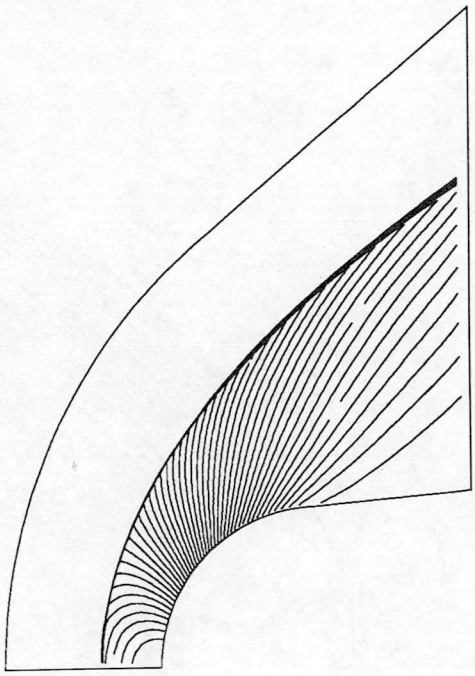

Figure C.7: *Pressure contours (Perfect gas)* - $\Delta p = 1000$

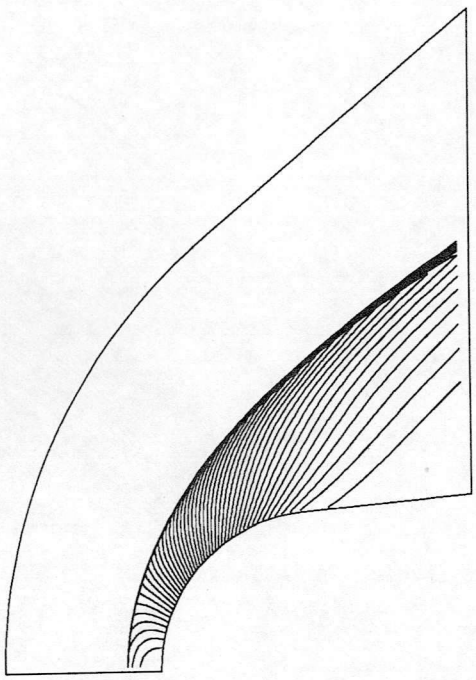

Figure C.8: *Pressure contours (Equilibrium gas)* - $\Delta p = 1000$

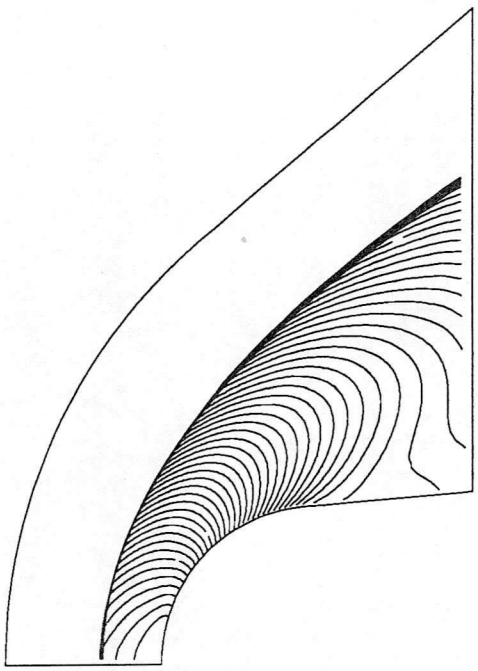

Figure C.9: *Temperature contours (Perfect gas)* - $\Delta T = 200$

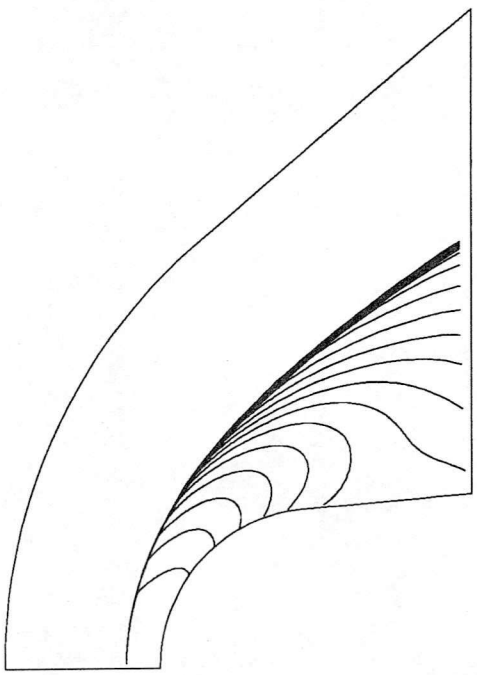

Figure C.10: *Temperature contours (Equilibrium gas)* - $\Delta T = 200$

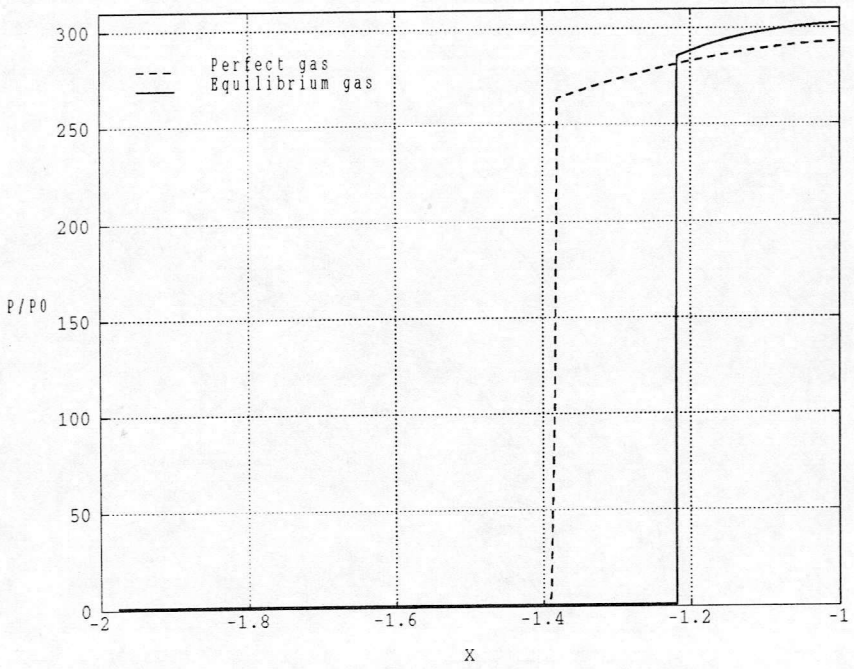

Figure C.11: *Pressure distribution along symmetric line*

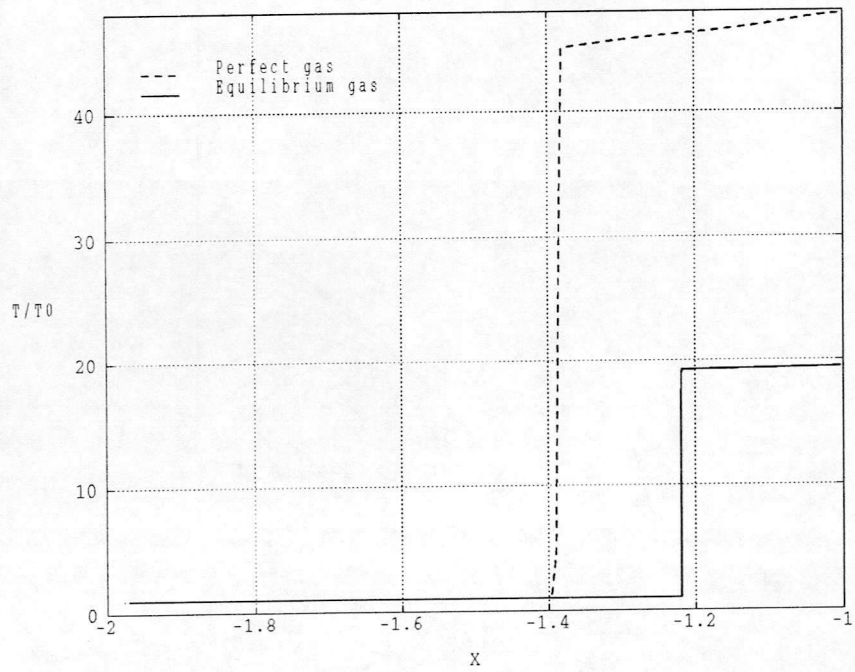

Figure C.12: *Temperature distribution along symmetric line*

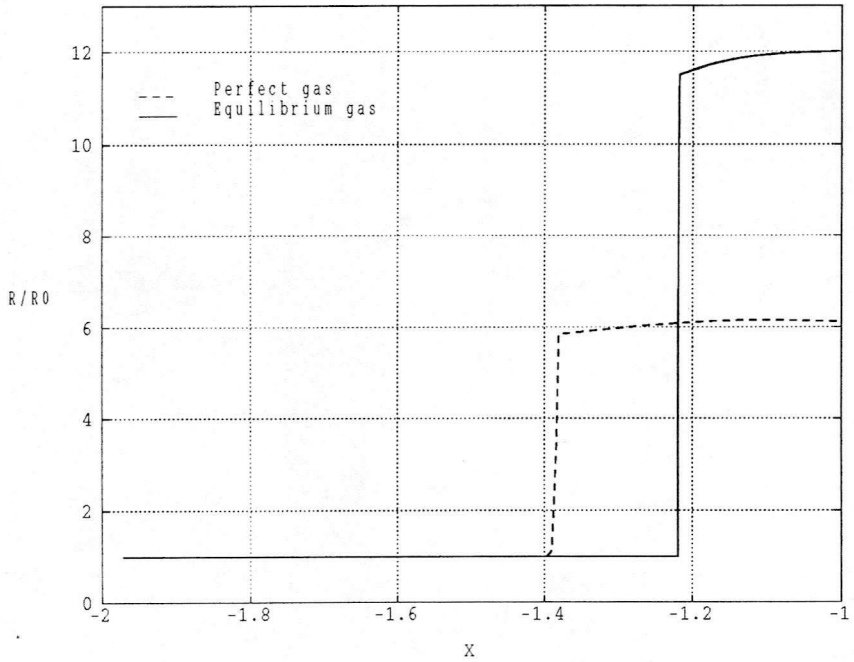

Figure C.13: *Density distribution along symmetric line*

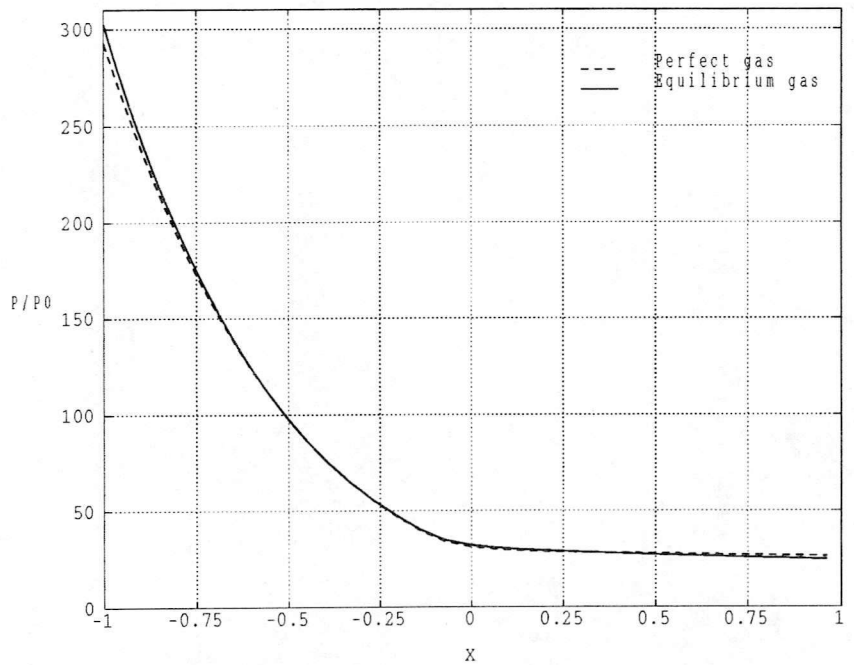

Figure C.14: *Pressure distribution along body surface*

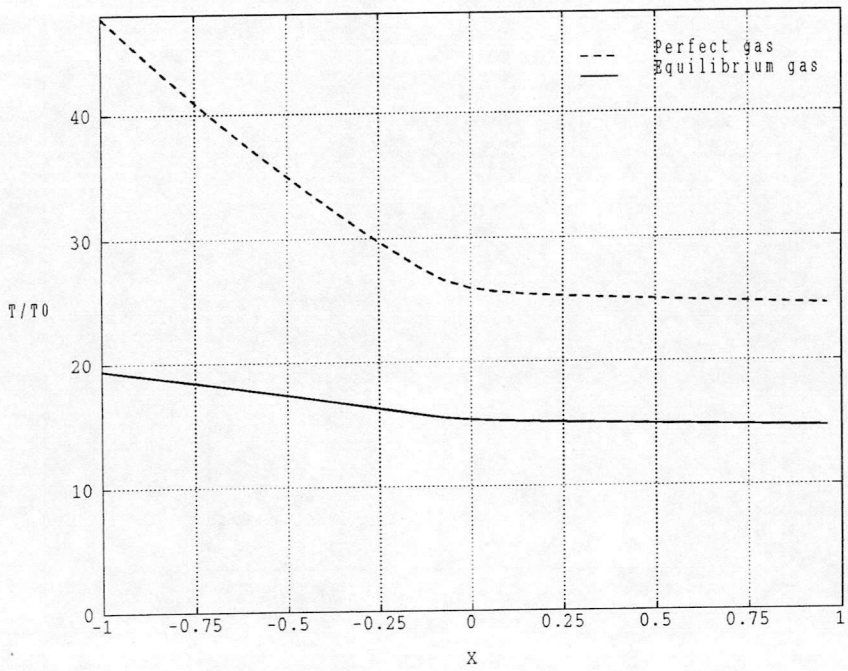

Figure C.15: *Temperature distribution along body surface*

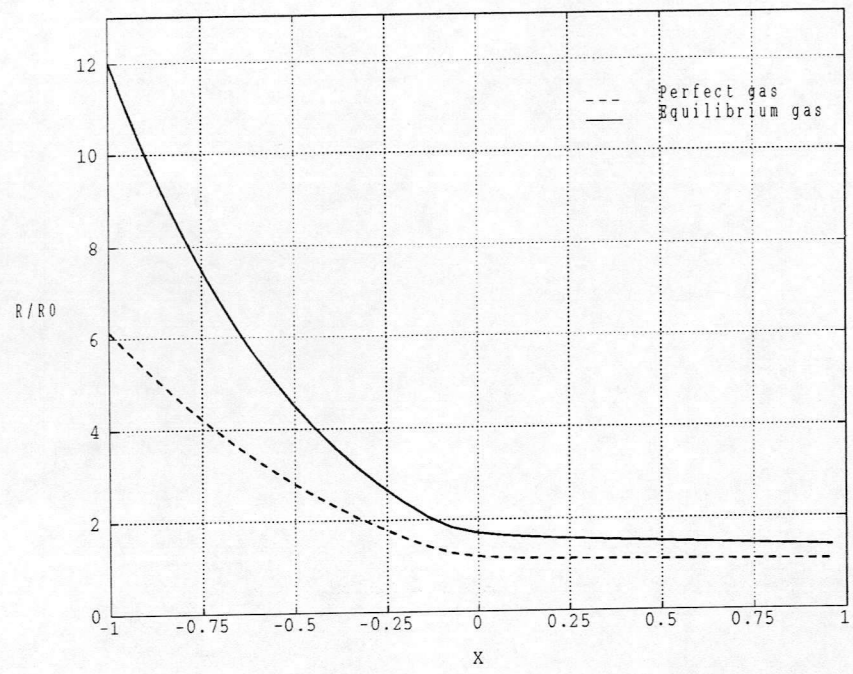

Figure C.16: *Density distribution along body surface*

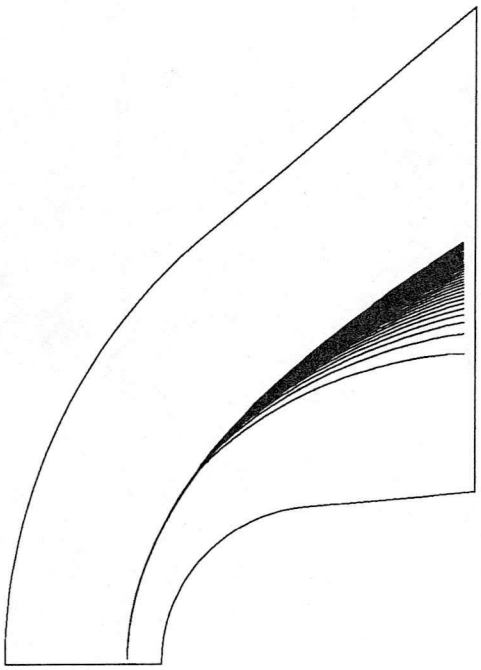

Figure C.17: *Species mole fraction contours for* O_2 - $\Delta x_{O_2} = 0.5 \times 10^{-2}$

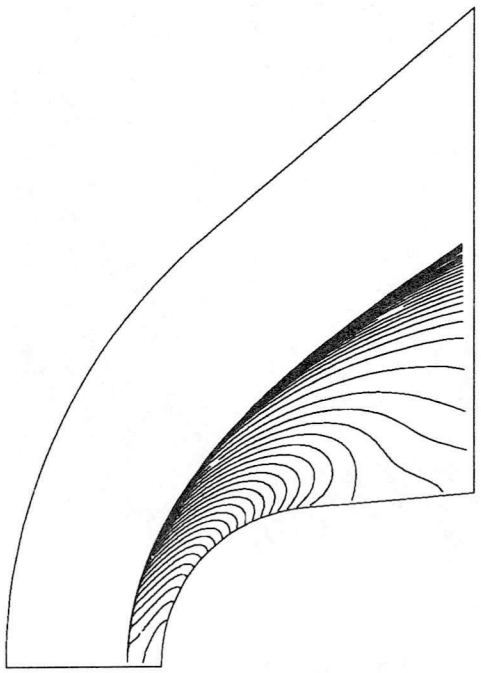

Figure C.18: *Species mole fraction contours for* N_2 - $\Delta x_{N_2} = 0.5 \times 10^{-2}$

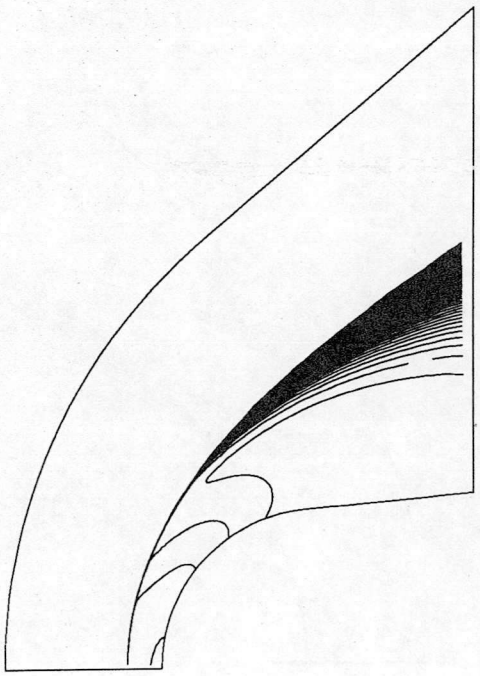

Figure C.19: *Species mole fraction contours for O* - $\Delta x_O = 0.5 \times 10^{-2}$

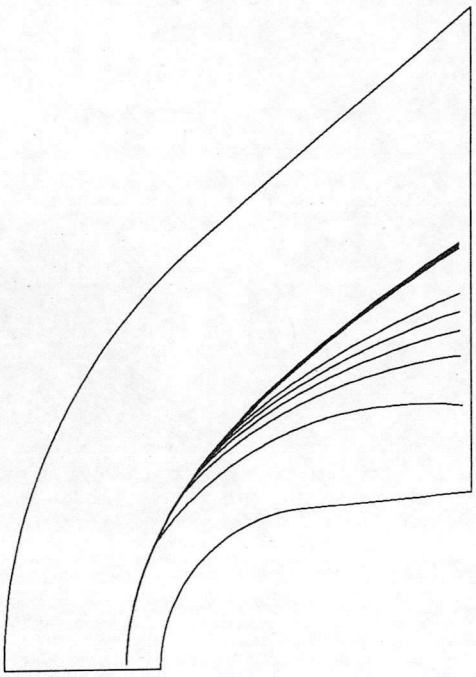

Figure C.20: *Species mole fraction contours for NO* - $\Delta x_{NO} = 0.5 \times 10^{-2}$

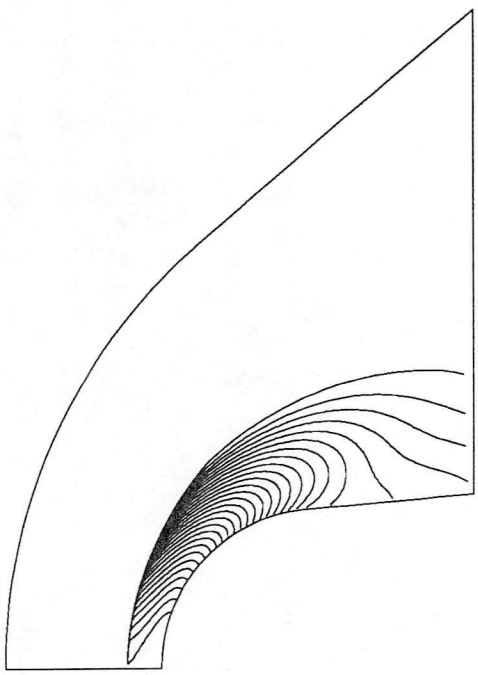

Figure C.21: *Species mole fraction contours for* N - $\Delta x_N = 0.5 \times 10^{-2}$

Appendix D

Hypersonic Hyperbola Problem

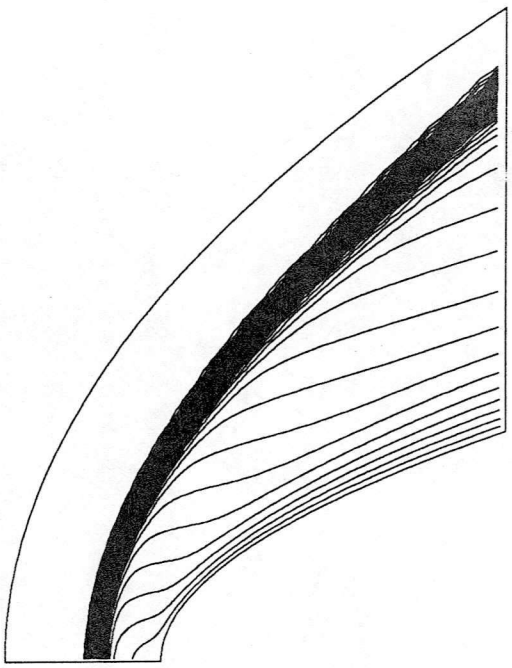

Figure D.1: *Mach number contours (Perfect gas)* - $\Delta M = 0.2$

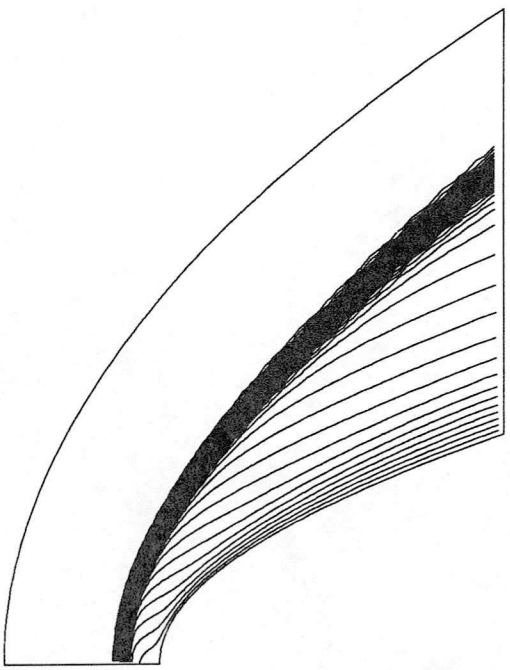

Figure D.2: *Mach number contours (Equilibrium gas)* - $\Delta M = 0.2$

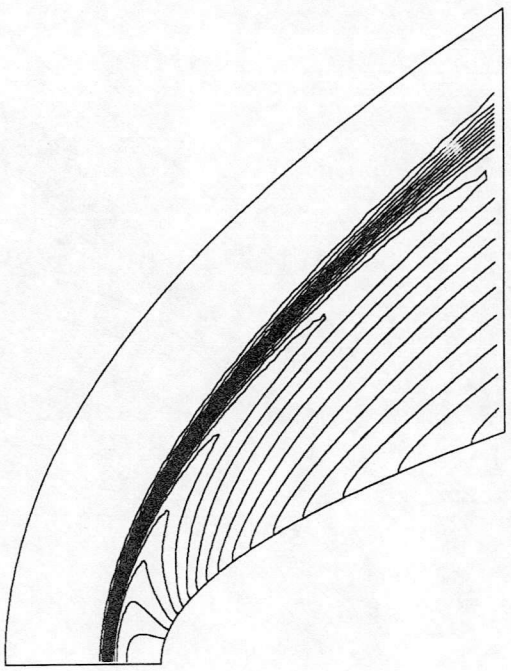

Figure D.3: *Density contours (Perfect gas)* - $\Delta\rho = 0.2 \times 10^{-3}$

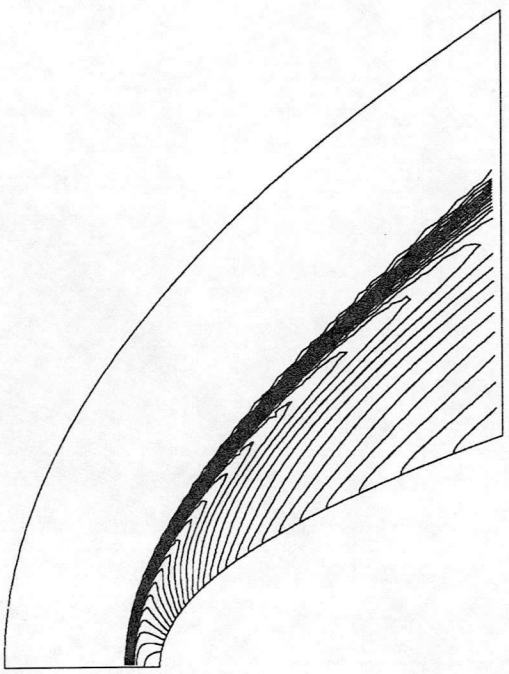

Figure D.4: *Density contours (Equilibrium gas)* - $\Delta\rho = 0.2 \times 10^{-3}$

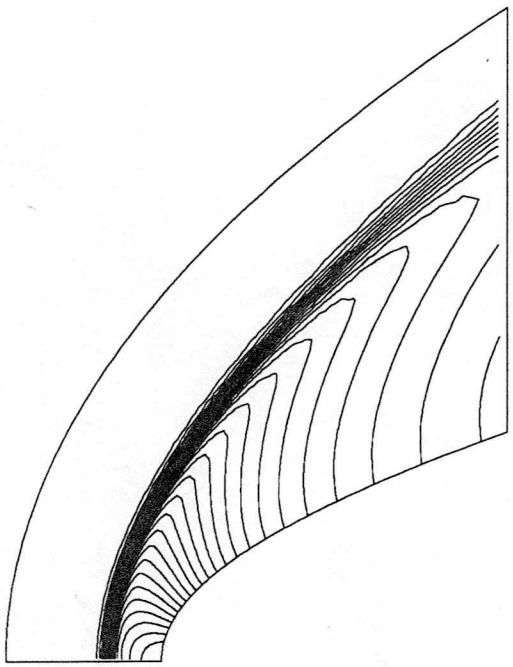

Figure D.5: *Pressure contours (Perfect gas)* - $\Delta p = 200$

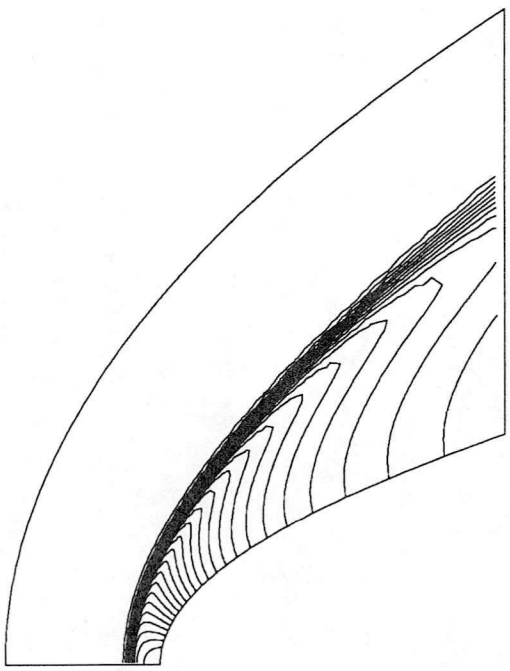

Figure D.6: *Pressure contours (Equilibrium gas)* - $\Delta p = 200$

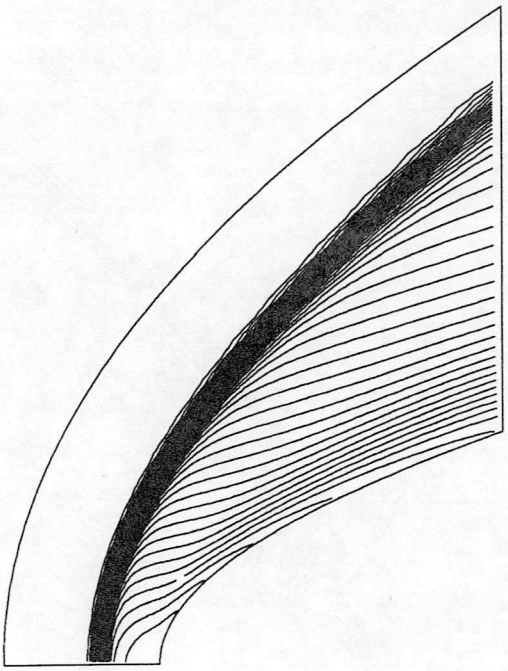

Figure D.7: *Temperature contours (Perfect gas)* - $\Delta T = 100$

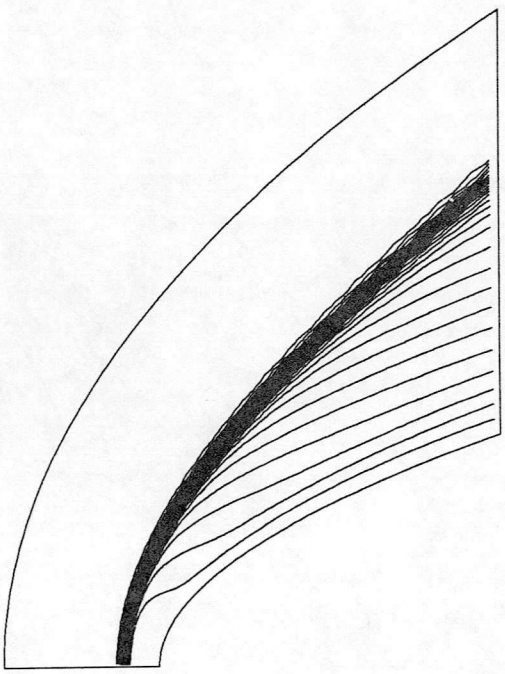

Figure D.8: *Temperature contours (Equilibrium gas)* - $\Delta T = 100$

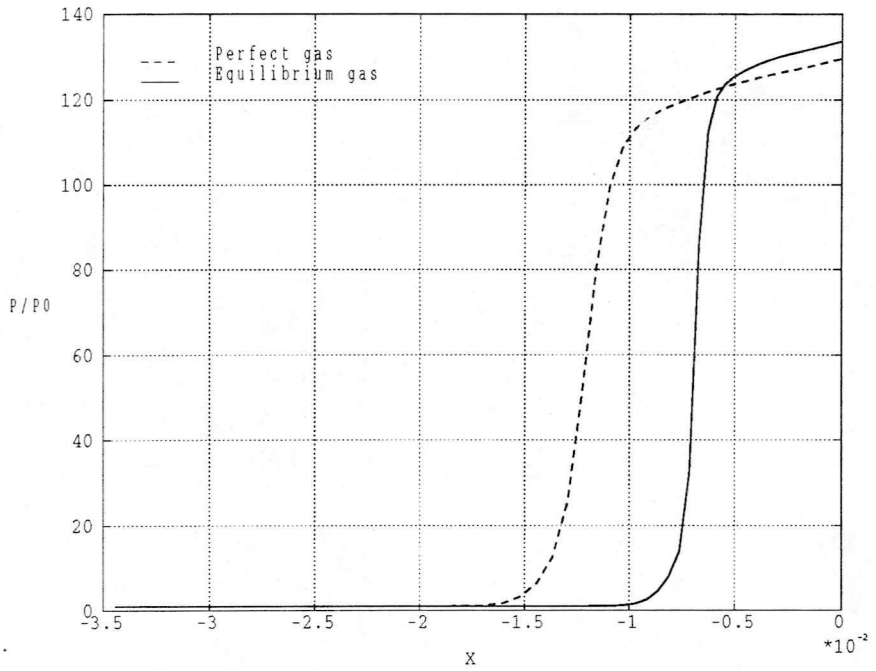

Figure D.9: *Pressure distribution along symmetric line*

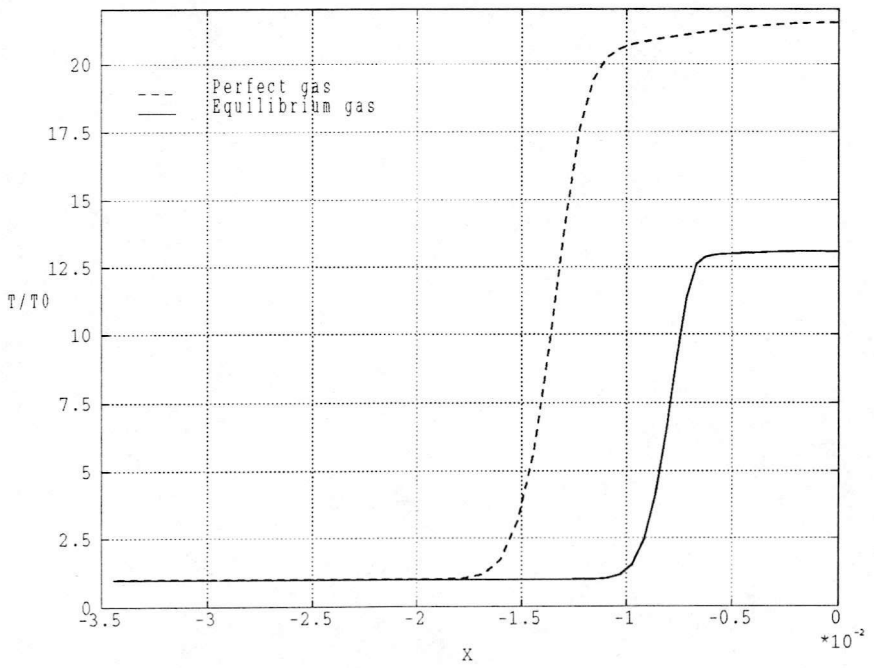

Figure D.10: *Temperature distribution along symmetric line*

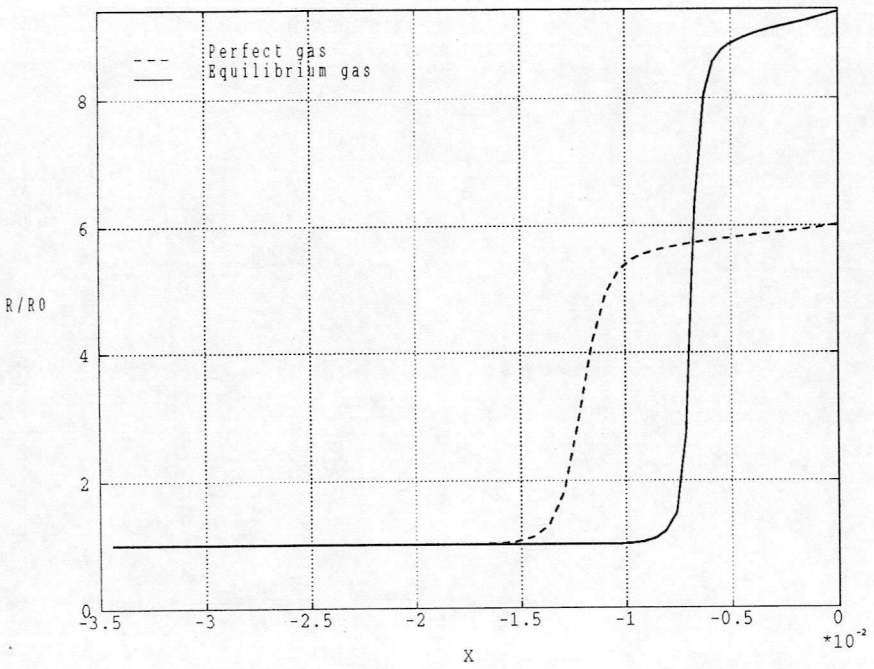

Figure D.11: *Density distribution along symmetric line*

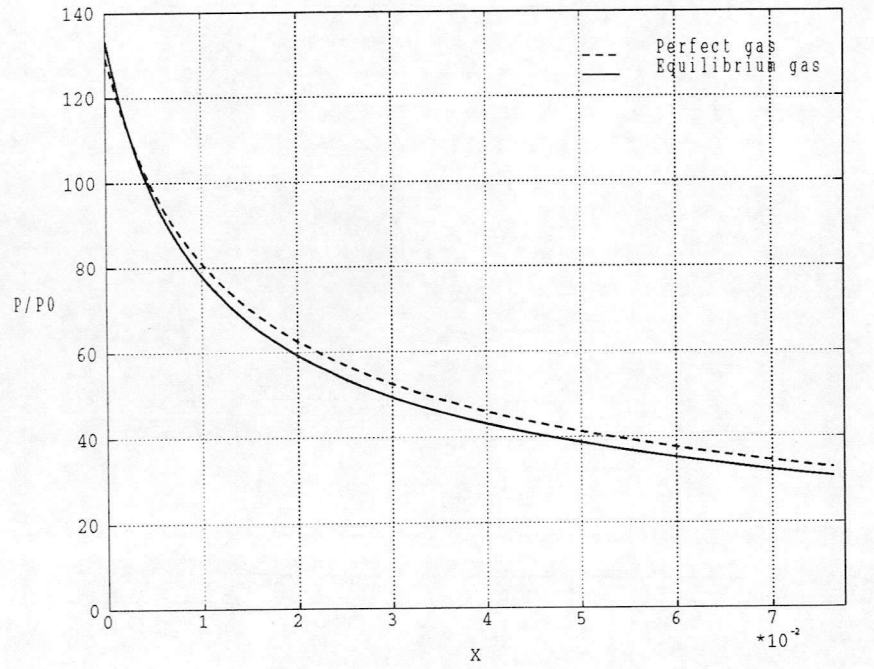

Figure D.12: *Pressure distribution along body surface*

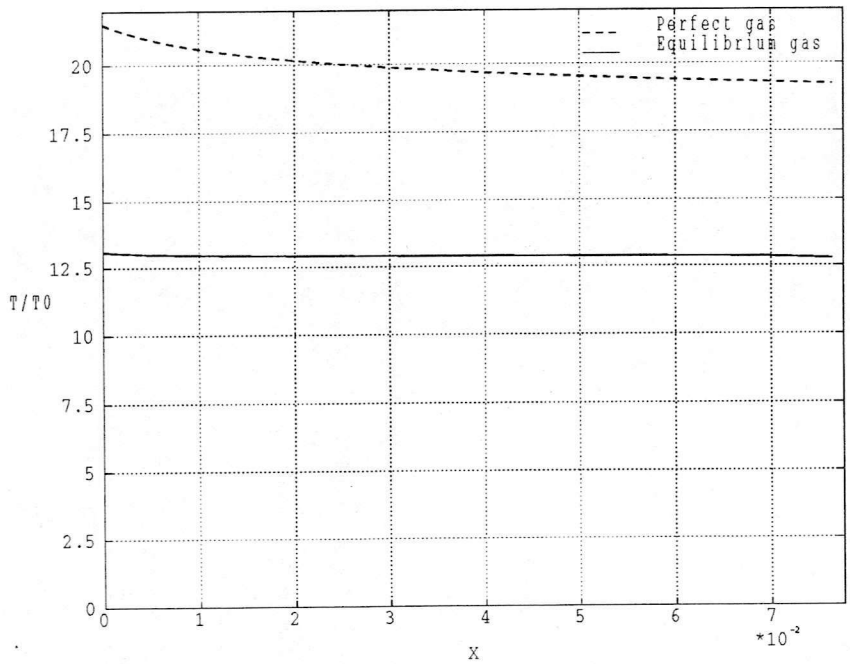

Figure D.13: *Temperature distribution along body surface*

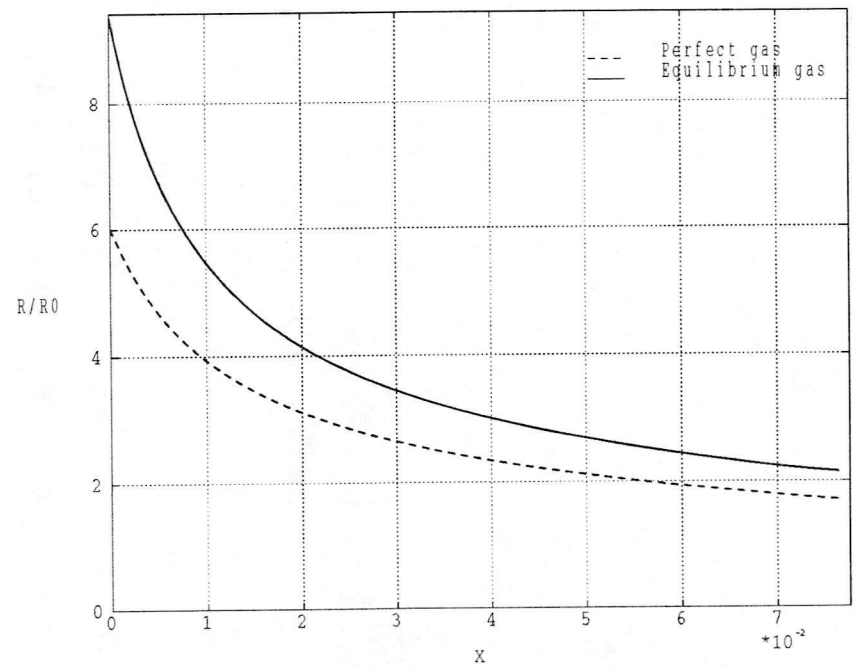

Figure D.14: *Density distribution along body surface*

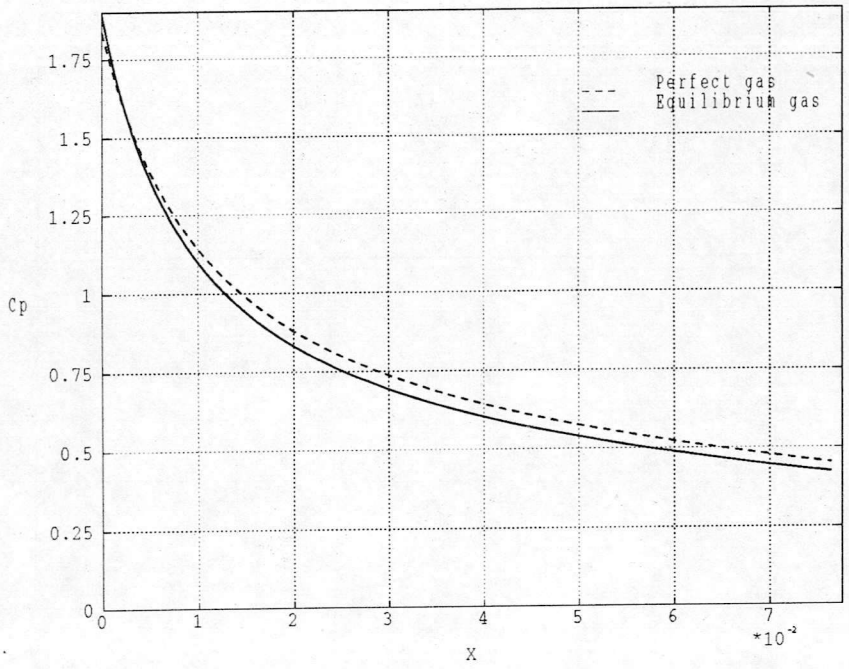

Figure D.15: *Pressure coefficient C_p distribution along body surface*

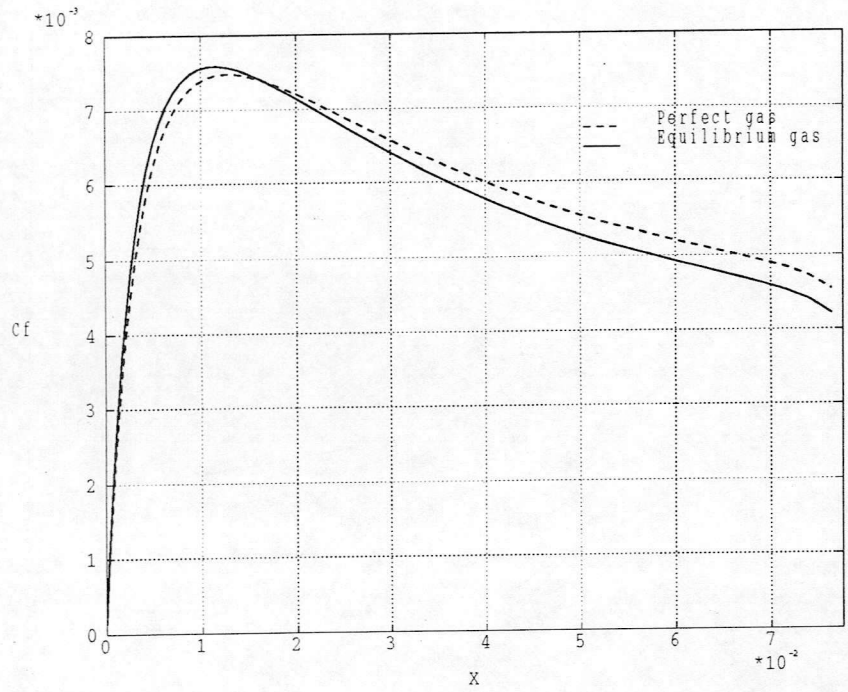

Figure D.16: *Skin friction coefficient C_f distribution along body surface*

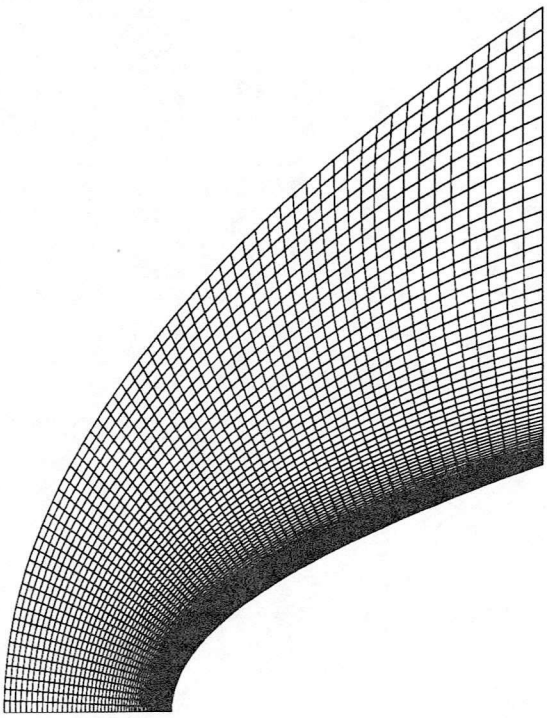

Figure D.17: *Mesh for perfect gas and equilibrium gas model* (60×60)

Bibliography

[1] Remi Abgrall. An extension of roe's upwind scheme to algebraic equilibrium real gas models. *Computers and Fluids*, 19(2):171–182, 1991.

[2] John D. Anderson. *Modern Compressible Flow With Historical Perspective.* McGraw-Hill, 1982.

[3] John D. Anderson. *Hypersonic and High Temperature Gas Dynamics.* McGraw-Hill, 1989.

[4] John Murray Anderson. Implementation of equilibrium air models within the framework of an existing euler code. *G.U. Aero Report 8906*, 1989.

[5] John Murray Anderson. A fast computational module for the calculation of equilibrium state variables and sonic speeds in chemically reacting air for applications in cfd. *G.U. Aero Report 9206*, 1992.

[6] B. Aupoix. An introduction to real gas effects. *AGARD-FDP-VKI Special Course*, 1988.

[7] Laurent Dubuc. Two dimensional navier-stokes solver using an upwind scheme on unstructured grids. *G.U. Aero Report*, 1992.

[8] Ramadas K. Prabhu & Wayne D. Erickson. A rapid method for the computation of equilibrium chemical composition of air to 15,000 k. *NASA Technical Paper 2792*, 1988.

[9] P. Glaister. An approximate linearised riemann solver for tthe euler equations for real gases. *Journal of Computation Physics*, 74:382–408, 1988.

[10] W. G. Vincenti & Ch. H. Kruger. *Introduction to Physical Gas Dynamics.* Robert E. Krieger, 1965.

[11] Bram Van Leer & Jian-Shun Shuen & Meng-Sing Liou. Splitting of inviscid fluxes for real gases. *Journal of Computational Physics*, 87:1–24, 1990.

[12] Marcel Vinokur & Jean-Louis Montagne. Generalized flux-vector splitting and roe average for an equilibrium real gas. *Journal of Computational Physics*, 89:276–300, 1990.

[13] J.-A. Desideri & R. Glowinski & J. Periaux. *Hypersonic Flows for Reentry Problems - Volume II : Test cases - Experiments and Computations.* Spinger Verlag, 1991.

[14] P. L. Roe. Approximate riemann solvers, parameter vectors and difference scheme. *Journal of Computational Physics*, 1981.

[15] M. A. Schmatz. Hypersonic three-dimensional navier-stokes calculations for equilibrium gas. *AIAA Paper 89-2183*, 1989.

[16] R. C. Reid & T. K. Sherwood. *The Properties of Gas and Liquids.* McGraw-Hill, 1966.

[17] Jian-Shun Shuen. Upwind differencing and lu factorization for chemical non-equilibrium navier-stokes equations. *Journal of Computational Physics*, 99:233–250, 1992.

[18] S. Srinivasan & J. C. Tannehill. Simplified curve fits for the transport properties of equilibrium air. *NASA Contractor Report 178411*, 1987.

[19] D. Drikakis & S. Tsangaris. On the accuracy and efficiency of cfd methods in real gas hypersonics. *International Journal for Numerical Methods in Fluids*, 16:759–775, 1993.

[20] Marcel Vinokur. Flux jacobian matrices and generalized roe average for an equilibrium real gas. *NASA Contractor Report 177512*, 1988.

[21] Yen Liu & Marcel Vinokur. Equilibrium gas flow computations. 1. accurate and efficient calculation of equilibrium gas properties. *AIAA Paper 89-1736*, 1989.

[22] B. Grossman & R. W. Walters. Analysis of flux-split algorithms for euler equations with real gas. *AIAA Journal*, 27(5):524–531, 1987.